早稲田大学大学院環境・エネルギー研究科

博士学位論文

Robust Design of FACTS Wide-Area Damping Controller Considering Signal Delay for Stability Enhancement of Power System

信号遅延を考慮した電力系統ロバスト安定化のためのFACTS広域制動コントローラの設計手法

2011 年 07 月

劉	芳
Liu	Fang

早稲田大学大学院環境・エネルギー研究科

博士学位論文

Robust Design of FACTS Wide-Area Damping Controller Considering Signal Delay for Stability Enhancement of Power System

信号遅延を考慮した電力系統ロバスト安定化のためのFACTS広域制動コントローラの設計手法

2011年 07月

早稲田大学大学院環境・エネルギー研究科

環境・電力システム研究

劉	芳
Liu	Fang

ABSTRACT

With the development of electric power system and the scale-up of power networks, the stability problems change more complex. Especially, the low frequency oscillations have become one important factor that influence the stable and the efficient operation of interconnected systems. This doctoral dissertation concerns on this stability problems and proposed a series of wide area damping control strategies to prevent these low frequency oscillation modes. The flexible and quick control features that FACTS controllers can benefit are developed, and the wide area information provided by WAMS is also combined to construct wide area damping control network. At the same time, the advanced robust design approaches are also proposed to increase the robustness against various operating conditions (e.g., line outage, line fault, load shedding, etc). These approaches sufficiently consider the delay effects of wide area control-input on the practical damping performance. Hence, they are very suitable for the design of wide area controller based on WAMS. Not only these, the coordination of multiple wide area damping controllers is also considered to reduce or even to eliminate the negative interaction of multiple controllers. The multi-delays caused by these multiple controllers are also involved during the process of controller design. All the proposed control concepts and the controller design approaches are validated through the nonlinear simulation on the 4-machine 2-area benchmark system and the 16-machine 5-area (New England Test System and New York Power System) NETS-NYPS interconnected systems.

ACKNOWLEDGMENTS

Foremost, I would like to express my deepest gratitude and apprectation to my supervisor, Professor R.Yokoyama, for his support, patience, and consistent encouragement throughout the course of my Ph.D study. His technical and editorial advice was essential to the successful completion of this dissertation. He is not only my supervisor but also encouraged and challenged me throughout my academic researches. Moreove, I would like to thank the other members of my review committee, Professor M. Katsuta, Professor S. Tomonari and Professor K. Iba for their helpful comments during the grueling thesis review process.

I am also grateful to my co-advisor, Dr. Y. Zhou of the TEPCO Systems Corporation, Professor M. Wu and Professor Y. He of Central South University for their invaluable guidance and mentorship for my doctoral course. A special thanks goes out to Professor J. She of Tokyo University of Technology. During my three-year doctoral study in Tokyo, he provided me with selfless help and guidance whatever in my study or in my life. He became more of a mentor and friend, than a professor for me.

It is also a pleasure to thank my colleagues from Yokoyama laboratory for their support and help. I must acknowledge Dr. T. Niimura for his suggestions on my writing English papers, Dr. K. Koyanagi and Dr. H. Takamori for their guidance of my power research throughout my graduate program. I also give my thanks to the doctoral students D. Yamasida, Y. Hida, B. Hu and J. Zhang for all of their computer and technical assistance in my study, and special thanks to our office staff Mrs H. Kano and Mrs Y. Inaba for all the instances in which their assistance helped me along the way.

To my family and friends I dedicate my heartfelt thanks and gratitude for the support and encouragement that they provided me through my entire life. None of my achievements would have been possible achieved without them in these years.

Financial assistance from the "National Construction High level University Government-sponsored Graduate Student Project" provided by the China Scholarship Council is also thankfully acknowledged.

Liu Fang

July 2011

Contents

List of Figures

List of Tables

Abbreviations

FACTS: flexible alternating current transmission systems

SVC: static var compensator

TCSC: thyristor controlled series compensator

UPFC : unified power flow controller

WAMS: wide-area measurement system

PMU: phasor measurement unit

TSO: transmission system operator

POD: power oscillation damping (controller)

PSS: power system stabilizer

AVR: auto voltage regulator

FWMs: free-weighting matrices (method)

WADCer: wide-area damping controller

WARD control: wide-area robust damping control

WACD: wide-area coordinated damping (controller)

Chapter 1
Introduction

1.1 Chapter Introduction

The low frequency oscillations (LFOs) especial the inter-area oscillations have become the key factor that influence the stable operation of interconnected electric networks, and meanwhile limit the transmission capacity of large-scale power systems. For these LFOs, especially these inter-area oscillations, in principle, it mainly represents as the power oscillations among different generators located in different areas of power systems. Such power oscillations further represents the negative interaction of different generators. Generally, the local power system control strategies, that adopt local control signals, cannot achieve the effective damping performance for these LFOs. However, in recent years, with more and more applications of wide area measurement systems (WAMS) in modern power systems, it provides some interested solutions to prevent these LFOs especial the inter-area oscillations. This doctoral dissertation mainly investigates these LFOs and the various wide area damping strategies developed based on advanced control theories and methods.

In this chapter, the background and the significance of this doctoral thesis will be discussed from the stability, the security, and the efficiency aspects of modern power systems. Based on this, the LFOs especial the inter-area oscillations are paid more attention. Furthermore, the overview of wide area measurement based power system damping control, which includes the introduction of wide area measurement systems (WAMS), the wide area control (WAC) strategies, and the main design approaches for wide area damping controller (WADCer). In addition, the advanced application of modern control theories and methods in WADC design is also investigated. Finally, the objective and the structure of this thesis will be presented briefly.

1.2 Background and Significance of This Doctoral Thesis

Nowadays, the continued interconnected enhancement of regional electric networks is being the developing trend of modern power systems in the worldwide, such as the interconnection of Europe networks (UCTE) [1-1] [1-2], the Japan power grid [1-3] [1-4], the national grids of China

(CSG) [1-5] [1-6], and the North American Power Grids [1-7] [1-8]. Basically, the interconnection of electric networks can efficiently utilize various power resources distributed in different areas, and achieve the optimal allocation of energy resources. It is advantage to optimize the economic dispatching of power energies, and get the relative cheaper power consumes, which means the decrease of system installed capacity and the investment. Moreover, on the fault or disturbance operating conditions, it can further provide the supporting powers of each area of interconnected networks, which can increase the reliability of the generation, transmission and the distribution systems.

However, for the interconnected electric networks, the LFOs especial inter-area oscillations are easily excited when there are faults (e.g. line-to-ground fault) or disturbances (e.g. line outage or load shedding) in the systems. Such oscillation phenomena are not typical but have the general meaning for the current interconnected networks. Take some practical interconnected systems in the worldwide as examples:

Figure 1.1 Placement of PMUs and WAMS central stations in Chinese power systems

(1) Chinese Power Systems. The PMU/WAMS has got wide application in Chinese power systems. Figure 1.1 shows the placement of PMUs and WAMS central stations in China [1-6]. Totally, the Chinese power systems mainly include Central, Northern, Eastern, Southern,

Northeastern, and Northwestern China networks. More than 105 PMUs and WAMS are distributed in these interconnected systems.

Figure 1.2 shows the online analysis result about the active power flow in the Northern and Central China interconnected line. From this it can be seen that there is a typical inter-area oscillation mode with the oscillation frequency around 0.26 Hz. This oscillation mode causes the power instability on the interconnected lines, and inevitably limits the interconnected ability. Thus, the necessary damping strategy should be performed to stabilize such oscillation mode.

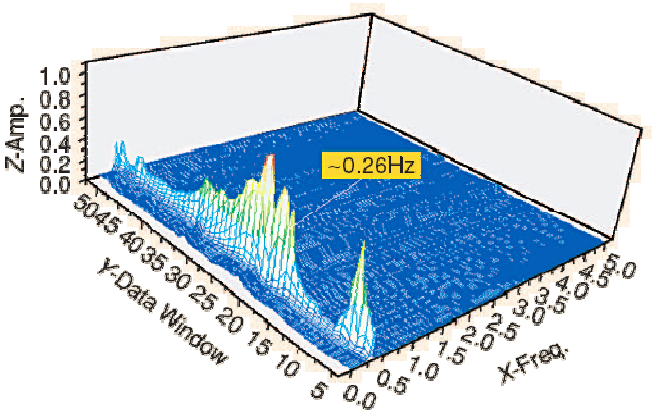

Figure 1.2 Inter-area oscillations in Chinese interconnected systems (November 5th 2003) [1-6]

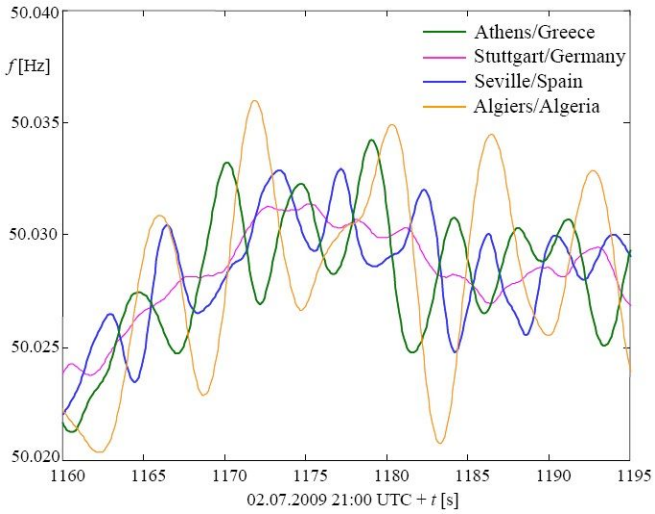

Figure 1.3 Frequency curves of different areas in UCTE network (July 2th 2009, 21:00 UTC+t [s]) [1-2]

(2) *European interconnected network (UCTE)*. Up to now, the European power system has developed a large-scale interconnected network whose area extends from Poland to Portugal in the east-west direction and from Denmark to Greece in the south-north direction. This big network covers 28 countries synchronously interconnected with 32 transmission system operators (TSOs). In the practical operating experience, the inter-area oscillations have been detected from the real-time operating data as shown in Figure 1.3 [1-2]. From this, it can be found that there are typical oscillations among four areas (Athens, Stuttgart, Seville, and Algiers). The oscillation frequency f_p and damping ratio ζ_p of the dominate oscillation mode is 0.15Hz and 5.3% [1-2], which is the typical inter-area oscillation mode.

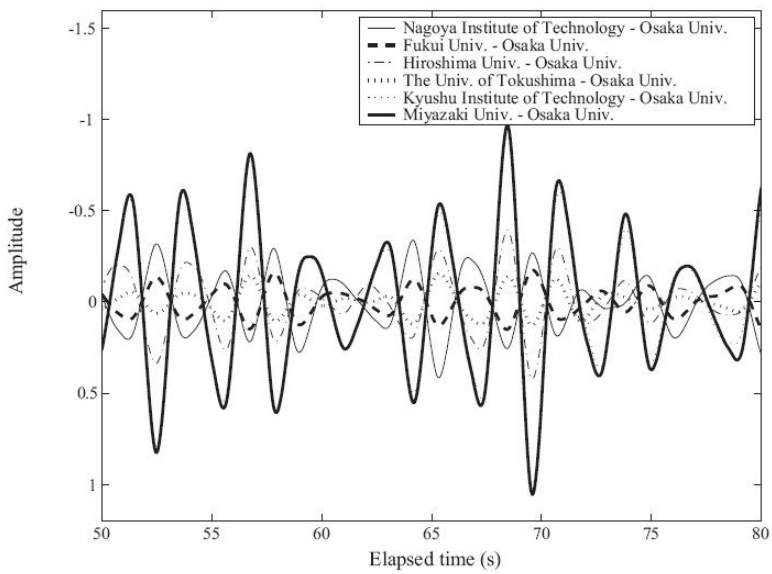

Figure 1.4 Inter-area oscillations in Japan 60Hz western system (August 21, 2003) [1-3]

(3) *Japan western 60Hz electric networks.* In Japan, there are one eastern 50Hz and one western 60Hz electric networks, respectively. For the 60Hz system, it consists of six major electric power companies [1-3], and each power system, who is operated by each power company, is interconnected through 500 kV transmission lines. In practice, such interconnected systems also exist inter-area oscillations, which can be detected by the PMUs located in campuses of Nagoya Institute of Technology, Fukui University, Osaka University, Hiroshima University, Tokushima University, Kyushu Institute of Technology, and Miyazaki University

[1-3]. Figure 1.4 shows the inter-area oscillations, which character as around 0.4 Hz oscillation frequency. These curves are obtained by monitoring the phase difference between different areas. From these, it can be found that there are obvious long-term oscillations in the western 60 Hz electric networks.

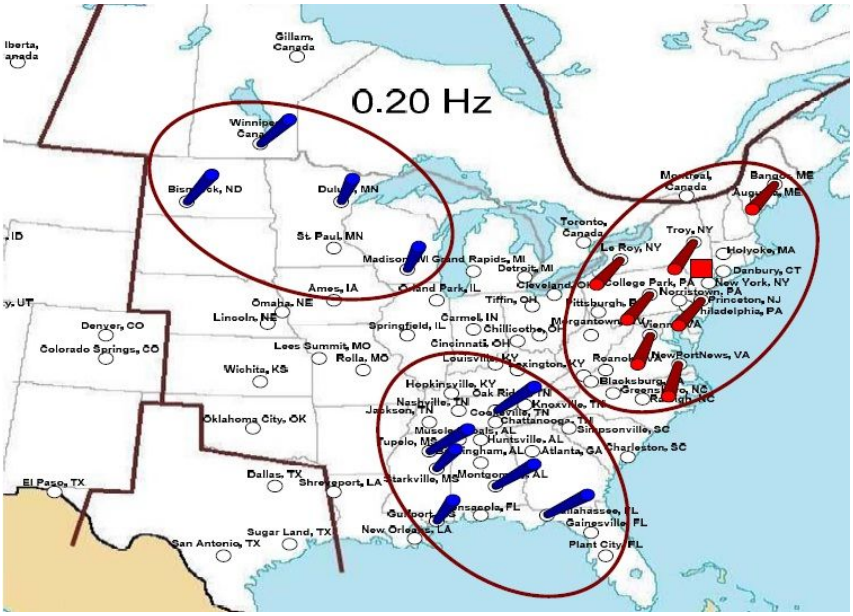

Figure 1.5 Mode shape for the 0.20 Hz dominant mode in the eastern interconnection of the North American system (August 11, 2009, New York) [1-7]

(4) *The North American power system*. The North American power system is a typical large-scale interconnected system with three different electric areas [1-7], where the eastern area is an important energy consuming area and it consists of a lot of heavy loads. The wide area measurement systems (WAMS), who bases on the phasor measurement units (PMUs), have been got a certain application in the North American power system. Hence, it changes convenient to monitor the dynamic behavior of the large-scale interconnected system. On August 11, 2009, there was some disturbance occurred in New York area, which leads to a 0.20 Hz inter-area oscillations, as shown in Figure 1.5. From the mode shape of the 0.20 Hz dominant mode, it is clearly seen that the inter-area oscillations represent as the interaction between the northeastern region and the northwestern & the southern regions of the Eastern area [1-7].

The inter-area oscillation has a number of serious damages on the stable and efficient operation of power system especial of the large-scale interconnected network. The long-term inter-area oscillation with the weak or negative damping ratio easily leads to cascading failures, and finally the power blackout could happen, such as the large-scale power blackout of USA western grid occurred on August 10, 1996 [1-7]. Not only that, once there are inter-area oscillations in the interconnected lines, the increase of transmission capacity could lead to more serious oscillations, which means that the inter-area oscillation limits the interconnected ability of power systems. Moreover, because more power energy cannot be exchanged among the interconnected areas, it makes disadvantage to achieve the optimal allocation of power resources, and realize the economical dispatching. In such cases, the technical advantages that network interconnection may benefit cannot be explored sufficiently. Thus, to ensure the stable and the efficient operation of interconnected systems, the damping strategies should be performed to prevent or eliminate such inter-area oscillation.

However, the conventional local control strategies, such as the power system stabilizer (PSS) or the FACTS damping controller that using local control signals, can usually play the effective roles on damping the local mode not the inter-area mode. In practice, the LFOs especial the inter-area oscillations usually represent the interaction among different interconnected areas. In such a case, the local control links to the local generation or transmission side cannot achieve the higher controllability. In recent years, the more application of WAMS in power systems provide the effective solution for inter-area oscillation damping. Because that WAMS can conveniently monitor the global operating variables, which makes the power system damping controller can select the effective control signals from the global range. In this thesis, such wide area measurement based power system damping control strategies are paid important attention, and various robust design methods are presented to handle with the controller design problems of wide area damping strategies.

1.3 Wide Area Measurement Based Power System Damping Control

1.3.1 Wide Area Measurement Systems (WAMS)

With the development of synchronized phasor measurement technology and modern communication technology, the WAMS technology has got relatively mature and more application in power system. In fact, WAMS is also the important part of smart grid, because the main function of WAMS is to measure and monitor the operation of power system, it can provide large number of operating information related to remote generators, transmission lines, and power customers. Such wealth of information can be flexibly utilized by transmission system operator (TSO), which agrees with the operating characteristic of smart grid with more sensors, more measurement, and more communication [1-9].

Generally, the WAMS mainly consists of three parts: (1) the PMUs distributed in the key components of power system; (2) the central station of upper monitoring and control; (3) the digital communication network that connects the previous two parts. For the part (1), it mainly includes the synchronized data sampling, which should represent a certain adaptive ability to ensure sampling accuracy when the operating condition changes (e.g. system frequency variation). For the part (3), it mainly charges of the transmission of wide area measurements. The related key equipments and technologies are the physical carrier of digital communication network, the communication protocol, the application of global position system (GPS), etc. For the part (2), the main task is to process these wide area measurement signals, monitor the system operating characteristic, and provide the decision support for TSO. At the same time, it can also provide control signals for the major control devices (e.g. PSS, HVDC controller, FACTS controller, etc) distributed in power system.

The initial overall project of PMU based WAMS was mainly introduced by the electric power research institute (EPRI) in the 1990s. Since then, the WAMS got more and more attention in the worldwide. In Japan, the Tohoku Electric Power Company developed the first GPS-based data acquisition system in 1993, which is with the purpose of wide area monitoring of power system behavior [1-10]. In recent years, the PMU-based Campus-WAMS has been also founded, which covers ten electric power companies of Japan [1-3]. In China, by the end of 2006, more than 300 PMUs have been installed in China Grid, which are mainly distributed in five regional areas (e.g.

Northern, Northeastern, Central, Southern, and Eastern China power grid), and five provincial power systems (e.g. Jiangshu, Henan, Guangdong, Yunan, and Guizhou provincial power grid) [1-6]. In the North America, up to now, there are 105 PMUs installed in the Eastern Interconnection (EI) and 56 PMUs in the Western Interconnection (WECC) [1-8].

1.3.2 Flexible AC Transmission Systems (FACTS) Technology

For the high and quick controllable ability that FACTS devices have, the FACTS controller can be used not only to stabilizing bus voltage, increase the transmission capacity and flexibly control power flow [1-11] [1-12], but also as the alternative technology to perform wide area oscillation damping control through introducing the suitable wide area signals [1-13] [1-14].

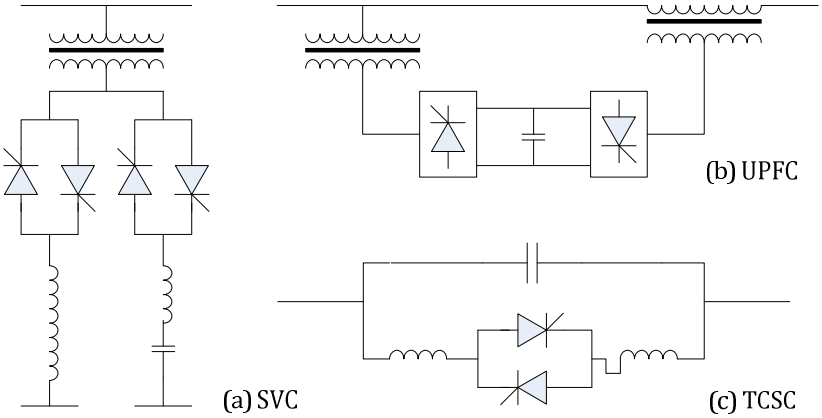

Figure 1.6 Basic types of FACTS devices

Typically, Figure 1.6 gives three structures of FACTS devices [1-15] that can be classified as series-, shunt-, and multi-types, respectively.

(1) For the shunt-type FACTS controller, it is always used to compensate the reactive power and stabilize the bus voltage, and the relatively mature shunt-type FACTS device is SVC (Static Var Compensator) shown in Figure 1.6(a). Normally, it constructed by TCR (Thyristor Controlled Reactor) and FC (Fixed Capacitor), sometimes TCR and TSC (Thyristor Switched Capacitor). At present, the advanced VSC-based shunt-type FACTS device that is STATCOM (Static Synchronous Compensator) has brought widely attention and a certain application in power systems. Due to the based voltage source converter and energy storage

(DC capacitor or battery) technologies, STATCOM can conveniently realize the 4-quadrant operation for active and reactive power (*P&Q*).

(2) For the series-type FACTS controller, it is always used to control power flow and limit short circuit current, and also can be used to damp various power oscillations very well. The typical series-type FACTS controller is TCSC (Thyristor Controlled Series Capacitor) shown in Figure 1.6(c), and like STATCOM, the VSC-based series-type FACTS controllers are SSSC (Static Synchronous Series Compensator) and IPFC (Interline Power Flow Controller), which can control P&Q parameters conveniently.

(3) For the multi-type FACTS controller as shown in Figure 1.6(b), it combines the technical advantages of shunt- and series-type FACTS controllers, such as the typical device named UPFC (Unified Power Flow Controller), which can be looked as the combination of STATCOM and SSSC. UPFC has the well-rounded compensating ability, and can not only provide the controlled reactive power compensation, but also realize the active and reactive power flow control independently.

Although there are wide range of FACTS controllers, as for the existing power oscillations in power systems, if the suitable wide-area control singles can be governed by PMU-based WAMS, and be selected as the wide area input of the POD (Power Oscillation Damping) controller of FACTS control system, then combine the advanced control theory and method with the fully consideration of the time-delay of the power systems, the various power oscillations especial the inter-area oscillations can be damped effectively to enhance the stability of power systems.

1.3.3 Design Methods of Wide Area Damping Controller (WADCer)

Up to now, to improve the stability of interconnected system, various oscillation damping controllers including the wide area damping controllers (WADCer), which are with different controller structures, have been proposed by means of different controller design methods. In principle, these controller design methods can be summarized as the following aspects:

(1) *Phase compensation design method*. This classic design method was proposed by F.P. Demello and C. Concordia in 1969 [1-16]. In this literature, they theoretically analyzed why the inter-area oscillation could be excited, and correspondingly, they proposed the design

concept of power system stabilizer (PSS) with lead-lag compensation blocks. The basic design concept of such controller is to calculate the phase of the dominant oscillation mode, and utilize the lead-lag blocks of PSS to compensate such phase. Although the PSS can provide the effective damping for simple oscillation mode, it needs the coordination of multi-PSSs linked with the generators distributed in different areas of power system. For this purpose, many papers presented various methods to coordinate multi-PSSs [1-17] or PSSs and FACTS controller [1-18].

(2) *Linear quadratic regulation (LQR) method*. The method is the typical application of advanced control theory in controller design of power system. In principle, the power system is linearized at different operating conditions, and the state-space models are thereby obtained. Then, by employing the LQR method, the coordination of various oscillation damping controllers (e.g., PSSs or/and FACTS controller) can be considered simultaneously. Generally, the LQR method is useful to coordinated optimize the controller gains or/and controller structures [1-19].

(3) *H_2/H_∞ control design methods*. As one typical modern robust control design method, the H_2/H_∞ control has been introduced into the control fields of power system [1-20] [1-21]. Generally, for this control design method, it is mixed synthesis with multi-objective control optimization, such as the constraint of pole placement and the guarantee of robustness, etc. In recent years, the linear matrix inequalities (LMIs) theory is introduced to solve the H_2/H_∞ controller, and such solution is generally converted as standard optimization problem in the framework of LMIs.

(4) *Intelligent control design methods.* Various intelligent algorithms, such as artificial neural network, fuzzy theory, genetic algorithm (GA), expert system (ES), etc, have been applied for power system damping controller design. In [1-22], the GA was used to simultaneously tune multiple power system damping controllers, and such tuning considers a pre-specified set of operating conditions, thus it represents a certain robustness. In [1-23], the neural networks were introduced for adaptive control coordination of PSSs and FACTS devices to damp power oscillations. In [1-24], a Mamdani fuzzy logic controller was designed for a FACTS device to enhance the small signal stability of multi-machine power system.

1.4 Advanced Application of Modern Control Theory in WADC Design

Although there are various design methods for FACTS damping controllers and the designed POD has the good performance in the ideal system, as for the actual complex power systems, there are some existing negative factors that influence the damping effects of FACTS POD to a certain degree. The time-delay characteristic of the remote or global transmitted signals is an important factor that cannot be ignored, and especially that power system itself is a typical time-delay system. So, it is important to do the related research on the time-delay stability of the modern power systems with multi-FACTS device, and make this as one of the guideline for the FACTS damping controller design.

The improvement of modern control theory and technology make the more alternative for the design method and structure of the FACTS damping controller [1-25] [1-26] [1-27] [1-28] [1-29] [1-30]. The LMI (Linear Matrix Inequalities) theory can be used to analyze the time-delay system and design the related feedback controller very well. Because that LMI-based robust controller can consider the time-delay of input signals and controlled system, it can be obtain the optimal control effects for the time-delay systems.

In addition, as for the complex power system with multi-FACTS controllers, the interaction among the FACTS controllers should be considered, because that it can also influence the control effects and the stability of the power system. As for this aspect, the LMI-based controller design method, which combines to the optimal algorithm such as genetic algorithm (GA), can be used to design the FACTS POD controller to improve the control effects for the power systems with time-delay characteristics.

1.5 Objective and Structure of the Doctoral Thesis

The overall objective of this doctoral thesis represents the following aspects: (1) Present a wide area damping control network, which mainly includes WAMS and the FACTS controllers, to enhance the stability of large interconnected systems; (2) The robust control design method, presented in [1-25] [1-26] [1-27] [1-28] [1-29] [1-30], are introduced to design the robust FACTS damping controller to implement wide area damping control strategy; (3) Solve the delay effects of wide area signals on the control performance of wide area damping controller.

The structure of this doctoral thesis is planned as follows:

Chapter 1. The background and significance of the research is presented. Then, the application of the WAMS and the FACTS device is introduced briefly. Moreover, the design methods of power system damping controller, and the advanced application of modern control theories in power system are also summarized.

Chapter 2. The eigenvalues based modal analysis method for small signal stability of power system is discussed, and the classic local power system stabilizers, which include different structures, are also analyzed. The characteristic of LFOs especial the inter-area mode is revealed.

Chapter 3. The basic framework of wide area damping control network is presented in this chapter. The operating principle that adopts FACTS device to realize the goal of oscillation damping is discussed in detail. Furthermore, the initial robust design, which considers the delay effects of wide area signal, is performed for a single-machine infinite-bus (SMIB) system with FACTS device.

Chapter 4. A free-weighting matrices (FWMs) approach is proposed to design FACTS wide area damping controller. All the controller design problems are solved in the LMI framework, and the time delay of wide area signals is involved during the processing of controller.

Chapter 5. An output-feedback-type controller that considers the signal time-varying delay is proposed for FACTS wide area damping control strategy. Unlike the classic static output-feedback controller, the proposed controller represents as the state-space or the transfer-function model, which is dynamic and can adaptive to the varying of time delay.

Chapter 6. A wide area coordinated robust damping control of multiple FACTS devices is proposed in this chapter for stability enhancement of large-scale interconnected systems. The control coordination of multiple FACTS controllers is considered during the robust design processing, thus it can greatly reduce the interaction among multiple FACTS controllers. At the same time, the signal varying delay of

different FACTS controllers is also considered, and it can reach good damping performance under multiple time varying delay.

Chapter 7. The conclusions and the possible future works are presented in this chapter.

Chapter References

[1-1] **C. D. Vournas, A. Metsiou, and B. M. Nomikos.** *Analysis of intra-area and interarea oscillations in South-Eastern UCTE interconnection*. IEEE Power & Energy Society General Meeting, 2009.

[1-2] **J. Lehner, M. Kaufhold, M. Treuer, and T. Weissbach.** *Monitoring of inter-area oscillations within the European interconnected network based on a wide area measuring system.* IEEE PES Transmission and Distribution Conference and Exposition, 2010.

[1-3] **T. Hashiguchi, Y. Mitani, O. Saeki, K. Tsuji, M. Hojo, and H. Ukai.** *Monitoring power system dynamics based on phasor measurements from demand side outlets developed in Japan Western 60 Hz system.* IEEE Power Systems Conference and Exposition, 2004.

[1-4] **Y. Ota, T. Hashiguchi, H. Ukai, M. Sonoda, Y. Miwa, and A. Takeuchi.** *Monitoring of interconnected power system parameters using PMU based WAMS.* IEEE Lausanne Power Tech, 2007.

[1-5] **P. Li, X. C. Wu, C. Lu, J. H. Shi, J. Hu, J. B. He, Y. Zhao, and A. D. Xu.** *Implementation of CSG's wide-area damping control system: overview and experience.* IEEE/PES Power System Conference and Exposition, 2009.

[1-6] **X. R. Xie, Y. Z. Xin, J. Y. Xiao, J. T. Wu, and Y. D. Han.** *WAMS applications in Chinese power systems.* IEEE Power & Energy Magazine. Vol. 4, No. 1, pp. 54-63, Jan.-Feb. 2006.

[1-7] **Z. Y. Yuan, X. Tao, Y. C. Zhang, C. Lang, P. N. Markham, R. M. Gardner, and Y. L. Liu.** *Inter-area oscillation analysis using wide area voltage angle measurements from FNET.* IEEE Power and Energy Society General Meeting, 2010.

[1-8] **Y. C. Zhang, P. Markham, X. Tao, C. Lang, Y. Z. Ye, Z. Y. Wu, W. Lei, J. Bank, J. Burgett, R. W. Conners, and Y. L. Liu.** *Wide-area frequency monitoring network (FNET) architecture and applications.* IEEE Transactions on Smart Grid. Vol. 1, No. 2, pp. 159-167, Sept. 2010.

[1-9] **A. Bose.** *Smart transmission grid applications and their supporting infrastructure.* IEEE Transactions on Smart Grid. Vol. 1, No. 1, pp. 11-19, June 2010.

[1-10] **H. Saitoh.** *GPS synchronized measurement applications in Japan.* IEEE PES Transmission and Distribution Conference and Exhibition, 2002.

[1-11] **Y. Xiao, Y. Song, C. C. Liu, and Y. Sun.** *Available transfer capability enhancement using FACTS devices.* IEEE Transactions on Power Systems, Vol. 18, Nov. 1, pp. 305-312, Feb. 2003.

[1-12] **Y. Xiao, Y. Song, and Y. Sun.** *Power flow control approach to power systems with embedded FACTS devices.* IEEE Transactions on Power Systems, Vol. 17, No. 14, pp. 943-950, Nov. 2002.

[1-13] **M. Zarghami, M. L. Crow, and S. Jagannathan.** *Nonlinear control of FACTS controllers for damping interarea oscillations in power systems.* IEEE Transactions on Power Delivery. Vol. 25, No. 4, pp. 3113-3121, Oct. 2010.

[1-14] **H. Nguyen-Duc, L. Dessaint, A. F. Okou, and I. Kamwa.** *A power oscillation damping control scheme based on Bang-Bang modulation of FACTS signals.* IEEE Transactions on Power Systems. Vol. 25, No. 4, pp. 1918-1927, Oct. 2010.

[1-15] **X. P. Zhang, C. Rehtanz, and B. Pal.** *Flexible AC Transmission Systems: Modeling and Control.* Springer, 2006, ISBN 3540306064.

[1-16] **F. P. Demello and C. Concordia.** *Concepts of synchronous machine stability as affected by excitation control.* IEEE Transactions on Power Apparatus and Systems. Vol. 88, No. 4, pp. 316-329, 1969.

[1-17] **P. Zhang and A. H. Coonick.** *Coordinated synthesis of PSS parameters in multi-machine power systems using the method of inequalities applied to genetic algorithms.* IEEE Transactions on Power Systems. Vol. 15, No. 2, pp. 811-816, 2000.

[1-18] **L. J. Cai and I. Erilich.** *Simultaneous coordinated tuning of PSS and FACTS damping controllers in large power systems.* IEEE Transactions on Power Systems. Vol. 20, No. 1, pp. 294-300, 2005.

[1-19] **R. Gupta, B. Bandyopadhyay, and A. M. Kulkarni.** *Power system stabiliser for multimachine power system using robust decentralised periodic output feedback.* IEE Proceedings of Control Theory Application. Vol. 152, No. 1, pp. 3-8, Jan. 2005.

[1-20] **R. Kutzner, B. Scholz, and M. Reimann.** *An advanced model-based approach to stabilize power system oscillations based on the H-infinite theory modelling and tuning guide, practical experience.* IEEE Power Engineering Society General Meeting, 2003.

[1-21] **Y. Zhang and A. Bose.** *Design of wide-area damping controllers for interarea oscillations.* IEEE Transactions on Power Systems. Vol. 23, No. 3, pp. 1136-1143, 2008.

[1-22] **Antonio L. B. do Bomfim, Glauco N. Taranto, and Djalma M. Falcao.** *Simultaneous tuning of power system damping controllers using genetic algorithms.* IEEE Transactions on Power Systems. Vol. 15, No. 1, pp. 163-169, Feb. 2000.

[1-23] **T. T. Nguyen and R. Gianto.** *Neural networks for adaptive control coordination of PSSs and FACTS devices in multimachine power system.* IET Generation, Transmission and Distribution. Vol. 2, No. 3, pp. 355-372, 2008.

[1-24] **S. Mohagheghi, G. K. Venayagamoorthy, S. Rajagopalan, and R. G. Harley.** *Hardware implementation of a Mamdani fuzzy logic controller for a static compensator in a*

multimachine power system. IEEE Transactions on Industry Applications. Vol. 45, No. 4, pp. 1535-1544, July/August 2009.

[1-25] **F. Liu, M. Wu, Y. He, Y. Zhou, and R. Yokoyama.** *Delay-dependent Robust Stability Analysis for Interval Neural Networks with Time-varying Delay.* IEEJ Transactions on Electrical and Electronic Engineering, 2010. (Accepted)

[1-26] **F. Liu, M. Wu, Y. He, and R. Yokoyama.** *Improved Delay-dependent Stability Analysis for Uncertain Stochastic Neural Networks with Time-varying Delay.* Neural Computing and Applications, Vol. 20, pp. 441-449, 2011.

[1-27] **F. Liu, M. Wu, Y. He, Y. Zhou, and R. Yokoyama.** *New Delay-dependent Stability Criteria for T-S Fuzzy Systems with Time-varying Delay.* Fuzzy Sets and Systems. Vol. 161, No. 15, pp. 2033-2042, 2010.

[1-28] **M. Wu, F. Liu, P. Shi, Y. He, and R. Yokoyama.** *Stability Analysis for Discrete-time Recurrent Neural Networks with Time-varying Delay.* IEEE Trans on Circuits and Systems, II. Vol. 55, No. 7, pp. 600-604, 2008.

[1-29] **M. Wu, F. Liu, P. Shi, Y. He, and R. Yokoyama.** *Exponential Stability Analysis for Neural Networks with Time-Varying Delay.* IEEE Trans on Systems, Man and Cybernetics, Part B. Vol. 38, No. 4, pp. 1152-1156, 2008.

[1-30] **F. Liu, M. Wu, Y. He, Y. Zhou, and R. Yokoyama.** *New Delay-dependent Stability Criteria for T-S Fuzzy Systems with a Time-varying Delay.* Proceedings of the 17th World Congress, the International Federation of Automatic Control. pp. 254-258, July 6-11, 2008, Seoul, Korea.

Chapter 2
Effective Analysis of Local PSSs on Oscillation Damping Based on Eigenvalues Analysis Method

2.1 Introduction

Power system oscillations were first reported in northern American power network in 1964 during a trial interconnection of the northwest power pool and the southwest power pool [2-1]. Up to now, Generally speaking, power oscillations could be divided into three kinds of types, that is, local mode, inter-area mode, and global mode. Local oscillations lie in the upper part of that range and consist of the oscillation of a single generator or a group of generators against the rest of the system. In contrast, inter-area oscillations and global oscillations are in the lower part of the frequency range and comprise the oscillations among groups of generators. As a classic oscillation mode, there are relative mature technologies and devices such as kinds of power system stabilizers equipped as a part of the additional excitation system of machine unit to provide the efficient damping ratio to suppress the local oscillation. Nevertheless, as for the inter-area and the global oscillation mode, the classic stabilizer cannot play an important role to damp such oscillation very well. The leaded result is that the line power transmitted from one area to another will form the instable oscillation with the unease attenuation characteristic.

As a result, if there is no effective solution to suppress these power system oscillations, the instability could lead the machine unit cut even the networks breakout. Nowadays, severe consequences have been coursed by large-scale blackouts, such as blackouts in the USA, Europe and many other countries in recent years. Moreover, blackouts not only lead to financial losses, but also lead to potential dangers to society and humanity. So it is necessary to pay attention to keep the stability and security of the electrical power systems. Up to now, many authors are trying to develop new methods to enhance the various types of oscillations in power system. Various theories and technologies are introduced to against such power oscillations, such as wide area measurement systems [2-2][2-3], FACTS devices[2-4][2-5][2-6], robust controllers and the design technologies [2-7][2-8], and so on, to enhance the stability and the security operating ability of the close-loop systems. In this chapter, we will deals with the application of power system stabilizer(PSS) to improve the power system damping oscillation by using eigenvalue analysis method.

2.2 Operating Principle of PSS on Oscillation Damping

The basic function of power system stabilizer (PSS) is to add damping to the generator rotor oscillations by controlling its excitation by using auxiliary stabilizing signal(s). Based on the automatic voltage regulator (AVR) and using speed deviation, power deviation or frequency deviation as additional control signals, PSS is designed to introduce an additional torque coaxial with the rotational speed deviation, so that it can increase low-frequency oscillation damping and enhance the dynamic stability of power system. Figure2.1 shows the torque analysis between AVR and PSS.

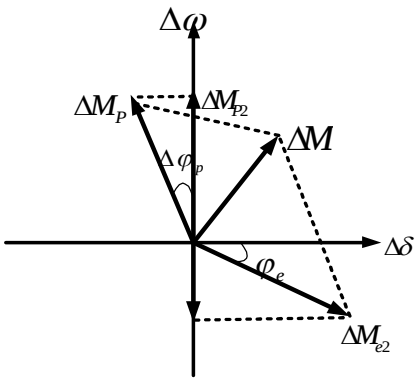

Figure 2.1 torque analysis between AVR and PSS

As shown in *Figure 2.1*, under some conditions, such as much impedance, heavy load need etc., the additional torque ΔM_{e2} provided by the AVR lags the negative feedback voltage ($-\Delta V_t$) by one angle φx , which can generate the positive synchronizing torque and the negative damping torque component to reduce the low frequency oscillations damping. On the other hand, the power system stabilizer, using the speed signal ($\Delta\omega$) as input signal, will have a positive damping torque component ΔM_{p2}. So, the synthesis torque with positive synchronous torque and the damping torque can enhance the capacity of the damping oscillation. *Figure* 2.2 shows the structure diagram of power system stabilizer (PSS).

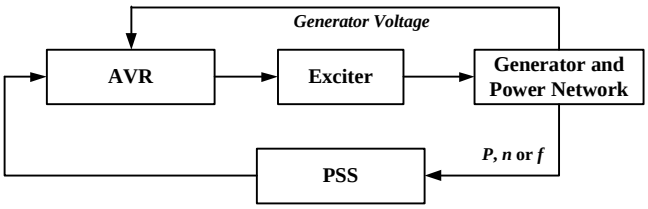

Figure 2.2 the structure diagram of power system stabilizer(PSS)

2.3 PSS Category

Power system stabilizers (PSS) are added to excitation systems to enhance the damping of power system during low frequency oscillation. For the potential power oscillation problem in the interconnected power networks, the power system stabilizers solution is usually selected as the relative practical method, which can provide the additional oscillations damping enhancement through excitation control of the synchronous machines.

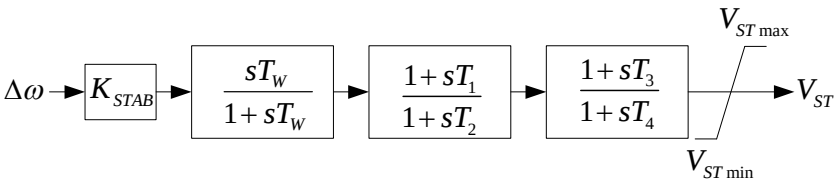

Figure 2.3 General power system stabilizer model

Figure2.3 shows the general power system stabilizer model with a single input, and from which, it can be seen that as for the additional damping control of the excitation system of the synchronous machines, basically the general input signal is the rotor speed deviation. The damping amount is mostly determined by the gain K_{STAB}, and the following sub-block has the high-pass filtering function to ensure the stabilizer has the relative better response effect on the speed deviation. There are also two first-order lead-lag transfer functions to compensate the phase lag between the excitation model and the synchronous machine.

Figure 2.4 shows the power system stabilizer mode with dual-input singles, which is designed by using combinations of power and speed or frequency as stabilizing singles. From it, it can be seen this model can be used to represent two distinct types of dual-input stabilizer implementations. One hand, as for electrical power input stabilizers in the frequency range of system oscillations, they can use the speed or frequency input for the generation of an equivalent mechanical power signal, to make the total signal insensitive to mechanical power change. On the other hand, by combining the speed /frequency and electrical power, they can use the speed directly (i.e., without phase-lead compensation) and add a signal proportional to electrical power to achieve the desired stabilizing signal shaping.

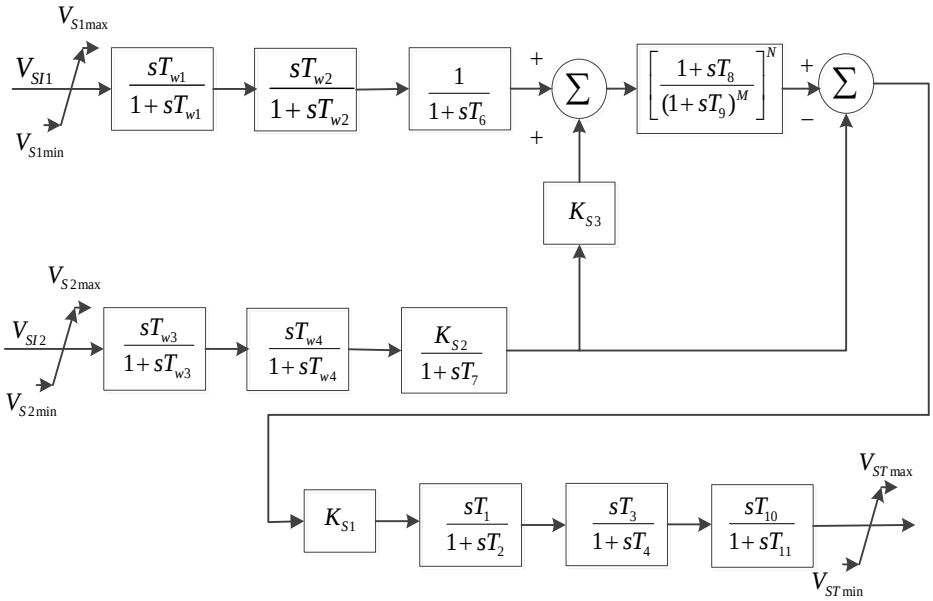

Figure2.4 Power system models with dual inputs

Although the conventional stabilizer model has a certain damping effect on the active power oscillation, the action on the special oscillation such as inter-area or global oscillation cannot be considered very well. To solve such oscillation problems, various methods have been provided with the special consideration of the inter-area or global oscillation. Here, the multi-band power system stabilize shown in Figure2.5 is studied in detail to the inter-area oscillation environment.

In essence, the standardized multi-band power system stabilizer is the multi-structure of the general stabilizer with three kinds of frequency bands action function to consider the mostly potential power system oscillations. In that case, the measured input signal, which has been transferred through high-pass filter sub-block, can be used by the related gain, phase compensation block, and limiter to generate the special output control signal for the local oscillation damping mode. Similarly, the measured input signal, and the related transfer function blocks are used to damp the impossible inter-area and global power oscillation.

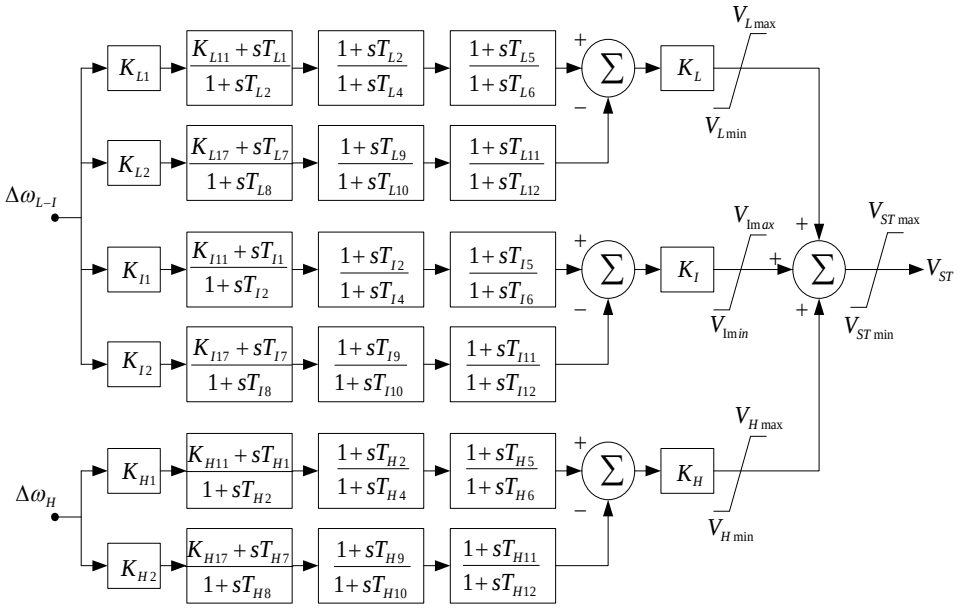

Figure2.5 Multi-band power system stabilizer model

2.4 Eigenvalues Analysis Method

2.4.1 Small Signal Modeling

The behaviour of a normal power system can be described by a set of first order nonlinear ordinary differential equations and a group of nonlinear algebraic equations. It can be written in the following form by using vector-matrix notation:

$$\begin{aligned} \dot{x} &= f(x,\ w,\ u) \\ 0 &= g(x,\ w,\ u) \\ y &= h(x,\ w,\ u) \end{aligned} \tag{2.1}$$

In which, x is vector of state variables, such as rotor angle and speed of generators. The column vector w is the vector of bus voltages. u, y is the input and output vector of variables respectively

Although power system is a nonlinear, it can be linearized by small signal stability at a certain operating point. $(x_0,\ w_0,\ u_0)$ is supposed to be a equilibrium point of this power system, then based on direct feedback, it can be expressed as the following standard form:

$$\begin{cases} \Delta\dot{x} = A\Delta x + B\Delta u \\ \Delta y = C\Delta x + D\Delta u \end{cases} \tag{2.2}$$

where Δx, Δy , and Δu express state, output, and input vector, respectively; A, B, C, and D expresses the state, control or input, output, and feed forward matrices, respectively.

2.4.2 Damping Ratio and Linear Frequency

The eigenvalues λ of A matrices can be obtained by solving the root of the following characteristic equation:

$$\det(\lambda I - A) = 0 \tag{2.3}$$

As for any obtained eigenvalues $\lambda_i = \sigma_i \pm j\omega_i$, the damping ratio ρ and oscillation frequency f can be defined as follows:

$$\rho_i = -\frac{\sigma_i}{\sqrt{\sigma_i^{\ 2} + \omega_i^{\ 2}}} \tag{2.4}$$

$$f_i = -\frac{\omega_i}{2\pi} \tag{2.5}$$

The above parameters ρ_i and ω_i can be used to evaluate the damping effects of the power system stabilizers on the power oscillation. It is obvious that the higher damping ratio and the lower oscillation frequency, the better damping effects to enhance the stability of the power system, so as for the solution with power system stabilizers to damp the power oscillation, the best scheme is that install the power system stabilizer for every machine in the power networks, in that case, it can inevitably obtain the best damping effects. Nevertheless, such installation scheme must increase the investment cost, which may be not the economical solution scheme. So, with the precondition of demand damping effects within the specific limits, the optimal arrangement for stabilizers in the areas and the machines of the power

networks could be valuably performed with the consideration of economical factor, which will be discussed in the case study.

2.4.3 Mode Shape and Participation Factor

if λ_i is an eigenvalue of A, v_i and w_i are non zero column and row vectors respectively such

that the following relations hold:

$$Av_i = \lambda_i v_i,\ i = 1, 2, \cdots, n \tag{2.6}$$

$$w_i A = \lambda_i w_i,\ i = 1, 2, \cdots, n \tag{2.7}$$

where, the vectors v_i and w_i are known as right and left eigenvectors of matrix A. And they are henceforth considered normalised such that

$$w_i \cdot v_i = 1 \tag{2.8}$$

Then the participation factor p_{ki} (the kth state variable x_k in the ith eigenvalue λ_i) can be given as

$$p_{ki} = |v_{ik}||w_{ki}| \tag{2.9}$$

where w_{ki} and v_{ki} are the ith elements of w_k and v_k , respectively.

2.5 Cases Study

2.5.1 Four-Machine Two-Area Test System with MB-PSSs

Figure 2.6 shows the two-area benchmark power system[2-9] for inter-area oscillation studies. From this, it can be seen that there are two machines in each area, and two-parallel 220km transmission lines are used to interconnect the both areas. In order to discuss the impacts of different stabilizer arrangement on the power oscillation damping, as for the area arrangement scheme, the following tests have been performed: (a) install stabilizers in both areas; (b) install stabilizers in area-1; (c) install stabilizers in area-2; (c) not install stabilizers. As for the machine arrangement scheme, the following tests have been

performed: (a) install stabilizers for G1~G4; (b) install stabilizers for G1 and G3; (c) install stabilizer for G1; (d) no machine installed stabilizer.

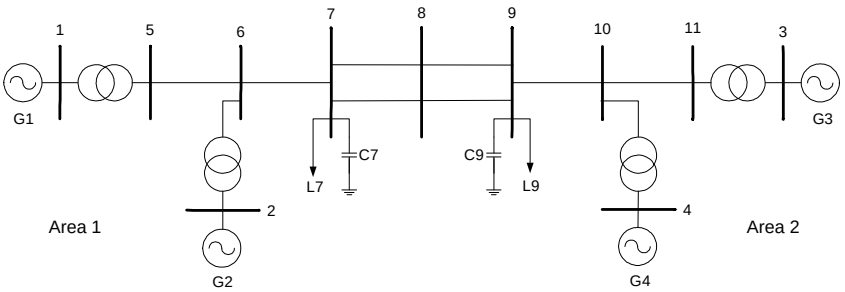

Figure2.6 Two-area test system

It is worth to remark that such testes mentioned above are achieved by small disturbance for the G1's reference voltage step from 1.0pu to 1.02pu with the duration time of 0.2s. In the corresponding situations, the small signal stability for the inter-area oscillation has been analyzed in detail with the eigenvalues analysis method.

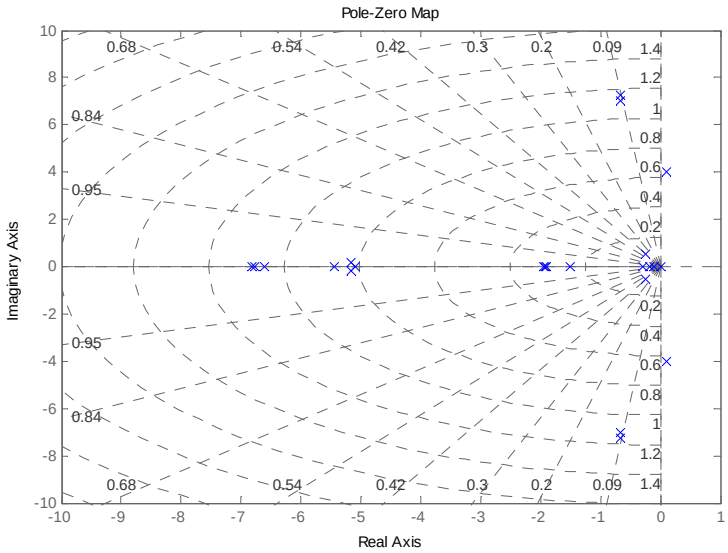

(a)

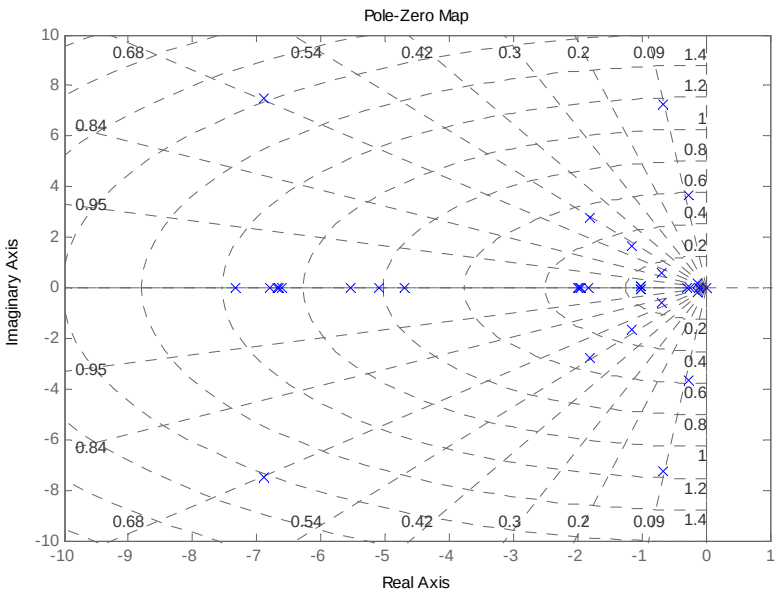
Pole-Zero Map
Imaginary Axis
Real Axis
0.68
0.54
0.42
0.3
0.2
0.09
0.84
0.95
1.4
1.2
1
0.8
0.6
0.4
0.2

(b)

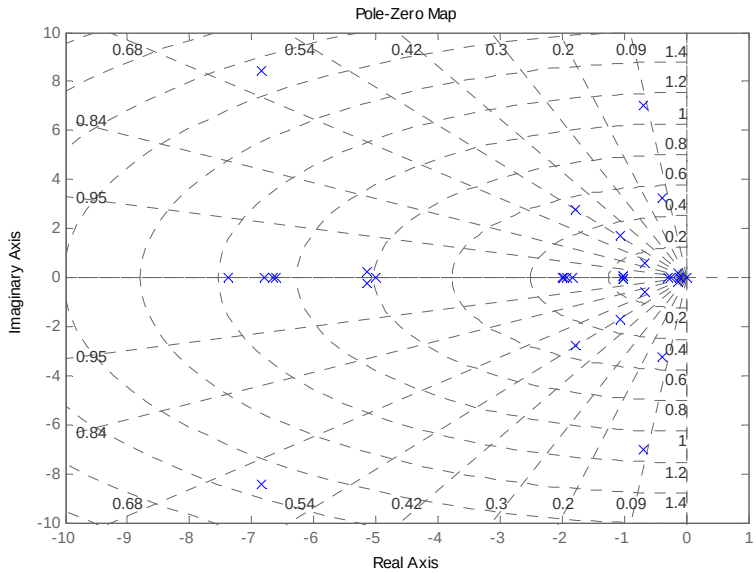
Pole-Zero Map
Imaginary Axis
Real Axis
0.68
0.54
0.42
0.3
0.2
0.09
0.84
0.95
1.4
1.2
1
0.8
0.6
0.4
0.2

(c)

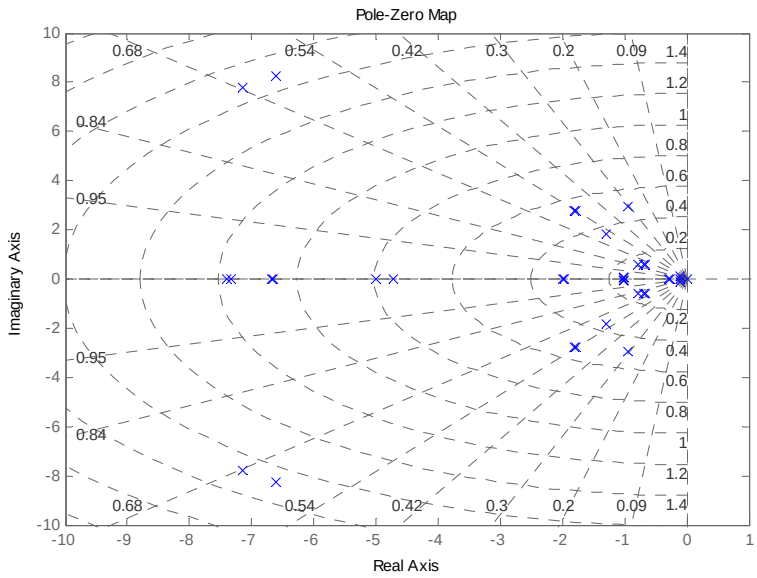

(d)

Figure 2.7 Dominant eigenvalues of the two-area test system, (a) no stabilizer; (b) with stabilizers in area-1; (c) with stabilizers in area-2; (4) with stabilizers in both areas.

Figure 2.7 shows dominant eigenvalues analysis results for the two-area test system with different area stabilizer arrangement. From Figure 2.7(a), it can be seen that as for the open-loop system without any installed stabilizer, there is some instability for the inter-area mode. By installing the stabilizers in area-1, the inter-area oscillation mode has been suppressed, and meanwhile the local mode in area-1 between G1 and G2 is also enhanced greatly shown in Figure 2.7(b). Such similar damping effect shown in Figure 2.7(c) is also achieved by installing stabilizers in area-2. If we stall the stabilizers in both area-1 and -2, both the inter-area mode and two local modes can be obtained the high damping ratio and lower oscillation frequency shown in Figure 2.7(d).

In order to represent the related oscillation effects, the time domain for the test system has been performed. Figure 2.8 shows the simulation results on the line power flow from area 1 to area 2. From this, it can be found that the arrangement on stabilizer installation for every machine in both areas has the best damping effects on inter-area oscillation, which is in unison with the above dominant eigenvalues analysis results. If there is no any stabilizer for machine in both areas, the inter-area oscillation cannot be avoided. The other arrangement schemes exists a certain difference. By comparative analysis, it can be found that

the arrangement scheme on installing the stabilizer for G1 in area-1 and G3 in area-2 is the relative optimal solution to damp the inter-area oscillation between area-1 and 2.

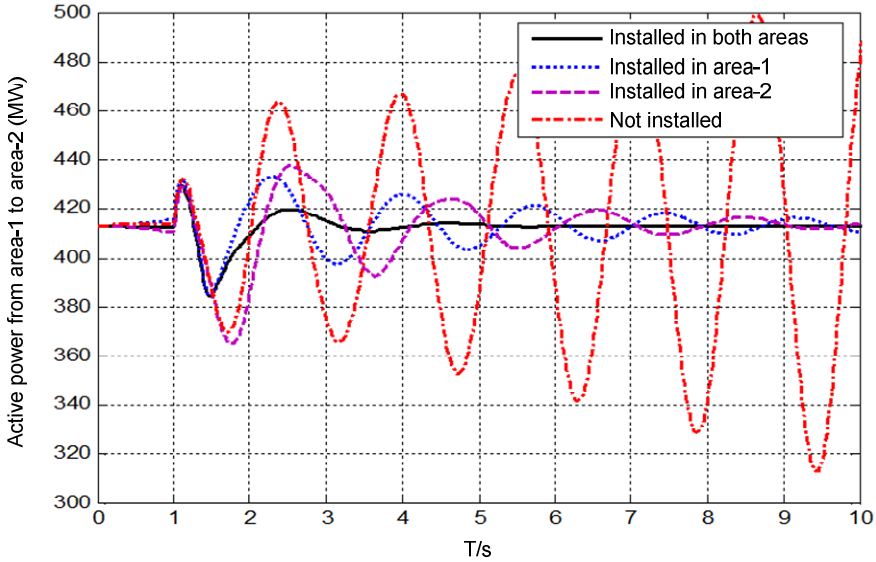

(a)

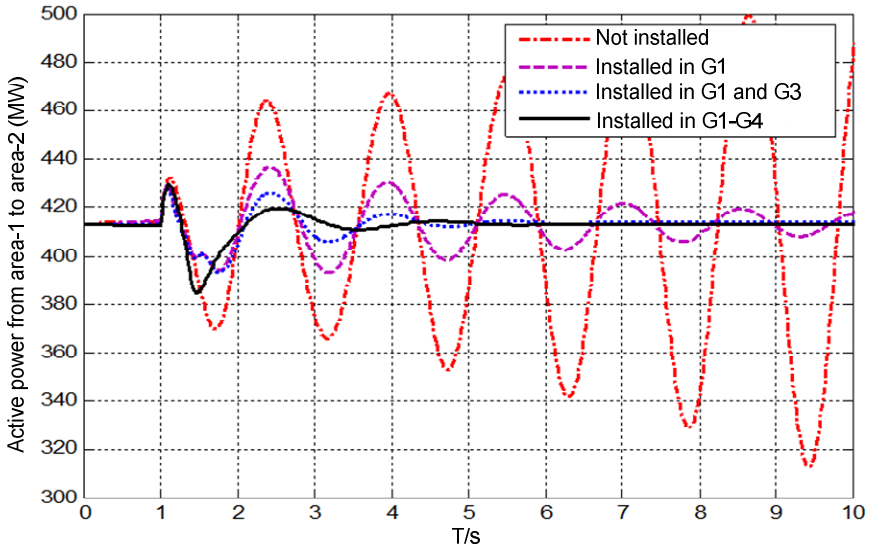

(b)

Figure 2.8 Oscillation damping effects of installed stabilizers, (a) different areas; (b) different machines

2.5.2 Sixteen-Machine Five-Area Test System with Various PSSs

In order to indicate the stabilization effects of multi-PSSs for large-scale power system, the 16-machine 5-area test system[2-10]showed in Figure 2.9 is simulated in this section. This is in fact the simplified New England and New York interconnected system. The first nine machines (G1-G9) and the second four machines (G10-G13) are belonged to the New England Test System (NETS) and the New York Power System (NYPS), respectively. In addition, there are other three machines (G14-G16) used as the dynamical equivalent of the three neighbour areas connected with NYPS area. It should be remarked that all the machines are described by the sixth-order dynamical model.

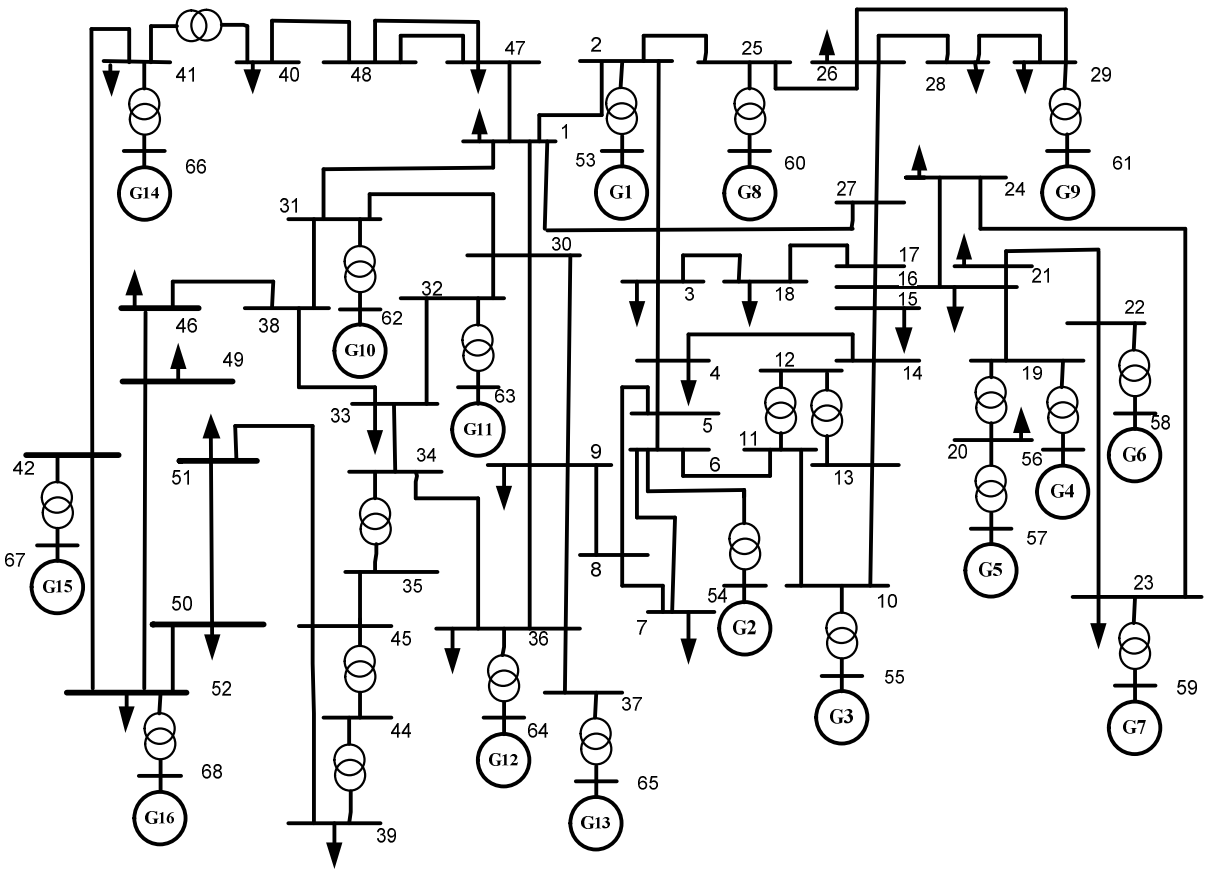

Figure 2.9. The 16-machine 5-area test system

The eigenvalue analysis mentioned in the above Section 2.4 has been performed on the linearized system model of the multi-machine test system without any PSS. The calculated dominate oscillation modes are shown in Table 2.1. From this, it can be seen that as for the system without PSSs, there are kinds of low frequency oscillations (LFOs) with the very weak damping ratios, which is disadvantage to the normal operation of the multi-machine test system.

Table 2.1 Dominant oscillation modes (without PSS)

Mode	Eigenvalues	Frequency (Hz)	Damping Ratio
1	-0.064±2.756i	0.439	0.023
2	-0.032±3.590i	0.571	0.009
3	-0.003±4.408i	0.702	0.001
4	-0.131±5.170i	0.823	0.025
5	0.408±7.673i	1.221	-0.053
6	0.240±7.722i	1.229	-0.031
7	0.647±7.790i	1.240	-0.083
8	-0.157±8.357i	1.330	0.019
9	0.291±8.462i	1.347	-0.034
10	0.477±8.615i	1.371	-0.055
11	0.167±8.690i	1.383	-0.019
12	-0.116±10.095i	1.607	0.012
13	0.092±10.188i	1.621	-0.009
14	-0.383±10.207i	1.625	0.037
15	0.516±12.543i	1.996	-0.041

Furthermore, according to the calculation results shown in Table 2.1 about the participation factor of each machine to the corresponding operation mode, it can be observed that under the normal operation condition, the system mainly has four inter-area oscillation modes and eleven local oscillation modes. Combined to Table 2.1, we can obviously obtain the common results about the LFO characteristics. That is to say, as for the inter-area modes, the oscillation frequency is less 1.0Hz, and as for the low-frequency local modes, the oscillation frequency is between 1.0Hz and 2.0Hz.

Table 2.2 Participation factor and oscillation modes

Mode	Participation factor (from G1 to G16)	Oscillation mode
1	0.0147,0.0110,0.0137,0.0127,0.0130,0.0167,0.0120,0.0093, 0.0142,0.0049,0.0046,0.0253,0.1400,0.0848,0.1006,0.0366	G1-G9 vs G10-G16
2	0.0022,0.0012,0.0017,0.0021,0.0023,0.0029,0.0020,0.0014, 0.0024,0.0001,0.0000,0.0001,0.0002,0.2065,0.0063,0.2730	G1,G4-G9,G14 vs G2,G3, G10-G13,G15,G16
3	0.0309,0.0141,0.0214,0.0383,0.0461,0.0546,0.0366,0.0191, 0.0392,0.0000,0.0006,0.0205,0.1746,0.0029,0.0003,0.0056	G1,G4-G8 vs G2,G3, G9-G16
4	0.0000,0.0000,0.0000,0.0001,0.0001,0.0001,0.0001,0.0000, 0.0000,0.0000,0.0000,0.0003,0.0029,0.1322,0.3144,0.0498	G1-G9,G12,G13,G15 vs G10,G11,G14,G16
5	0.0001,0.0059,0.0038,0.0037,0.0048,0.0102,0.0039,0.0008, 0.0140,0.0013,0.0006,0.4178,0.0681,0.0000,0.0000,0.0001	Local oscillation mode
6	0.0176,0.0979,0.0734,0.0429,0.0565,0.1126,0.0381,0.0040, 0.0758,0.0103,0.0010,0.0422,0.0017,0.0001,0.0000,0.0000	Local Oscillation mode
7	0.0123,0.0898,0.0728,0.0015,0.0014,0.0038,0.0029,0.0111, 0.3152,0.0000,0.0000,0.0019,0.0004,0.0000,0.0000,0.0000	Local Oscillation mode
8	0.0055,0.0005,0.0007,0.0167,0.2878,0.1593,0.0536,0.0031, 0.0005,0.0019,0.0001,0.0001,0.0001,0.0000,0.0000,0.0000	Local Oscillation mode
9	0.1377,0.0427,0.0108,0.0007,0.0023,0.0102,0.0082,0.0783, 0.0166,0.1799,0.0043,0.0077,0.0013,0.0002,0.0000,0.0002	Local Oscillation mode
10	0.0027,0.1864,0.2582,0.0001,0.0002,0.0015,0.0007,0.0014, 0.0006,0.0018,0.0000,0.0000,0.0000,0.0000,0.0000,0.0000	Local Oscillation mode
11	0.1213,0.0008,0.0035,0.0001,0.0004,0.0084,0.0012,0.0710, 0.0047,0.2569,0.0032,0.0029,0.0021,0.0001,0.0000,0.0002	Local Oscillation mode
12	0.0025,0.0001,0.0005,0.1471,0.0727,0.1056,0.1381,0.0007, 0.0003,0.0000,0.0000,0.0000,0.0000,0.0000,0.0000,0.0000	Local Oscillation mode
13	0.0001,0.0000,0.0000,0.1957,0.0345,0.0365,0.1852,0.0001,	Local Oscillation mode

	0.0000,0.0000,0.0000,0.0000,0.0000,0.0000,0.0000,0.0000	
14	0.1793,0.0000,0.0001,0.0001,0.0001,0.0002,0.0001,0.3086, 0.0000,0.0000,0.0000,0.0000,0.0000,0.0000,0.0000,0.0000	Local Oscillation mode
15	0.0007,0.0002,0.0001,0.0001,0.0000,0.0000,0.0000,0.0002, 0.0000,0.0100,0.4323,0.0021,0.0043,0.0001,0.0000,0.0002	Local Oscillation mode

To describe the existing oscillation modes vividly, the angle eigenvectors for mode 1-8 have been drawn as shown in Figure 2.10 and 2.11. By comparing there two figures, we can obviously find the difference between inter-area mode and local mode. In practice, with the demand of competitive power markets and the large-scale transmission and distribution of electric energy, more and more regional electric networks are interconnected to gradually form the relative bigger scale electric power systems. In that case, the dynamic performance changes more complex, which lead to various instability problems such as voltage instability, power oscillations, and so on. Especial for the inter-area oscillation mode, it could be the typical LFO modes existing in the modern power system, which should be considered carefully. Generally, as for the typical common selection for stabilization of power system, PSS can provide a certain damping for the LFO mode especial for the local mode. Also, as for the inter-area oscillation damping, the multi-band PSS mentioned in the above section should be a better alternative.

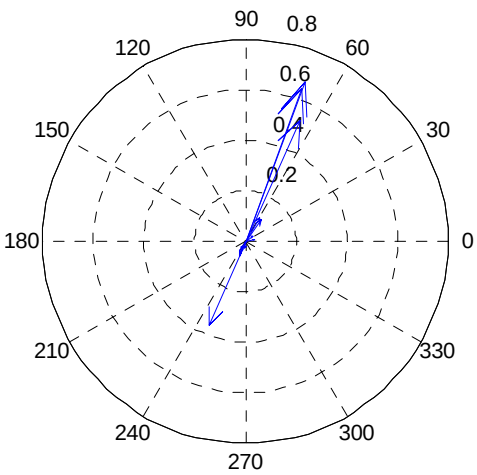

(a)

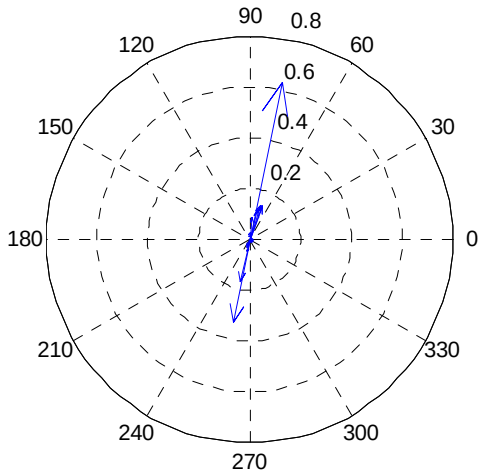

(b)

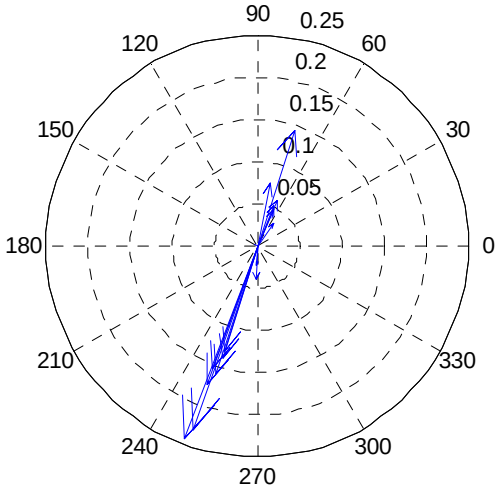

(c)

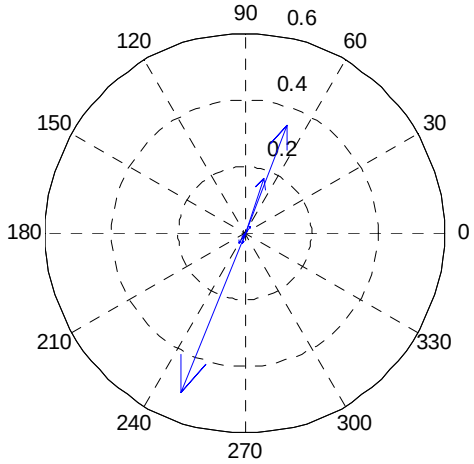

(d)

Figure 2.10. Inter-area oscillation modes. (a) mode-1, (b) mode-2, (c) mode-3, (4) mode-4

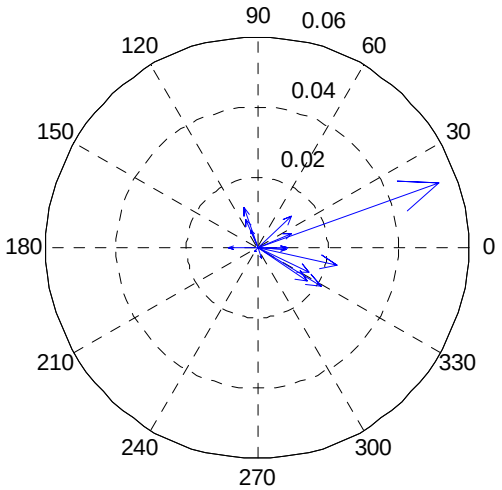

(a)

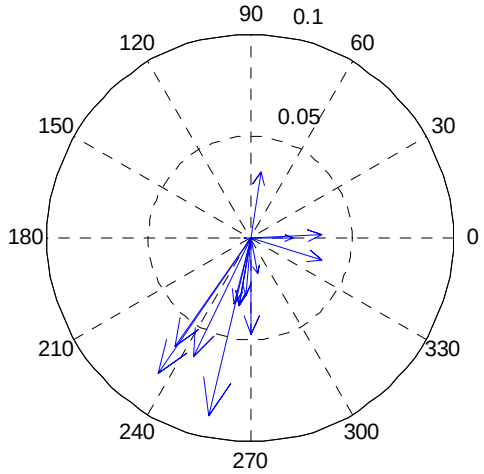

(b)

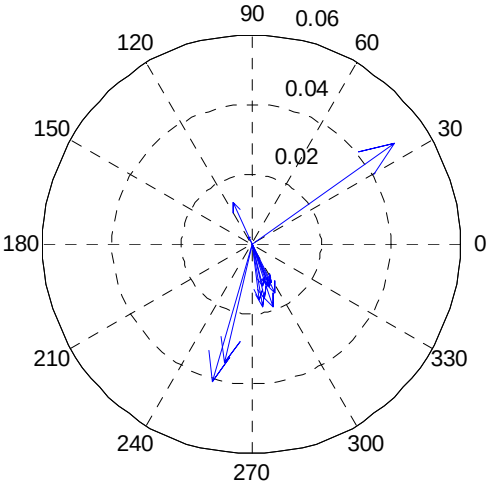

(c)

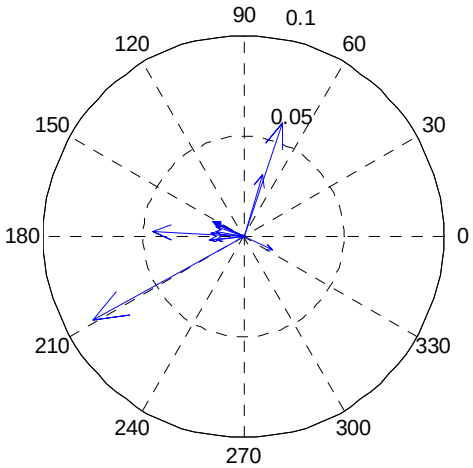

(d)

Figure 2.11. Local oscillation modes. (a) mode-5, (b) mode-6, (c) mode-7, (4) mode-8

In order to reveal the stabilizing effects of the general PSS on the LFO modes, the PSS with the classical structure shown in Figure 2.3 has been installed to each machine in the multi-machine test system. As for the lead-lag time constants for the phase lag compensation, they can be determined using the method given in [2-9].

The eigenvalues analysis for the linearized model of the multi-machine test system with 16-PSSs has been performed. The calculated dominate oscillation modes are shown in Table 2.3. By comparing with Table 2.1, it can be seen that with the implement of PSSs installation, the damping ratios for both the inter-area and the local modes are greater than 0.1, which indicates the very well stabilization effects of PSS on LFO mode.

In order to evaluate the stabilization performance of PSSs on the LFO modes, the nonlinear simulation on the multi-machine test system has been performed by setting the line-to-ground fault nearby Bus-1. The fault starts from 10.0-s and continuous 50-ms. Figure 2.12 and 2.13 show the dynamic responses of the test system for such large disturbance. From Figure 2.12, it can be seen that the system without PSSs exists the serious power oscillations, which is directly reflected by the instability of machine speed shown in Figure 2.12(a). However, with the implement of PSSs, such oscillations are damped very well, which can be shown in Figure 2.12(b).

Table 2.3. Dominant oscillation modes (with PSS)

Mode	Eigenvalues	Frequency (Hz)	Damping Ratio
1	-0.598±2.667i	0.424	0.219
2	-0.690±3.489i	0.555	0.194
3	-0.676±4.209i	0.670	0.159
4	-0.674±5.037i	0.802	0.133
5	-1.205±7.434i	1.183	0.160
6	-1.494±7.543i	1.201	0.194
7	-1.560±8.152i	1.297	0.188
8	-1.810±8.337i	1.327	0.212
9	-1.738±8.540i	1.359	0.199
10	-1.271±8.622i	1.372	0.146
11	-2.767±8.879i	1.413	0.297
12	-1.724±11.114i	1.769	0.153
13	-2.913±11.414i	1.817	0.247
14	-3.024±11.822i	1.882	0.248
15	-2.056±12.353i	1.966	0.164

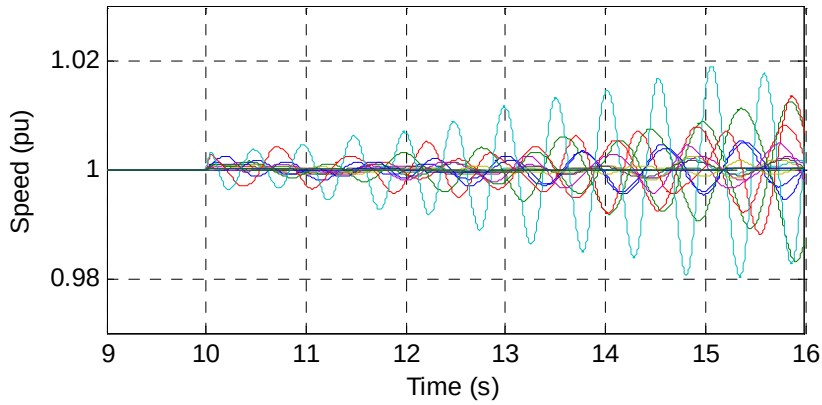

(a)

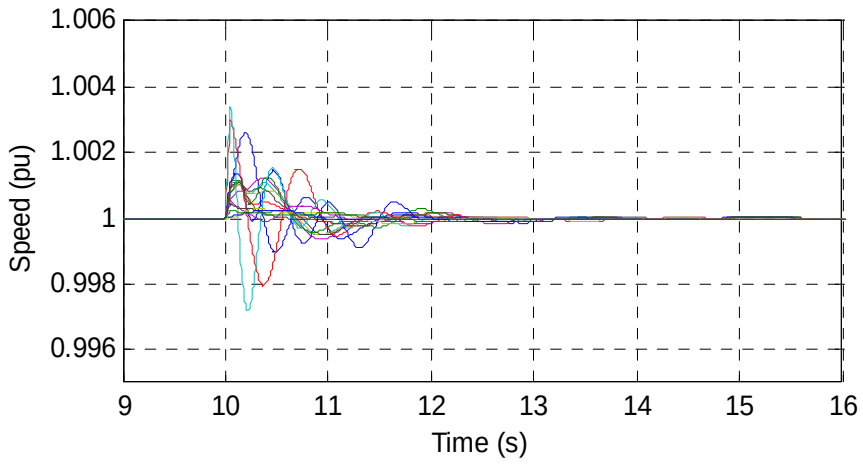

(b)

Figure 2.12. Dynamic response of speed of G1-G16 to a line-to-ground fault. (a) without PSSs, (b) with PSSs.

Furthermore, as for the multi-machine test system with five areas, the power flow in the backbone lines, which play an important role on the network interconnection, can be obtained as shown in Figure 2.13. From this, it can be seen that, the installation of PSSs can improve the system dynamic performance very well, and all the backbone lines can transmit the power stably.

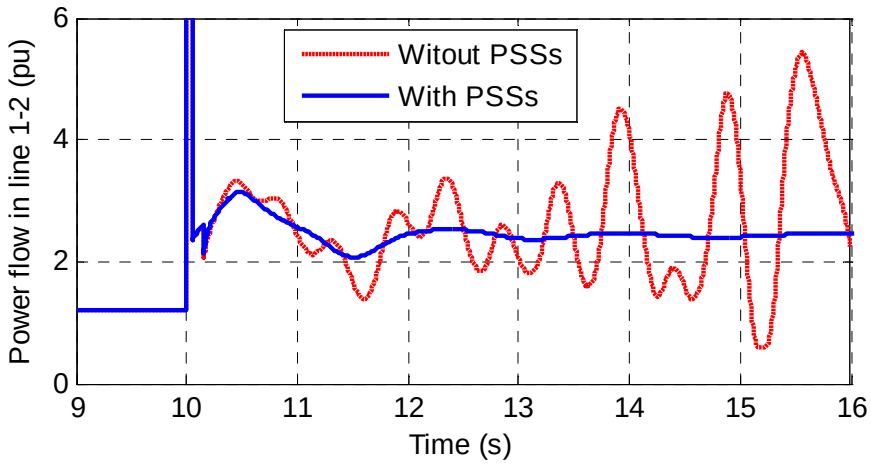

(a)

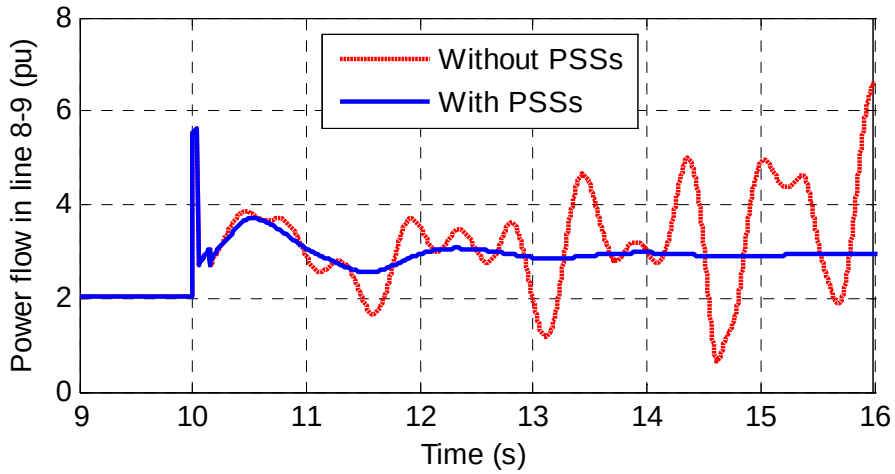
Without PSSs
With PSSs
Power flow in line 8-9 (pu)
Time (s)
0
2
4
6
8
9
10
11
12
13
14
15
16

(b)

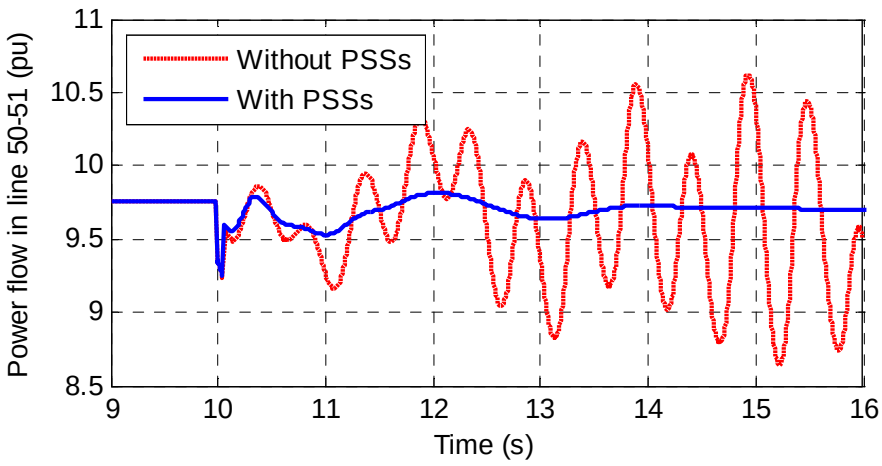
Without PSSs
With PSSs
Power flow in line 50-51 (pu)
Time (s)
8.5
9
9.5
10
10.5
11
9
10
11
12
13
14
15
16

(c)

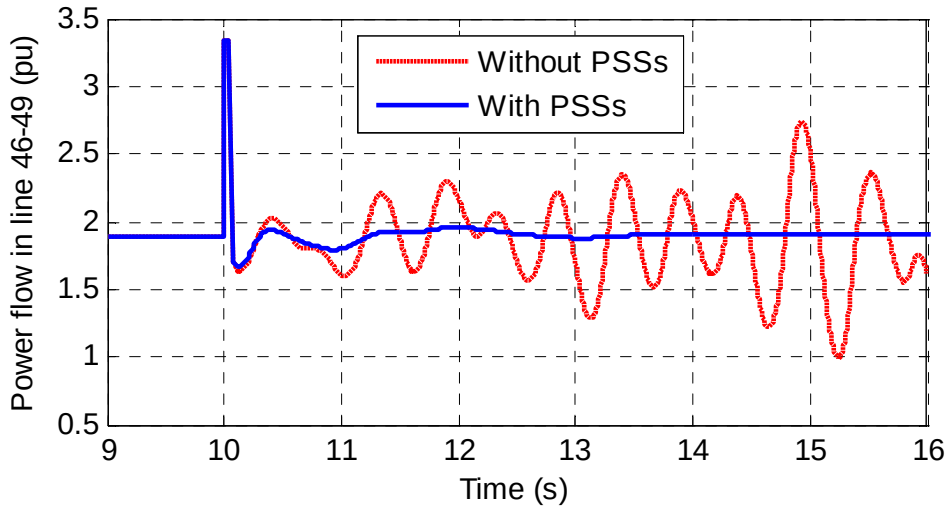

(d)

Figure 2.13 Dynamic response of power flow in the interconnected backbone lines. (a) line 1-2, (b) line 8-9, (c) line 50-51, (d) line 46-49.

2.6 Conclusion

This chapter presents the power system stabilizer with the consideration of local, inter-area, and global mode to damp the potential power oscillation. Based on this, the eigenvalues analysis method has been introduced to analyze the damping effects of various arrangement schemes of such stabilizer. The case study on the typical 4-machines 2-area test system and 16-machines 5-areas shows that although the best arrangement scheme that install the stabilizer for every machine and area can obtain the best oscillation damping effect, it is not the economical solution scheme especial to the large power networks, and the scheme that arrange stabilizer for one area one machine is the optimal arrangement with the consideration of economical factor. This paper has a certain meaning to the optimal stabilizer arrangement for power networks, and the future researches on the arrangement rules with evolutionary algorithm and the coordinated FACTS device to obtain the better power oscillation damping effects could be concerned and performed.

Chapter References

[2-1] **F.R. Schleif, and J. H. White.** *Damping for the northwest-southwest tieline oscillations -an analogue study*. IEEE Trans. Power Appar. Syst., Vol. 85, No. 12, 1239-1247, 1966.

[2-2] **X.P. Zhang, C. Rehtanz, and B. Pal.** *Flexible AC Transmission Systems: Modeling and Control*, Springer, 3540306064, Germany.

[2-3] **S. Ray, and G. K. Venayagamoorthy**. *Real-time implementation of a measurement-based adaptive wide-area control system considering communication delays.* IET Gener. Transm. Distrib., Vol. 2, No. 1, (Jan. 2008), 62-70, 1751-8687, 2008.

[2-4] **I. Kamwa, and R. Grondin.** *PMU configuration for system dynamic performance measurement in large, multiarea power systems.* IEEE Trans. Power Syst., Vol.17, No. 2, 59-69, 0272-1724, 2002.

[2-5] **P. Pourbeik, and M. J. Gibbard.** *Damping and synchronizing torques induced on generators by FACTS stabilizers in multi-machine power systems*. IEEE Trans. Power Syst., Vol.11, No. 4, 1920-1925, 0885-8950, 1996.

[2-6] **P. Pourbeik, and M. J. Gibbard.** *Simultaneous coordination of power system stabilizers and FACTS device stabilizers in a multi-machine power system for enhancing dynamic performance.* IEEE Trans. Power Syst., Vol.13, No. 2, 473-479, 0885-8950, 1998.

[2-7] **R. De Oliveira, R. Ramos, and N. Bretas.** *A mixed procedure based on classical and modern control to design robust damping controllers.* IEEE Trans. Power Syst., Vol. 22, No. 3, 1231-1239, 0885-8950, 2007.

[2-8] **B. C. Pal, A.H. Coonick, and B. J. Cory.** *Robust damping of inter-area oscillations in power systems with superconducting magnetic energy storage devices.* IET Gener. Transm. Distrib., Vol. 146, No. 6, (Nov. 1999), 633-639, 1350-2360, 1999.

[2-9] **P. Kundur.** *Power Stability and Control.* New York: McGraw-Hill, 1994.

[2-10] **G. Rogers.** *Power System Oscillations.* Norwell, MA: Kluwer, 1999.

Chapter 3
Basic Framework and Operating Principle of FACTS Wide Area Damping Control Strategy

3.1 Introduction

With the technical development and cost reduction of power electronics, more and more FACTS devices are being applied into power system especial into modern power system towards to smart grid [3-1] [3-2] [3-3]. FACTS devices can conveniently adjust network parameters (e.g. reactance) flexibly and benefit power flow optimization, transmitted power increase, bus-voltage stability enhancement, and so on. At the same time, with more and more application of synchronized phasor measurement (PMU) technology, WAMS technology are being applied into power system, which is also one obvious technical feature of the coming smart grid [3-4] [3-5] [3-6]. Therefore, it would be wonderful to construct WAMS-based FACTS supplementary wide area damping control strategy, that combines the quick and flexible control ability of FACTS devices and the global monitoring ability of WAMS, to prevent the low frequency oscillation (especial the inter-area oscillation) and enhance the global stability of power system.

In this chapter the basic framework of wide area damping control will be represented, and the operating principle that using the supplementary control function of FACTS device to construct the wide area damping control strategy will be investigated in detail. The delay effect of wide area control signal on the damping performance is also discussed. A case study will be performed to represent the basic system modeling method, the advanced robust control design method, and the basic damping performance that handles with the time delay of wide area signal.

3.2 Wide Area Damping Control Framework

The application of wide area measurement system (WAMS) technology in power system makes it convenient to monitor and transmit system operating variables within global range. Generally, by way of global position system (GPS), optical fiber communication, or other advanced communication technologies, WAMS can perform synchronized measurement and centralized

processing of remote phasor data. Furthermore, to enhance system stability, optimize power flow, increase protection ability, or other positive purpose for operating improvement of power system, it could be possible to utilize the WAMS technology and select remote signal as the feedback control input to implement various wide area control and protection strategies. In this thesis, the wide area damping control is concerned deeply for stability enhancement of power system. Figure 3.1 shows the basic framework that utilizes the main control devices and WAMS to implement wide area damping control strategy.

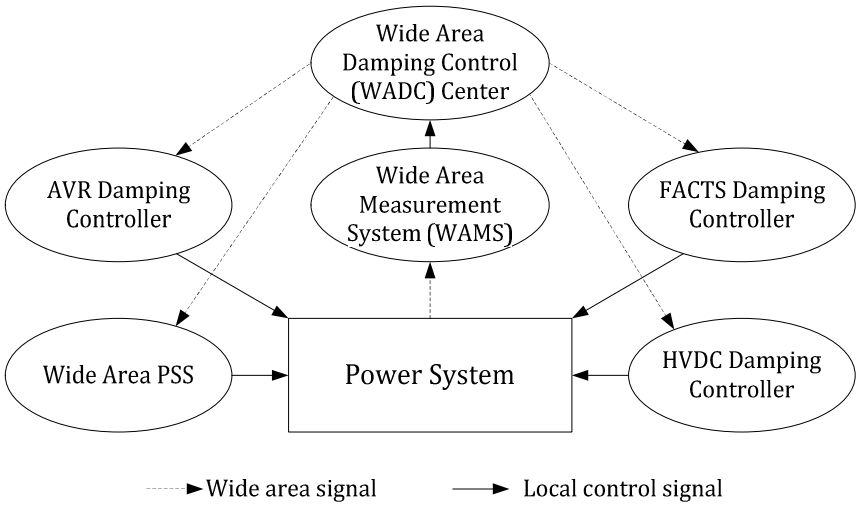

Figure 3.1 Basic framework of wide area damping control

According to Figure 3.1, it can be seen that the framework of wide area damping control basically includes control devices, WAMS, WADC, and power system. The WAMS is used to synchronously measure and process the global operating variables, and at the same time, these processed variables are then submitted to wide area damping control (WADC) center. The WADC center is used to select the suitable control-input signals, and then through the centralized wide area damping controller, it sends the wide-area feedback-control signals to the local control devices. The local control devices, such as FACTS controller, AVR, PSS, HVDC, and so on, receive the corresponding wide area feedback signals and implement the separate supplementary damping control. In the control framework, WADC is a very important part, which mainly includes the choice of wide area control-input signals and the generation of wide area control-output signals. For the WADC design, nowadays there are various design methods that can be utilized to guide the

controller design, such as the classic phase-compensation method [3-7] [3-8], the linear control design method [3-9], the robust design method [3-10] [3-11], and so on.

Furthermore, it should be noted that during the transmission and processing of wide-area signals, there inevitably exists time delays that endanger the practical damping performance. From Figure 3.1, it can be found that the transmission delay mainly includes the following two parts: 1) when the measured signals are transmitted from different areas of power system to WAMS center, the time delays must be generated. 2) Similarly, when the wide area control signals are transmitted from WADC center to local control devices, another time delays are also generated. Besides these, for the wide area signals in both WAMS and WADC center, the signal process inevitably wastes time which also leads to a certain amount of time delays. Many research results show that the time delays even a little time delays may worse or even fail the control performance. However, for the controller design, the conventional design methods mentioned in the above section cannot consider or handle with the delay effect very well. In this thesis, the delay effect is paid the deep attention, and multi-type advanced controller design methods will be proposed to decrease or eliminate the effect of time delay on the wide area damping performance, which will be discussed in the following chapters.

Moreover, as Figure 3.1 shows, various power system control devices can be used to introduce wide area supplementary control-input signal to implement oscillation damping control, such as power system stabilizer (PSS), automatic voltage regulator (AVR), control devices of flexible ac transmission system (FACTS) and high-voltage direct current (HVDC) transmission system, and so on. In practice, the choice of wide area control device should comprehensively consider the practical control performance, the investment cost, and other potential factors. In this thesis the FACTS devices are used to implement wide area damping control strategy. Because that compare with PSS and AVR, FACTS devices are convenient to perform centralized control, and they can also play effective damping role on critical inter-area oscillation modes. For AVR and PSS, both of them are associated to generator located in different area of power system, and they are usually designed to damp local oscillation modes related to their associated generators. In such a case, if they are used to perform wide area control strategy, the coordination of various AVR or PSS associated to various generators, and the damping effect on both local and inter-area oscillation modes, should be considered carefully. In addition, with more and more application of FACTS devices in power

system, it changes more and more convenient to use their supplementary control functions and implement wide area damping on inter-area oscillation among different areas, and at the same time, PSS and AVR can keep on effective damping on local oscillation related to their associated generators.

3.3 Operating Principle of FACTS Wide Area Damping Control

In essence the purpose of FACTS wide area damping control is to shift all the system eigenvalues into the left hand side of the *S*-plane, so that the needed minimum damping ratio can be satisfied and the system damping can be increased into the acceptable level. The operating principle on system damping increase by means of FACTS wide area damping control can be revealed through the simplified wiring diagram of single-machine infinite-bus (SMIB) system installed with FACTS device, as shown in Figure 3.2. In this SMIB system, one shunt-type FACTS device (e.g. SVC, STATCOM) is installed at the middle of the transmission line.

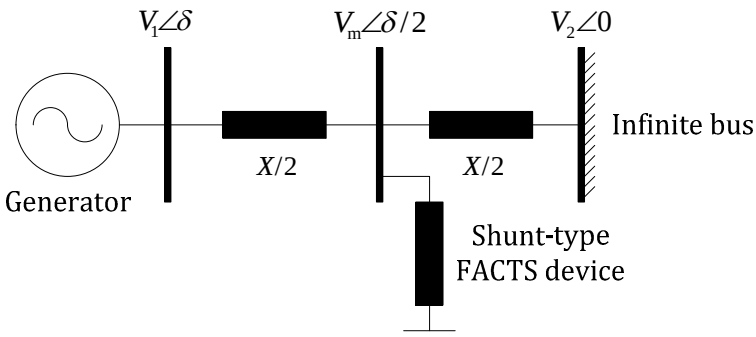

Figure 3.2 Simplified wiring diagram of single-machine infinite-bus (SMIB) system with FACTS device

According to Figure 3.2, the magnitude value of the buses can be expressed as:

$$\begin{cases} V_1 = |V_1|\sin(\omega t + \delta) \\ V_2 = |V_2|\sin \omega t \\ V_m = |V_m|\sin(\omega t + \delta/2) \end{cases} \tag{3.1}$$

The electromagnetic power of the generator can be written as:

$$P_E = \frac{2VV_m}{X}\sin\frac{\delta}{2} \tag{3.2}$$

The increment equation of the generator electrical power can be obtained by linearizing the above equation, that is:

$$\Delta P_E = \frac{\partial P_E}{\partial V}\Delta V + \frac{\partial P_E}{\partial V_m}\Delta V_m + \frac{\partial P_E}{\partial \delta}\Delta\delta \tag{3.3}$$

Assume that the bus voltage associated to the generator keeps on constant, then combine the rotor motion equation of generator, the above equation can be further expressed as:

$$M\frac{d^2(\Delta\delta)}{dt^2} + \frac{\partial P_E}{\partial V_m}\Delta V_m + \frac{\partial P_E}{\partial \delta}\Delta\delta = 0 \tag{3.4}$$

Because that the installed FACTS device can control the voltage of the associated bus, if the bus voltage is controlled as the following functional relationship:

$$\Delta V_m = K\frac{d(\Delta\delta)}{dt} \tag{3.5}$$

where K is a constant value.

Then the increment equation (3.4) can be further rewritten as:

$$M\frac{d^2(\Delta\delta)}{dt^2} + \left.\frac{\partial P_E}{\partial V_m}\right|_0 K\frac{d(\Delta\delta)}{dt} + \left.\frac{\partial P_E}{\partial \delta}\right|_0 \Delta\delta = 0 \tag{3.6}$$

According to the above equation, the system damping can be represented as:

$$2\zeta = \frac{K}{M}\frac{\partial P_E}{\partial V_m} \tag{3.7}$$

Beside the voltage stability control that FACTS device can benefit for power system, from the above equation, it can be also seen that the application of FACTS device can also provide a certain positive damping, and such technical feature is advantage to develop oscillation damping control through

introducing supplementary wide area damping signal for FACTS controller. Figure 3.3 represents the general configuration.

As Figure 3.3 shows, the wide area damping controller (WADCer) is in fact the supplementary controller of local FACTS controller, and there is the supplementary wide area control-output as one part of the control-input of the local FACTS controller. The WAMS is in charge of collection, transmission, and processing wide area signals through a cluster of PMUs located in different areas of power system. Combining Figure 3.1 and the related analysis, the WAMS center sends the processed wide area signals to WADC center. Following this the WADC center further analyzes these wide area signals and selects the suitable wide area signal as the control-input of WADCer. The WADCer is in charge of generating an effective wide area control-output that can provide enhanced damping through the simultaneous action of local FACTS controller and WADCer on the power system with FACTS device.

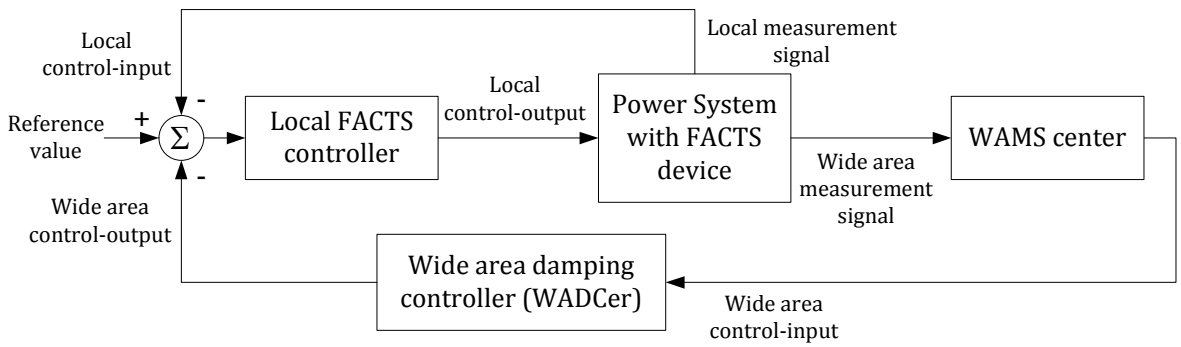

Figure 3.3 General configuration of FACTS wide area damping control

3.4 System Modeling

3.4.1 SMIB System with FACTS WADCer

The single line diagram of SMIB system with shunt-type FACTS device (SVC) is shown more in detail in Figure 3.4. As Figure 3.4 shows, there are two kinds of control-input signals for the SVC controller with WADCer. One is the wide area signal transmitted from the remote generator, that is the rotor angle in electrical degree δ and angular velocity ω of the remote generator, and another is the local signal measured from the bus shunted with SVC device, that is, the bus voltage V_s. The

control target of the SVC controller with WADCer is to damp the system power oscillation through wide area damping control, and in the meantime to maintain the stability of the local bus voltage.

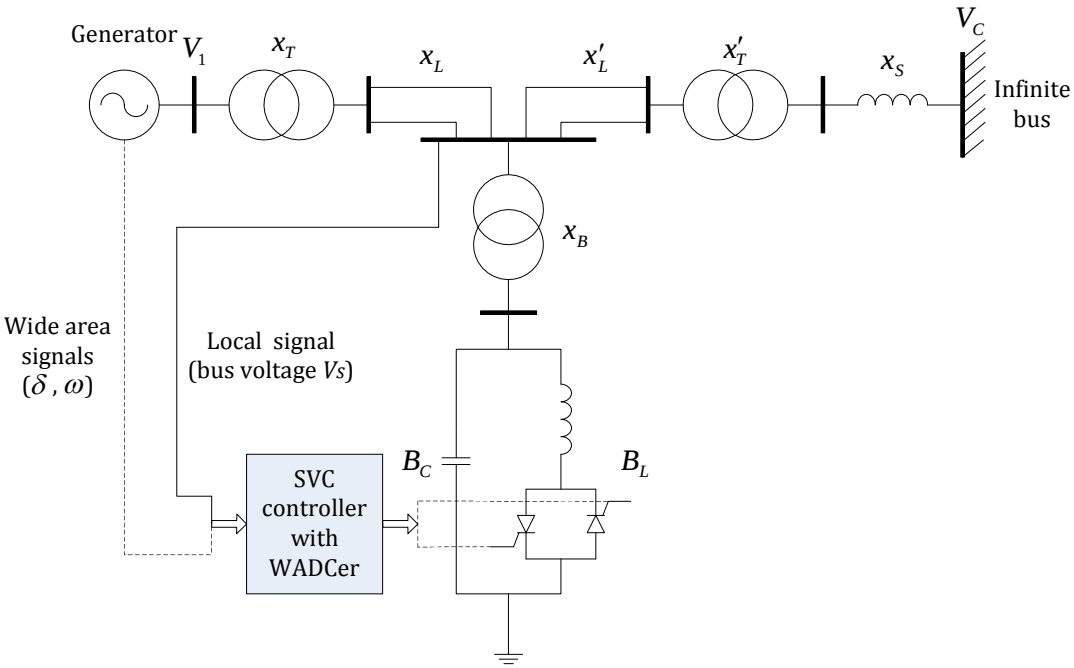

Figure 3.4 Single line diagram of SMIB system with SVC device

3.4.2 System Modeling Based on Direct Feedback Linearization (DFL) Theory

For the controller design, the system model that can reflect the small signal stability of the test system should be obtained in advance. In this chapter, the direct feedback linearization (DFL) theory[3-12] [3-13] is presented to perform the system modeling.

According to the electrical connection diagram shown in Figure 3.4, the equivalent circuit diagram of the SMIB system can be established as shown in Figure 3.5, in which, E expresses the transient voltage of the generator; x_1 and x_2 express the equivalent reactance of the sending and the receiving end, respectively; and $x_1 = x_d' + x_T + x_L$, $x_2 = x_L' + x_T' + x_S$, where x_d' expresses the d-axis transient reactance of the equivalent generator, x_T and x_T' express the equivalent leakage reactance of the transformers of the sending and the receiving end, respectively; x_L and x_L' express the equivalent

reactance of the transmission line divided by the shunted SVC device, and x_S expresses the system equivalent reactance; B_{SVC} expresses the equivalent susceptance of the SVC, and $B_{SVC}=B_C+B_L$, where, B_C and B_L express the equivalent susceptance of the mechanically switched capacitor (MSC) and the thyristor controlled reactor (TCR), respectively.

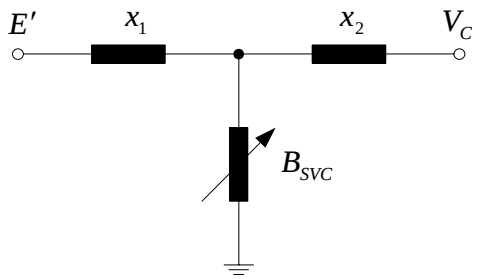

Figure 3.5 Equivalent circuit diagram of SMIB system with SVC device

Assume that the generator is expressed by second-order model, that is, E' is kept constant, and the mechanical power P_m of the generator is also kept constant, then, the state equation of the above system can be obtained as follows:

$$\begin{cases} \Delta\dot{\delta} = \omega - \omega_0 \\ \Delta\dot{\omega} = -D(\omega - \omega_0)/H + \omega_0(P_m - P_e)/H \\ \Delta\dot{B}_L = (-B_{\mathrm{SVC}} + B_{\mathrm{SVC0}} + K_C u_B)/T_C \end{cases} \tag{3.8}$$

where

$$P_e = \frac{E'V_C}{x_1 + x_2 + x_1 x_2 B_{SVC}} \sin\delta \tag{3.9}$$

in which, ω_0 expresses the synchronous speed, and $\omega_0=2\pi f_0$; P_e expresses the electromagnetic power; D and H express the damping coefficient and the inertia time constant of the generator, respectively; K_C and T_C express the magnification times and the inertia time constant of the adjustable system of the SVC, respectively; V_C expresses the infinite bus voltage; and the other parameters are as the mentioned above.

In order to ensure the voltage stability of the bus shunted with SVC device, the additional state variable about the local bus voltage should be introduced according to internal model control, that is:

$$\Delta V_S = \int (V_S - V_{S0})dt \tag{3.10}$$

The additional voltage state variable can be expressed as:

$$\Delta \dot{V}_S = V_S - V_{S0} \tag{3.11}$$

where

$$V_S = \frac{\sqrt{(x_2 E')^2 + (x_1 V_C)^2 + 2x_1 x_2 V_C E' C \cos\delta}}{x_1 + x_2 + x_1 x_2 B_{SVC}} \tag{3.12}$$

Combining the above equation with Equation (3.9), the following equation can be obtained:

$$V_S = \frac{\sqrt{(x_2 E')^2 + (x_1 V_C)^2 + 2x_1 x_2 V_C E' C \cos\delta}}{E' V_C \sin\delta} P_e \tag{3.13}$$

Because the voltage control could be considered near the operational point, $\Delta \dot{V}_S$ can be further obtained by the method of Taylor Series Expansion:

$$\Delta \dot{V}_S = \frac{\partial V_S}{\partial \delta} \Delta\delta \Big|_0 + \frac{\partial V_S}{\partial P_e} \Delta P_e \Big|_0 = S_\delta \Delta\delta + S_{P_e} \Delta P_e \tag{3.14}$$

If we select the following equation as the virtual controllers:

$$\Delta \dot{P}_e = P_m - P_e = P_m - \frac{E' V_C}{x_1 + x_2 + x_1 x_2 B_{SVC}} \sin\delta \tag{3.15}$$

Then, following the direct feedback linearization (DFL) theory, by combining Equation (3.8) with the above Equations (3.14) and (3.15), the initial linearized state equation can be obtained as:

$$\dot{x}(t) = Ax(t) + B_1 u(t) \tag{3.16}$$

where

$$A=\begin{bmatrix} 0 & \omega_0 & 0 & 0 \\ 0 & -\dfrac{D}{H} & \dfrac{\omega_0}{H} & 0 \\ 0 & 0 & 0 & 0 \\ S_\delta & 0 & S_{P_e} & 0 \end{bmatrix},\ B_1=\begin{bmatrix} 0 \\ 0 \\ 1 \\ 0 \end{bmatrix}.$$

The above equation is the linearized model of SMIB system with SVC device, which can be used for the robust linear design of SVC local controller with WADCer in next chapters.

3.5 Conclusion

In this chapter, the overall framework of wide area damping control is presented and analyzed briefly. Based on such framework, the control concept that utilizes the flexible and quick control feature of FACTS device to implement the WAMS-based wide area damping control is described in detail. The operating principle of FACTS wide area damping control is presented by studying a SMIB system with shunt-type FACTS device, which indicates that FACTS device can not only achieve local control strategy (e.g. bus voltage stability, power flow control) but also realize the oscillation damping through wide area control strategy. Such damping performance is achieved by enhancing system damping ratio through introducing the suitable wide area control-input. Furthermore, the general configuration of FACTS wide area damping control is presented, which is advantage to guide the control design represented in the following chapters. Finally, the system linearized modelling method (direct feedback linearization, DFL) are described.

Chapter References

[3-1] **A. Bose.** *New smart grid applications for power system operations.* IEEE Power and Energy Society General Meeting, 2010.

[3-2] **M. Zarghami, M.L. Crow, and S. Jagannathan.** *Nonlinear control of FACTS controllers for damping interarea oscillations in power systems.* IEEE Transactions on Power Delivery. Vol. 25, No. 4, pp. 3113-3123, Oct. 2010.

[3-3] **R. Eriksson and L. Soder.** *Wide-area measurement system-based subspace identification for obtaining linear models to centrally coordinate controllable devices.* IEEE Transactions on Power Delivery. Vol. 26, No. 2, pp. 988-997, Apr. 2011.

[3-4] **A. Bose.** *Smart transmission grid applications and their supporting infrastructure.* IEEE Transactions on Smart Grid. Vol. 1, No. 1, pp. 11-19, June 2010.

[3-5] **J. De La Ree, V. Centeno, J.S. Thorp, and A.G. Phadke.** S*ynchronized phasor measurement applications in power systems.* IEEE Transactions on Smart Grid. Vol. 1, No. 1, pp. 20-27, June 2010.

[3-6] **A. Chakrabortty, J.H. Chow, and A. Salazar.** *A measurement-based framework for dynamic equivalencing of large power systems using wide-area phasor measurements.* IEEE Transactions on Smart Grid. Vol. 2, No. 1, pp. 68-81, March 2011.

[3-7] **F.P. Demello and C. Concordia.** *Concepts of synchronous machine stability as affected by excitation control.* IEEE Transactions on Power Apparatus and Systems. Vol. 88, No. 4, pp. 316-329, 1969.

[3-8] **L.J. Cai and I. Erilich.** *Simultaneous coordinated tuning of PSS and FACTS damping controllers in large power systems.* IEEE Transactions on Power Systems. Vol. 20, No. 1, pp. 294-300, 2005.

[3-9] **R. Gupta, B. Bandyopadhyay, and A.M. Kulkarni.** *Power system stabiliser for multimachine power system using robust decentralised periodic output feedback.* IEE Proceedings of Control Theory Application. Vol. 152, No. 1, pp. 3-8, Jan. 2005.

[3-10] **Y. Zhang and A. Bose.** *Design of wide-area damping controllers for interarea oscillations.* IEEE Transactions on Power Systems. Vol. 23, No. 3, pp. 1136-1143, 2008.

[3-11] **R. Kutzner, B. Scholz, and M. Reimann.** *An advanced model-based approach to stabilize power system oscillations based on the H-infinite theory modelling and tuning guide, practical experience.* IEEE Power Engineering Society General Meeting, 2003.

[3-12] **C.L. Zhu, R.J. Zhou, and Y.Y. Wang.** *A new decentralized nonlinear voltage controller for multimachine power systems.* IEEE Transactions on Power Systems. Vol. 13, No. 1, pp. 211-216. Feb. 1998.

[3-13] **S.V. Grcar, S. V. J. Kumar, and N. Yadaiah.** *Control strategies for transient stability of multimachine power systems-a comparison.* IEEE International Conference on Power System Technology,2004.

Chapter 4
FWMs Approach Based FACTS Wide Area Damping Control with Considering Signal Time Delay

4.1 Chapter Introduction

With the rapid growth of electric power systems and the increasing needs for the multi-area power networks, the inter-area oscillation become a serious hazard since it may cause power system unstable or blackout. Lots of measurements has been taken to damp the inter-area oscillation in multi-area power networks. Especial for the FACTS devices based on power oscillation damping (POD) control, it has aroused widespread attention, and some kinds of FACTS devices with such POD control function have been applied into the transmission fields successfully [4-1] [4-2]. But the conventional FACTS POD control usually utilizes only local signals such as bus voltage, line active power, and so on, which limits the oscillation damping effects on some operating conditions. So the research on the WAMS-based FACT POD control strategies has aroused more and more concerns in recent years [4-3] [4-4] [4-5]. As said in the previous chapters, as for the wide-area control, the negative effects of the unavoidable time-delay can not be ignored.

In this chapter, in order to improve the power system damping and robustness for the FACTS device, a free-weighting matrices (FWMs) approach based Lyapunov functional stability theory is proposed to design the FACTS WADCer, which can consider efficiently the effect of signal delay on the control performance. The FWMs approach will be described and the detail nonlinear simulations on two typical test systems will be performed to evaluate the performance of the proposed SVC-type FACTS WADCer.

4.2 Description of Free-Weighting Matrices (FWMs) Approach

Research on the stability of time-delay systems began in the 1950s, including frequency-domain approaches and time-domain methods. Figure 4.1 gives an overall picture of the research on the stability of time delay systems, such as

$$\begin{cases} \dot{x}(t) = Ax(t) + Bx(t-h) + Cu(t) \\ x(t) = \phi(t) \end{cases} \tag{4.1}$$

in which A, B, and C are the constant real matrices with appropriate dimensions. h is the time delay. u(t) is the input single. $\phi(t)$ is the initial condition.

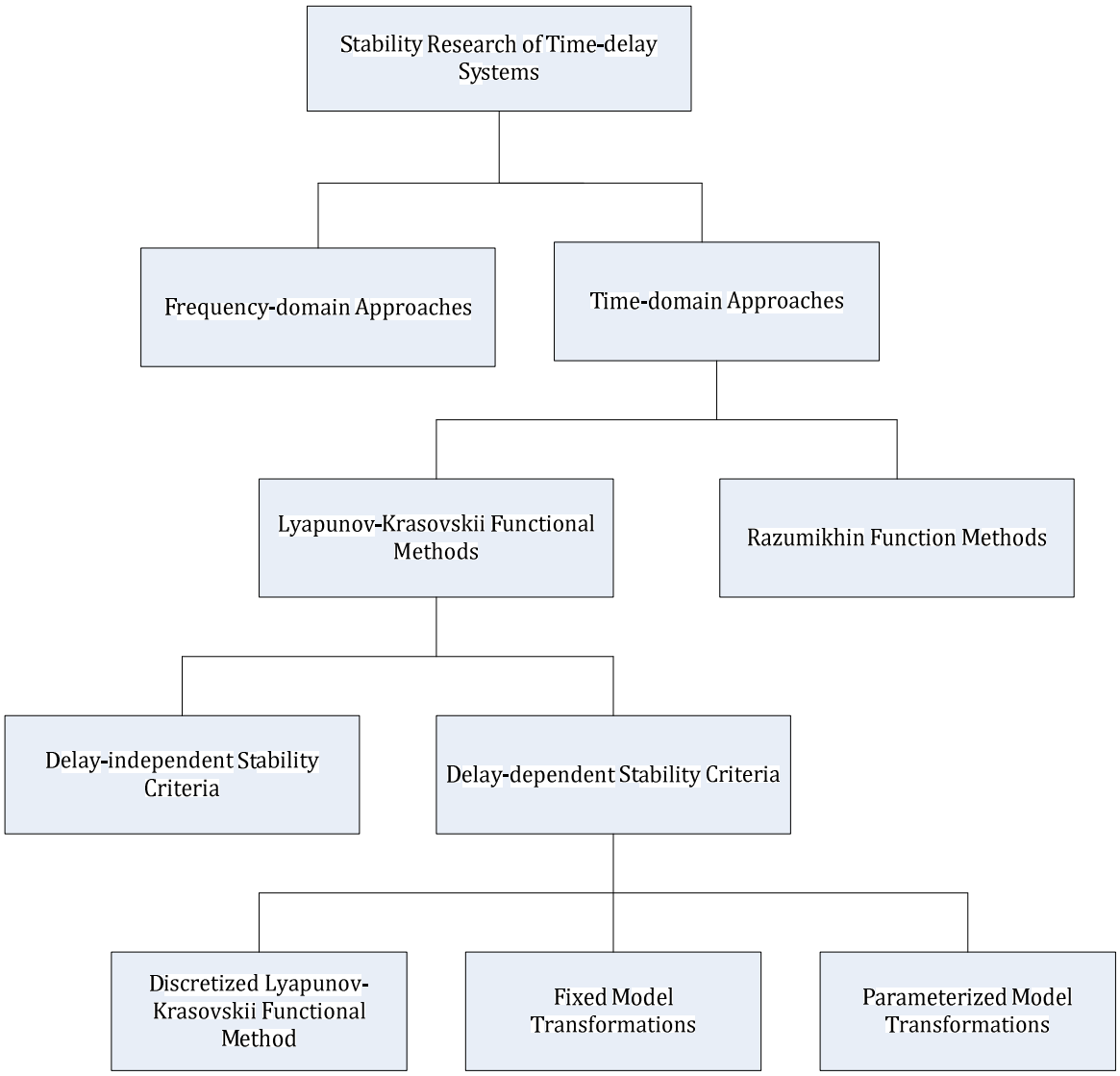

Figure 4.1 General stability research methods of typical time delay system

About frequency-domain approaches, it determines the stability of a system from the distribution of the roots of its characteristic equation or from the solutions of a complex Lyapunov matrix function equation. If and only if $f(\lambda) = \det(\lambda I - A - Be^{-h\lambda}) = 0$ have negative real part, the time delay system (4.1) is stable. Since this equation is transcendental, it is difficult to solve. So the time-

domain methods are very important in the stability analysis of linear systems. Among them, two classes of sufficient conditions have received lots of attention: delay-dependent criteria and delay-independent criteria. Since the delay-dependent stability criteria make use of information on the size of delay, while the delay-independent stability criteria do not include such information, the delay-dependent conditions are generally less conservative than the delay-independent ones especially when the time delays are small.

So far, three methods of studying delay-dependent problems have been devised: the discretized Lyapunov-Krasovskii functional method, fixed model transformations, and parameterized model transformations. The discretized Lyapunov functional method [4-6] [4-7] [4-8] is one of the most efficient among them, but it is difficult to extend to the synthesis of a control system. Another method involves a fixed model transformation, which expresses the delay term in terms of an integral. Four basic model transformations have been proposed [4-9]. Combined with Park's or Moon et al.'s inequalities [4-10], the descriptor model transformation method is the most efficient [4-9], [4-11] [4-12]. However, there is room for further investigation.

Recently, the proposed a free-weighting matrices (FWMs) approach based on the Lyapunov functional stability theory to handle with the stability/stabilization problem for many kinds of time-delay system and many advantageous results are obtained [4-13] [4-14] [4-15]. For the controllers' design problems, FWMs approach can reduce the conservativeness of the designed controller compared with the conventional fixed model transformations methods. That is as for the fixed model transformations, when calculating the derivative of Lyapunov function, some inequalities such as Park and Moon have to be used to estimate the upper bound of cross product terms. Different from this, when using FWMs approach to handle with the delay-dependent stability problem, the bounding techniques on some cross product terms don't need to be involved.

The well-used Lyapunov functional has the following form:

$$V(t,x_t) = x^T(t)Px(t) + \int_{t-h}^{t} x^T(s)Qx(s)ds + \int_{-h}^{0}\int_{t+\theta}^{t} \dot{x}^T(s)Z\dot{x}(s)dsd\theta \tag{4.2}$$

where, the first and second terms of Lyapunov functional can be viewed as things like the kinetic and potential energy of a mechanical system, and the third term is introduced to make the derivation simple. $P = P^T$, $Q = Q^T$, $Z = Z^T$ are to be determined. Then calculate the derivative of Lyapunov functional in (4.2):

$$\dot{V}(x_t) = \dot{x}^T(t)Px(t) + x^T(t)P\dot{x}(t) + x^T(t)Qx(t) - x^T(t-h)Qx(t-h) + h\dot{x}^T(t)Z\dot{x}(t) - \int_{t-h}^{t} \dot{x}^T(s)Z\dot{x}(s)ds \tag{4.3}$$

In order to obtain the LMIs-based stability criteria, by employing the conventional fixed model transformations and Lyapunov stability theorem, it usually added the right side of the following terms into the derivative of $V(t, x_t)$ in (4.3):

$$0 = 2x^T(t)PB[x(t) - x(t-\tau) - \int_{t-\tau}^{t} \dot{x}(s)ds] \tag{4.4}$$

where, B is coefficient matrix and P is Lyapunov matrix.

From this, it is obvious to see that as for the conventional solutions such as fixed model transformations, when we solve the inequalities which ensure $\dot{V}(x_t) < 0$, B and P have to be adjusted and they cannot be selected freely, which is the serious limitation for the conventional solutions.

However, in order to reduce the conservativeness, when we dealt with the derivative of Lyapunov functional in (4.2), we employed two new free-weighting matrices M and N, to explain the relationship between the New-Leibniz formula instead of P and B, which can be called free-weighting matrices (FWMs) approach.

So in the process of derivative calculation of (4.3), it equals to add the following right sides of Eq.(4.5) into $\dot{V}(x_t)$, then we can also obtain some LMIs inequalities to ensure $\dot{V}(x_t) < 0$. From this, it can be seen for FWMs approach, it needn't to select B and P, and just to optimize M and N by solving LMIs. So, the FWMs approach can reduce the conservativeness of the controller to the time-delay system. In the next Section 4.4, we will describe the solving process by FWMs approach in detail.

$$0 = [x^T(t)M + \dot{x}^T(t)N][x(t) - x(t-\tau) - \int_{t-\tau}^{t} \dot{x}(s)ds] \tag{4.5}$$

4.3 General Configuration of FACTS-WADCer Based on FWMs Approach

The concept on FACTS-WADCer can be described through Figure 4.2, which shows one power systems installed with SVC-type FACTS device and its supplementary wide-area robust damping controller. As Figure 4.2 shows, the closed-loop feedback control formed by SVC-type FACTS-WADCer can be used to damp the potential power oscillations. For the wide-area robust damping

controller, its control input signals select the operating variables from global range of power systems, and such selection can be performed based on small signal analysis (SSA) or other methods [4-16]. In addition, the application of WAMS for the transmission of the wide-area control signals inevitably causes time delay, thus, a power system with WAMS application is in essence a typical time-delay system. In this chapter, the first-order Pade approximation is used to model the time-delay characteristic of the wide-area control signals. Meanwhile, the high-pass and the low-pass filters (HPF and LPF) are necessary to process the control-input signals with the purpose of retaining the concerned oscillation frequency information.

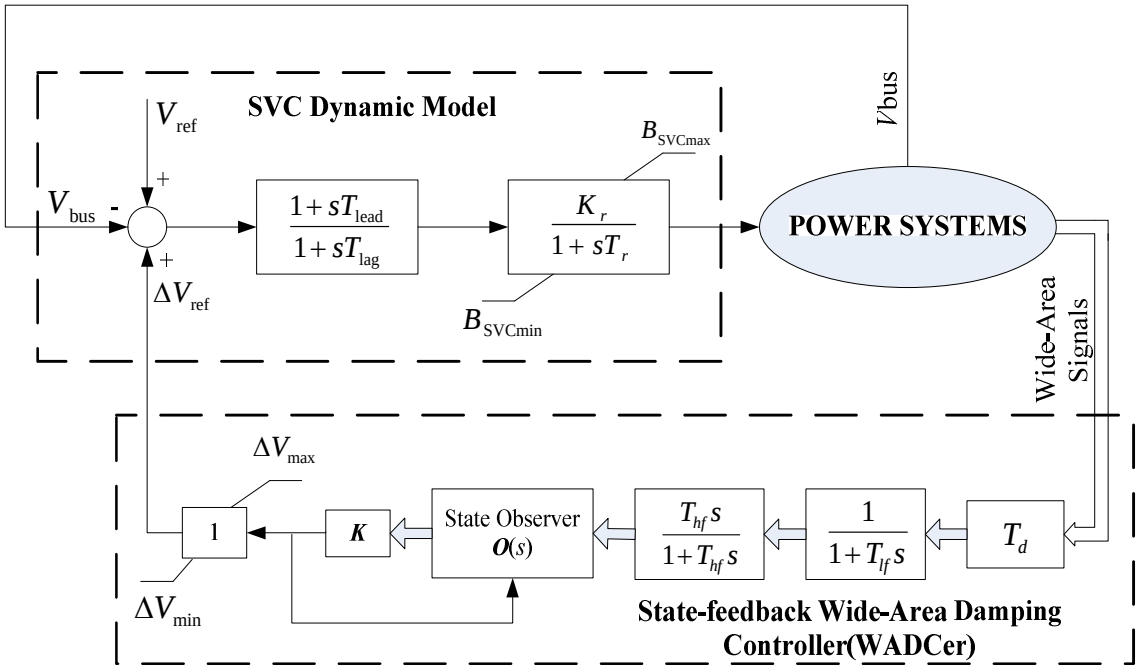

Figure 4.2 Control block diagram of SVC-type FACTS device with state-feedback WADCer

Furthermore, for the robust wide-area FACTS damping controller, the extremely important part is the state-feedback control gain matrix K, which can be optimally designed by employing the proposed FWMs approach. In addition, the designed K is the gain matrix for the state variables. However, the operating state variables cannot be completely observed very well for the practical system, thus, the state observer O(s) is introduced to implement the observation on the state variable. In this chapter, the practical pole-placement method is used to design the O(s), and the structure of O(s) will be also given in next section.

4.4 FWMs Approach Based FACTS-WADCer Design

In Chapter 3, the power system model, which includes generators, loads, various controllers, FACTS devices, etc, is described using a set of differential-algebraic equations [4-17] [4-18]. In this way, the open-loop system model can be modeled, which uses the output of the FACTS supplementary control as the input and while the wide-area control signals as the output of the open-loop power system. Furthermore, when the time-delay τ is considered as the transmission delay of the control input of the FACTS wide-area robust damping controller, then the general linearized power system model can be modified as follows

$$\begin{cases} \dot{x}(t) = Ax(t) + Bu(t) \\ y(t) = Cx(t) \end{cases} \tag{4.6}$$

where, A is the state matrix, B is the input matrix, and C is the output matrix.

The state-feedback controller that will be designed can be simplified as follows:

$$u(t) = Kx(t-\tau) \tag{4.7}$$

Then the closed-loop model constructed by open-loop model (4.6) and FACTS-WADCer (4.7) can be written as:

$$\begin{cases} \dot{x}(t) = Ax(t) + BKx(t-\tau) \\ y(t) = Cx(t) \end{cases} \tag{4.8}$$

The objective of this section is to develop a new delay-dependent stabilization criterion that provides the optimal controller gain K and time-delay h （$h = \max(\tau)$）, such that the resulting closed-loop system (4.8) is asymptotically stable. For this purpose, the following lemmas will be employed in the proofs of our results. And the notion $*$ stands for the symmetric matrix.

Lemma (Schur complement) [4-19]: Given a symmetric matrix $S = S^T = \begin{bmatrix} S_{11} & S_{12} \\ S_{12}^T & S_{22} \end{bmatrix}$ ($S_{11} \in \Re^{r\times r}$), the following three conditions are equal.

(1) $S < 0$

(2) $S_{11} < 0, S_{22} - S_{12}^T S_{11}^{-1} S_{12} < 0$

(3) $S_{22} < 0, S_{11} - S_{12} S_{22}^{-1} S_{12}^T < 0$

Theorem: For given scalar *h*, there exists a state-feedback controller of (4.7) such that the closed-loop system (4.8) is asympotically stable if there exist $L = L^T > 0$, $Q_1 = Q_1^T > 0,\ R = R^T > 0$, $Y = \begin{bmatrix} Y_{11} & Y_{12} \\ Y_{12}^T & Y_{22} \end{bmatrix} \geq 0$ and any appropriately dimensioned matrices M_1, M_2 and *V*, such that the following matrix inequalities are feasible.

$$\bar{\Phi} = \begin{bmatrix} AL + LA^T + M_1 + M_1^T + Q_1 + hY_{11} & BV - M_1 + M_2^T + hY_{12} & hLA^T \\ * & -M_2 - M_2^T - Q_1 + hY_{22} & hV^T B^T \\ * & * & -hR \end{bmatrix} < 0 \tag{4.9}$$

$$\bar{\Psi} = \begin{bmatrix} Y_{11} & Y_{12} & M_1 \\ * & * & M_2 \\ * & * & LR^{-1}L \end{bmatrix} > 0 \tag{4.10}$$

Moreover, the feedback controller gain is $K = VL^{-1}$.

Proof: It is clear from Newton-Leibniz formula that

$$x(t) - x(t-\tau) - \int_{t-\tau}^{t} \dot{x}(s)ds = 0 \tag{4.11}$$

So from Eq.(4.11), for any appropriately dimensioned matrices N_1 and N_2, the following equation is true:

$$0 = 2(x^T(t)N_1 + x^T(t-\tau)N_2)[x(t) - x(t-\tau) - \int_{t-\tau}^{t} \dot{x}(s)ds] \tag{4.12}$$

On the other hand, for any semi-positive definite matrix $X = \begin{bmatrix} X_{11} & X_{12} \\ X_{12}^T & X_{22} \end{bmatrix} \geq 0$, the following equation holds:

$$h\xi^T(t)X\xi(t)-\int_{t-\tau}^{t}\xi^T(t)X\xi(t)ds>0 \tag{4.13}$$

where $\xi(t)=[x^T(t),\ x^T(t-\tau)]^T$

Construct the following Lyapunov candidate function:

$$V(x_t)=x^T(t)Px(t)+\int_{t-\tau}^{t}x^T(s)Qx(s)ds+\int_{-h}^{0}\int_{t+\theta}^{t}\dot{x}^T(s)Z\dot{x}(s)dsd\theta \tag{4.14}$$

Where $P=P^T>0$, $Q=Q^T>0,\ Z=Z^T>0$ are to be determined.

Calculating the derivatives of $V(x_t)$ defined in (4.14) along the trajectories of system (4.8) yields:

$$\begin{aligned}
\dot{V}(x_t)&=\dot{x}^T(t)Px(t)+x^T(t)P\dot{x}(t)+x^T(t)Qx(t)-x^T(t-\tau)Qx(t-\tau)+h\dot{x}^T(t)Z\dot{x}(t)-\int_{t-h}^{t}\dot{x}^T(s)Z\dot{x}(s)ds\\
&=x^T(t)[PA+A^TP]x(t)+2x^T(t)PBKx(t-\tau)+x^T(t)Qx(t)-x^T(t-\tau)Qx(t-\tau)\\
&\quad+h[Ax(t)+BKx(t-\tau)]^TZ[Ax(t)+BKx(t-\tau)]-\int_{t-h}^{t}\dot{x}^T(s)Z\dot{x}(s)ds\\
&=x^T(t)[PA+A^TP+hA^TZA+Q+hX_{11}+N_1+N_1^T]x(t)+x^T(t)[PBK+hA^TZBK-N_1+N_2^T+hX_{12}]x(t-\tau)\\
&\quad+x^T(t-\tau)[PBK+hA^TZBK-N_1+N_2^T+hX_{12}]^Tx(t)+x^T(t-\tau)[-N_2-N_2^T-Q+hX_{22}+hK^TB^TZBK]x(t-\tau)\\
&\quad-\int_{t-\tau}^{t}[\dot{x}^T(s)Z\dot{x}(s)+\xi^T(t)X\xi(t)+2(x^T(t)N_1+x^T(t-\tau)N_2)\dot{x}(s)]ds
\end{aligned}$$

Then adding the terms on the right of equations (4.12) and (4.13) to $\dot{V}(x_t)$, it becomes

$$\begin{aligned}
\dot{V}(x_t)&\le x^T(t)[PA+A^TP]x(t)+2x^T(t)PBKx(t-\tau)+x^T(t)Qx(t)-x^T(t-\tau)Qx(t-\tau)\\
&\quad+h[Ax(t)+BKx(t-\tau)]^TZ[Ax(t)+BKx(t-\tau)]-\int_{t-\tau}^{t}\dot{x}^T(s)Z\dot{x}(s)ds\\
&\quad+h\xi^T(t)X\xi(t)-\int_{t-\tau}^{t}\xi^T(t)X\xi(t)ds+2(x^T(t)N_1+x^T(t-\tau)N_2)[x(t)-x(t-\tau)-\int_{t-\tau}^{t}\dot{x}(s)ds]\\
&=x^T(t)[PA+A^TP]x(t)+2x^T(t)PBKx(t-\tau)+x^T(t)Qx(t)-x^T(t-\tau)Qx(t-\tau)\\
&\quad+h[Ax(t)+BKx(t-\tau)]^TZ[Ax(t)+BKx(t-\tau)]\\
&\quad+h\xi^T(t)X\xi(t)+2(x^T(t)N_1+x^T(t-\tau)N_2)[x(t)-x(t-\tau)]\\
&\quad-\int_{t-\tau}^{t}\dot{x}^T(s)Z\dot{x}(s)ds-\int_{t-\tau}^{t}\xi^T(t)X\xi(t)ds-2(x^T(t)N_1+x^T(t-\tau)N_2)\int_{t-\tau}^{t}\dot{x}(s)ds
\end{aligned}$$

$$
\begin{aligned}
&= x^T(t)[PA + A^T P + hA^T ZA + Q + hX_{11} + N_1 + N_1^T]x(t) + x^T(t)[PBK + hA^T ZBK - N_1 + N_2^T + hX_{12}]x(t-\tau) \\
&\quad + x^T(t-\tau)[PBK + hA^T ZBK - N_1 + N_2^T + hX_{12}]^T x(t) + x^T(t-\tau)[-N_2 - N_2^T - Q + hX_{22} + hK^T B^T ZBK]x(t-\tau) \\
&\quad - \int_{t-\tau}^{t} [\dot{x}^T(s)Z\dot{x}(s) + \xi^T(t)X\xi(t) + 2(x^T(t)N_1 + x^T(t-\tau)N_2)\dot{x}(s)]ds \\
&= \begin{bmatrix} x(t) \\ x(t-\tau) \end{bmatrix}^T \begin{bmatrix} PA + A^T P + Q + hX_{11} + N_1 + N_1^T + hA^T ZA & PBK - N_1 + N_2^T + hX_{12} + hA^T ZBK \\ * & -N_2 - N_2^T - Q + hX_{22} + hK^T B^T ZBK \end{bmatrix} \begin{bmatrix} x(t) \\ x(t-\tau) \end{bmatrix} \\
&\quad - \int_{t-\tau}^{t} \begin{bmatrix} x(t) \\ x(t-\tau) \\ \dot{x}(s) \end{bmatrix}^T \begin{bmatrix} X_{11} & X_{12} & N_1 \\ * & X_{22} & N_2 \\ * & * & Z \end{bmatrix} \begin{bmatrix} x(t) \\ x(t-\tau) \\ \dot{x}(s) \end{bmatrix} ds
\end{aligned}
\tag{4.15}
$$

Define

$$
\Xi = \begin{bmatrix} PA + A^T P + Q + hX_{11} + N_1 + N_1^T + hA^T ZA & PBK - N_1 + N_2^T + hX_{12} + hA^T ZBK \\ * & -N_2 - N_2^T - Q + hX_{22} + hK^T B^T ZBK \end{bmatrix} \tag{4.16}
$$

$$
\Psi = \begin{bmatrix} X_{11} & X_{12} & N_1 \\ * & X_{22} & N_2 \\ * & * & Z \end{bmatrix} \tag{4.17}
$$

From Eq. (4.15), we can see if $\Xi < 0$ and $\Psi > 0$, then $\dot{V}(x_t) < 0$. That means the closed-loop system (4.8) is asymptotically stable. Using **Lemma**, it is easy to obtain $\Xi < 0$ is equal to

$$
\Phi = \begin{bmatrix} PA + A^T P + Q + hX_{11} + N_1 + N_1^T & PBK - N_1 + N_2^T + hX_{12} & hA^T Z \\ * & -N_2 - N_2^T - Q + hX_{22} & hK^T B^T Z \\ * & * & -hZ \end{bmatrix} < 0 \tag{4.18}
$$

In order to solve the controller gain *K*, define

$$
\begin{aligned}
&L = P^{-1},\ M_1 = P^{-1}N_1P^{-1},\ \ M_2 = P^{-1}N_2P^{-1} \\
&R = Z^{-1},\ V = KP^{-1},\ \ Q_1 = P^{-1}QP^{-1}, \\
&Y = diag\{P^{-1}, P^{-1}\}Xdiag\{P^{-1}, P^{-1}\}
\end{aligned}
$$

Pre- and post-multiply its left and right sides of Eq. (4.18) by $diag\{P^{-1}, P^{-1}, Z^{-1}\}$, respectively, that is,

$$\begin{bmatrix} P^{-1} & 0 & 0 \\ 0 & P^{-1} & 0 \\ 0 & 0 & Z^{-1} \end{bmatrix} \begin{bmatrix} PA+A^TP+Q+hX_{11}+N_1+N_1^T & PBK-N_1+N_2^T+hX_{12} & hA^TZ \\ * & -N_2-N_2^T-Q+hX_{22} & hK^TB^TZ \\ * & * & -hZ \end{bmatrix} \begin{bmatrix} P^{-1} & 0 & 0 \\ 0 & P^{-1} & 0 \\ 0 & 0 & Z^{-1} \end{bmatrix}$$

$$= \begin{bmatrix} AL+LA^T+M_1+M_1^T+Q_1+hY_{11} & BV-M_1+M_2^T+hY_{12} & hLA^T \\ * & -M_2-M_2^T-Q_1+hY_{22} & hV^TB^T \\ * & * & -hR \end{bmatrix} < 0$$

It is clear that (4.18) becomes (4.9).

Similarly, pre- and post-multiply its left and right sides of Eq.(4.17) by $diag\{P^{-1}, P^{-1}, P^{-1}\}$, respectively, (4.17) becomes (4.10). This completes the proof of Theorem.

Since the conditions in Theorem are no longer LMIs owing to the nonlinear terms $LR^{-1}L$ in (4.10), we cannot use a convex optimization algorithm to find a minimum value. However, we can use the cone complementarity linearization algorithm [4-20], which is based on LMIs, to solve this problem. The nonlinear optimization object and constraints can be constructed as follows.

Minimize $tr\{FF_1+LL_1+RR_1\}$

Subject to: $$\begin{bmatrix} AL+LA^T+M_1+M_1^T+Q_1+hY_{11} & BV-M_1+M_2^T+hY_{12} & hLA^T \\ * & -M_2-M_2^T-Q_1+hY_{22} & hV^TB^T \\ * & * & -hR \end{bmatrix} < 0$$

$$\begin{bmatrix} Y_{11} & Y_{12} & M_1 \\ * & Y_{22} & M_2 \\ * & * & F \end{bmatrix} > 0 \tag{4.19}$$

$$\begin{cases} \begin{bmatrix} F & I \\ I & F_1 \end{bmatrix} > 0, \begin{bmatrix} F_1 & L_1 \\ L_1 & R_1 \end{bmatrix} > 0, \\ L>0, F>0, R>0, \\ \begin{bmatrix} F & I \\ I & F_1 \end{bmatrix} > 0, \begin{bmatrix} F_1 & L_1 \\ L_1 & R_1 \end{bmatrix} > 0, \end{cases} \tag{4.20}$$

Based on the solution of the above nonlinear optimization object, the optimal controller gain matrix K and the maximum time delay $h=\max(\tau)$ can be searched out by the following proposed iteration algorithm.

Algorithm

Step 1: Choose a small initial time-delay h to ensure that there exists a feasible solution for (4.9), (4.19) and (4.20).

Step 2: Initially set a set of feasible matrix variable values for (L', L_1', V', M_1', M_2', F', F_1', Q_1', R', R_1', Y'), which should satisfy (4.9), (4.19) and (4.20). Then, set k=0.

Step 3: Solve the above nonlinear optimization problem expressed by the LMI constrains (4.9), (4.19) and (4.20). Then, set $F_{k+1} = F, F_{1,k+1} = F_1, L_{k+1} = L, L_{1,k+1} = L_1, R_{k+1} = R, R_{1,k+1} = R_1$.

Step 4: If inequality (4.10) is feasible, then increase h by a small amount and return to **Step 2**. If inequality (4.10) is unfeasible within a specified number of iterations, then stop. Otherwise, set k=k+1and go to **Step 3**.

According to Theorem and Algorithm, we can obtain the optimized feedback controller gain K and the maximum time delay h, In addition, it is necessary to remark that in the practical power system, since the operating state variables cannot be completely observed, it is preferable to use feedback control with measurable states for practical applications. For this purpose, the state observer O(s) should be introduced to implement the observation on the state variable transmitted by WAMS. In this chapter, the state observer is designed with the conventional pole-placement method [4-21]. Finally, the designed SVC-type FACTS wide-area robust damping control, which considers the time-delay of wide-area measurement signals, can be expressed as Figure 4.3 shows.

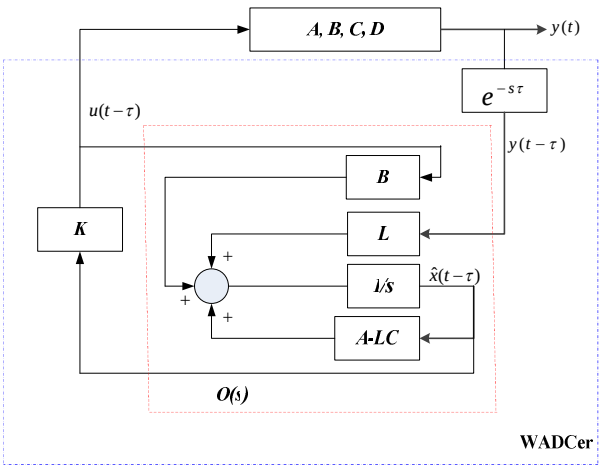

Figure 4.3 Configuration of SVC-type FACTS-WADCer including state observer

4.5 Cases Study

4.5.1 Four-Machine Two-Area System

In this case, the four-machine two-area benchmark system [4-17] for inter-area oscillation study is used to validate the proposed robust FACTS-WADCer. Figure 4.4 shows the system modified with a shunt FACTS device on bus-8. Such FACTS device is mainly used to improve the voltage profile and the interconnected ability of the areas. In this system, G1 and G2 are located in area-1, and G3 and G4 are in area-2.

Many research results have demonstrated that there is a typical inter-area oscillation mode between area-1 and area-2, and such oscillation further represents the power oscillation between G1 and G3. Thus, in this case, the rotor angle and speed deviation of the both machines are selected as the wide-area feedback input for the FACTS device. In addition, the classic shunt FACTS device, that is SVC, is used to implement the supplementary wide-area control.

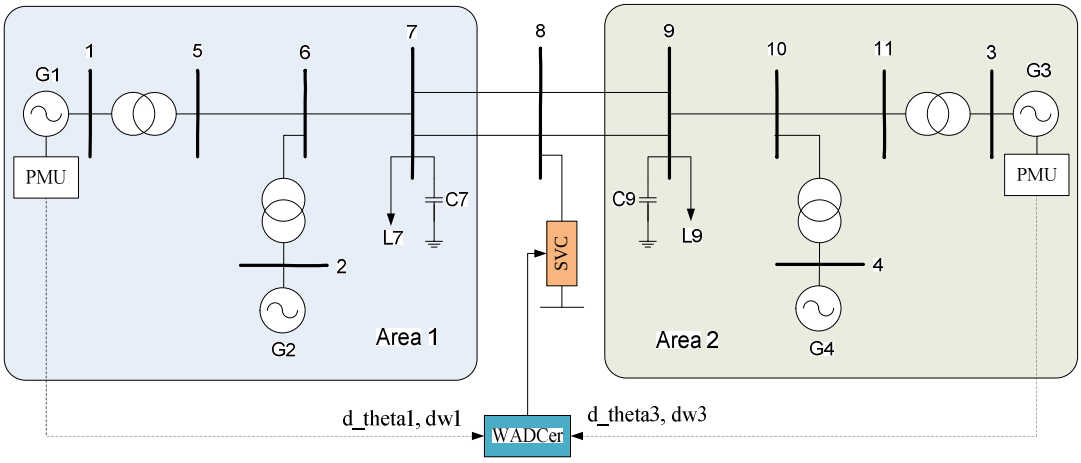

Figure 4.4 The four-machine Two-area system

The nonlinear dynamical simulation is performed by set three-phase ground-fault on bus-8 for the duration of 190ms. Figure 4.5 shows the response of line power flow from area-1 to area-2. From this, it can be seen that as for the system without the SVC wide-area damping control, such large disturbance leads to serious power oscillation occurrence in the interconnected system. However, when the presented control is applied, such oscillation is damped effectively, even there is 180ms delay time for the wide-area control signals, the designed controller still maintains good damping

effects. Figure 4.6 shows the relative angular between G1 and G3. From this, it can be seen that there is the oscillation on one generator in one area against another generator in another area, and such oscillation is the direct reason on the power oscillation of the interconnected system. However, with the implement of the SVC wide-area control, such oscillation is damped very well, which further verifies the correctness of the designed controller.

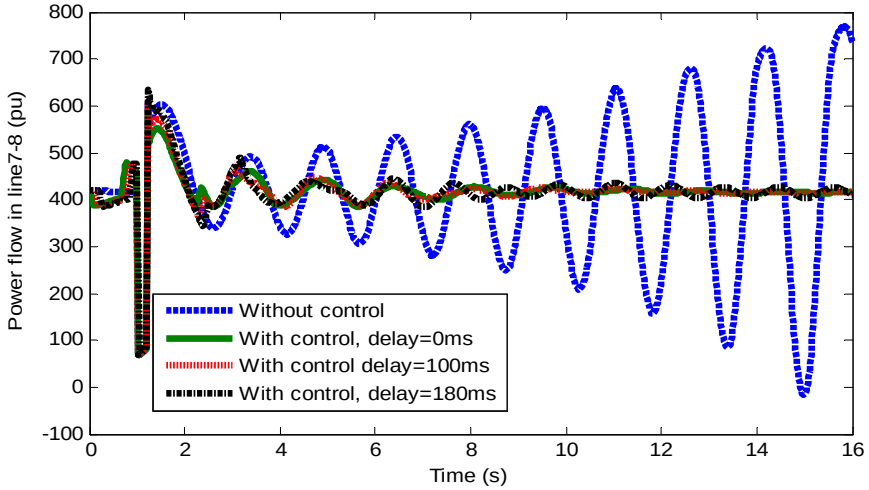

Figure 4.5 Power flow from area-1 to area-2

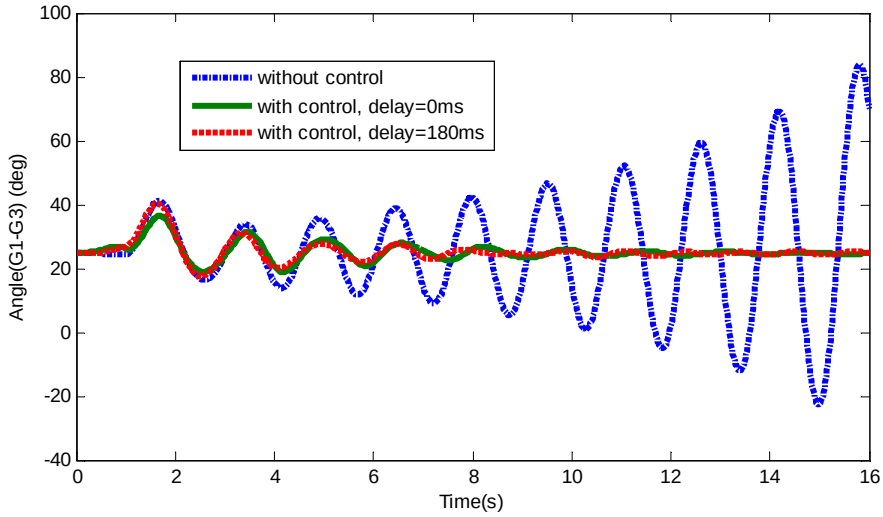

Figure 4.6 Dynamic response of the system with SVC-type FACTS-WADCer

Furthermore, to compare the damping performance of the conventional local control strategy to that of the proposed wide-area control strategy, four simulation cases are performed on the four-machine two-area benchmark system, that is:

1) Case-1: One general local power system stabilizer (PSS) is installed on G1 located in Area-1;

2) Case-2: Two local PSSs are installed on G1 (in Area-1) and G3 (in Area-2);

3) Case-3: All the generators in the two areas are installed with the local PSSs;

4) Case-4: Don't install any local PSS, and only perform the FACTS wide-area robust damping(WARD) control.

Figure 4.7 shows the results about the above four simulation cases. From this, it can be clearly seen that when it just implements the local control strategy, the single or part local PSSs cannot provide the sufficient damping on the inter-area oscillation occurrencing between different areas. Although when all the generators install the local PSSs, it can achieve the accepted damping performance like the implementation of the FACTS-WARD control, it should be noted that the coordination among plenty of PSSs in different areas could be difficult in the practical large-scale power systems. However, as for the FACTS-WARD, there is no the related problem, and it just to introduce the supplementary control of FACTS device to construct the wide-area damping control strategy to prevent the inter-area oscillations.

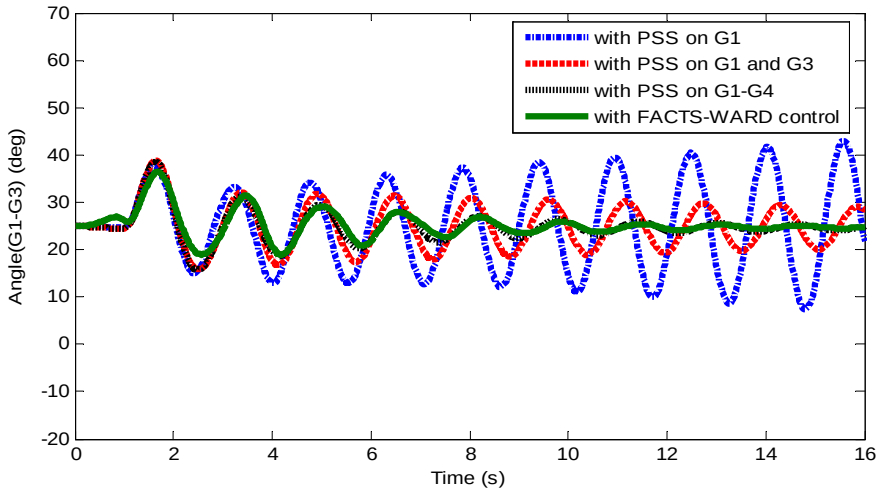

Figure 4.7 Dynamic response of the system with local PSS or with SVC-type FACTS-WARD controll

4.5.2 Sixteen-Machine Five-Area Test System

As Figure 4.8 shows, the 16-machine five-area test system [4-18] modified with a shunt FACTS device on bus-51 is simulated in this chapter to validate the proposed FWMs based robust controller design approach for FACTS wide-area damping control. This is in fact the simplified New England and New York interconnected system. So, the first nine machines (G1-G9) and the second

four machines (G10-G13) belong to the New England Test System (NETS) and the New York Power System (NYPS), respectively. In addition, there are three more machines (G14-G16) used as the dynamical equivalent of the three neighbor areas connected with NYPS area. It should be remarked that all the machines are described by the sixth-order dynamical model.

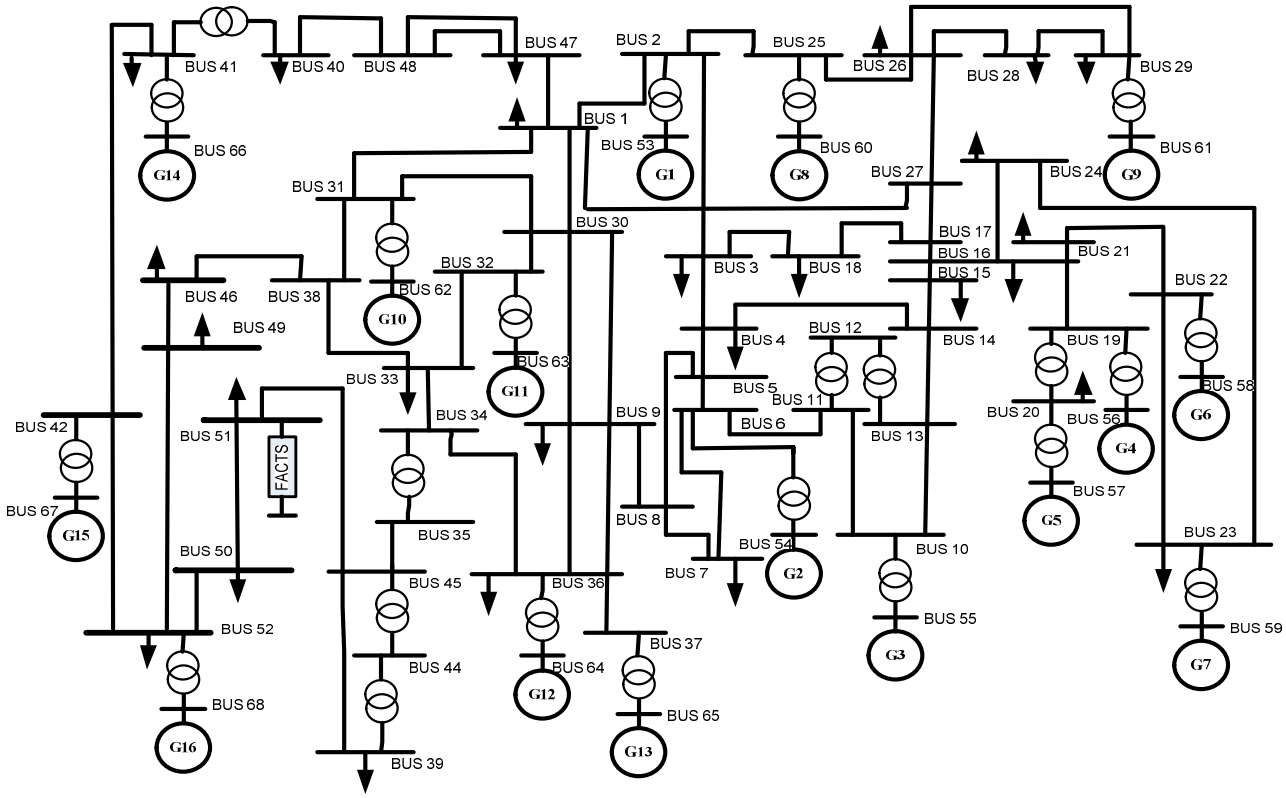

Figure 4.8 The sixteen-machine five-area test system

As the classic shunt-type FACTS device, SVC is installed on the interconnected bus to improve the voltage profile of the system. The mode analysis on the test system shows that there is an inter-area oscillation mode (oscillation frequency is 0.57Hz and damping ratio is 0.017) between G14 and G16 under the specific operating condition. As for such low-frequency oscillator (LFO) mode, the SVC wide-area supplementary control strategy could be a better alternative than the conventional local PSS control strategy. However, to implement the effective wide-area damping control, it is very important to select the suitable wide-area feedback signals. The residue analysis results show that the inter-area mode represents high observability on the real line current between bus-68 and bus-52. Thus, such line current is selected as the feedback stabilizing signal for SVC wide-area damping

control. Furthermore, based on the linearized model of the test system, the robust control design can be performed step by step as the above proposed method.

A three-phase short-circuit fault with 100ms duration is applied nearby the bus-51 to assess the control performance under the large disturbance. Figures. 4.9-4.14 show the nonlinear simulation results on the system dynamic response. Figure 4.9 shows the relative angular between G14 and G16. From this, it can be seen that the low-frequency oscillation between G14 and G16 is damped very well by the presented SVC-type FACTS-WADCer. Meanwhile, the power oscillations about the power flow nearby the machine and at the interconnected backbone line are also damped significantly as Figure 4.10 shows. The output variation of the SVC is shown in Figure 4.11, which indicates that the SVC with wide-area supplementary control plays the quick action against the oscillation damping.

To further reveal the control performance of the presented robust controller under different delays of the wide-area control signal, the 100ms and the 200ms delay caused by signal transmission is simulated respectively. Figures 4.12 -4.14 show the comparison about the dynamic response under such different delays. From these, it can be seen that with the increase of the time delay from 0 to 200ms, the designed controller always maintains the good oscillation damping effect, which indicates the robustness of the presented controller against the transmission delays of the wide-area feedback signal.

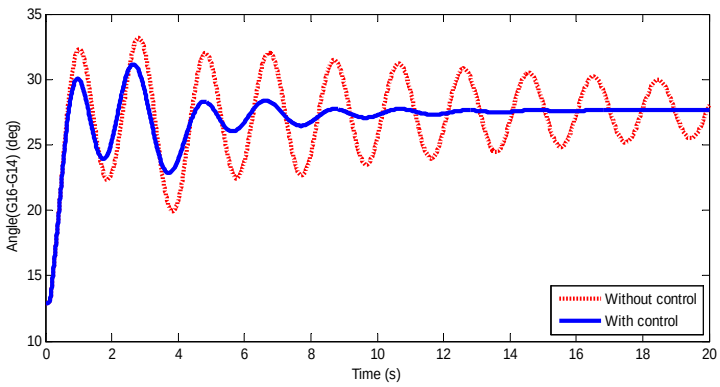

Figure 4.9 Dynamic response of the system with SVC-type FACTS-WADCer

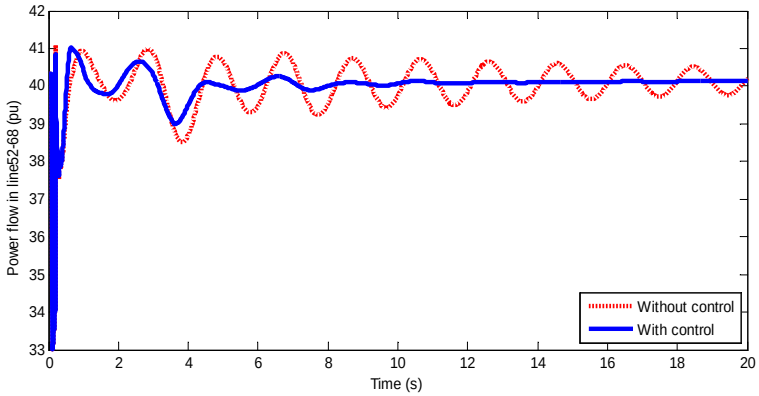

(a)

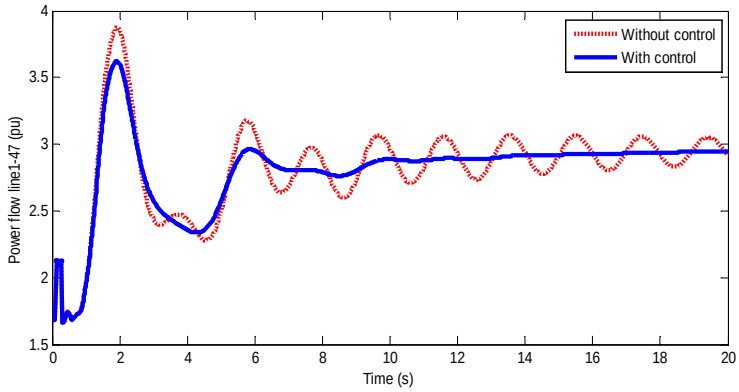

(b)

Figures 4.10 Power flow in the tie-line. (a) line 52-68, (b) line 1-47

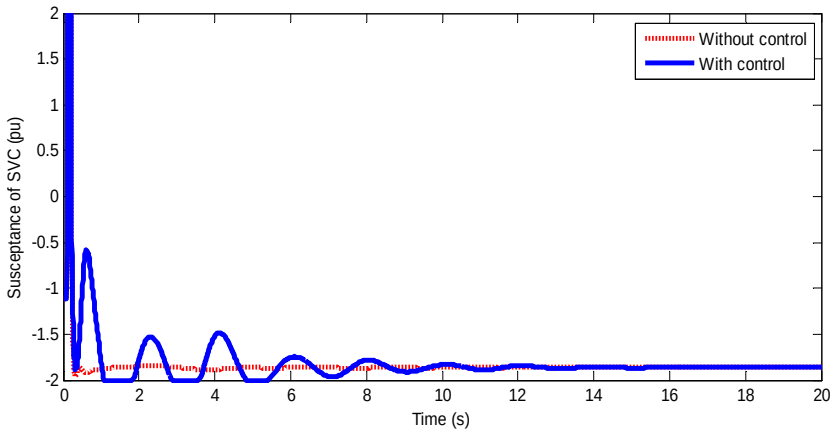

Figure 4.11 Output of the SVC

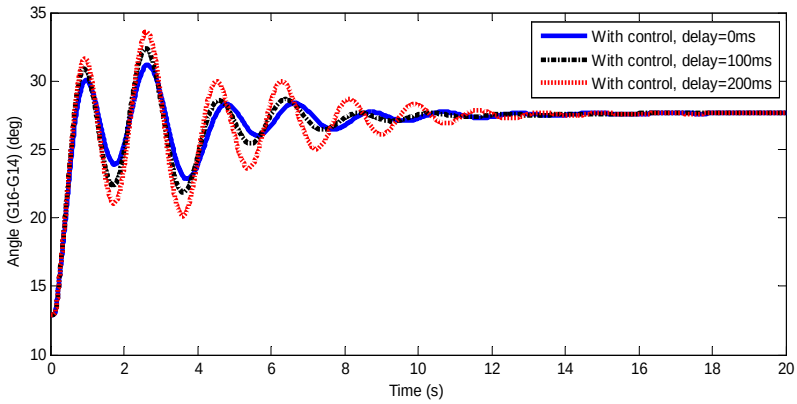

Figure 4.12 Dynamic response of the system with SVC-type FACTS-WADCer under different time delays

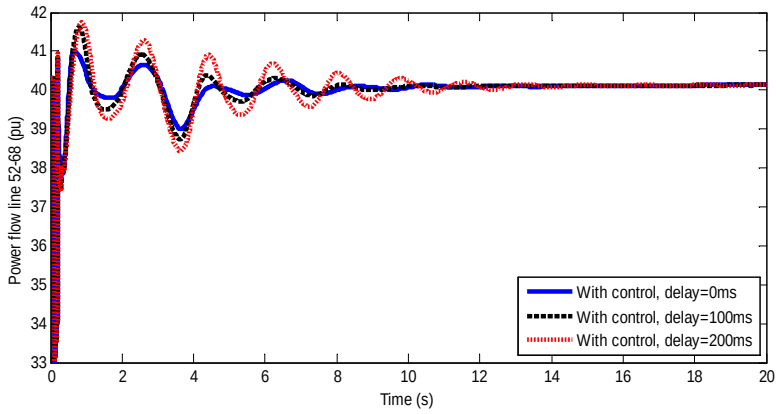

(a)

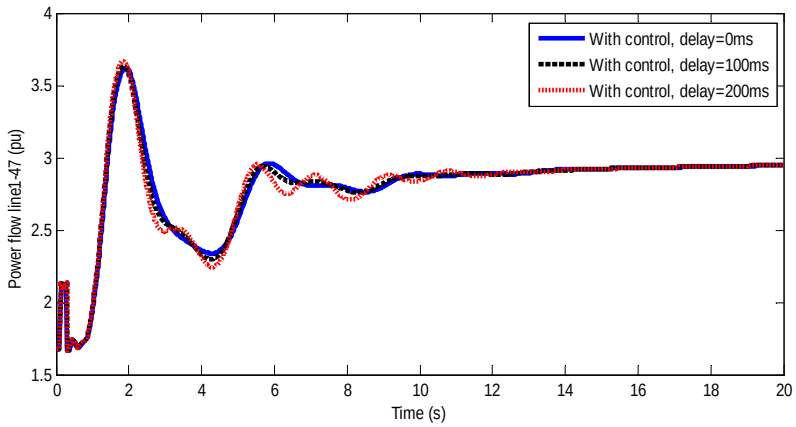

(b)

Figure 4.13 Power flow in the tie-line under different time delays. (a) line 52-68, (b) line 1-47

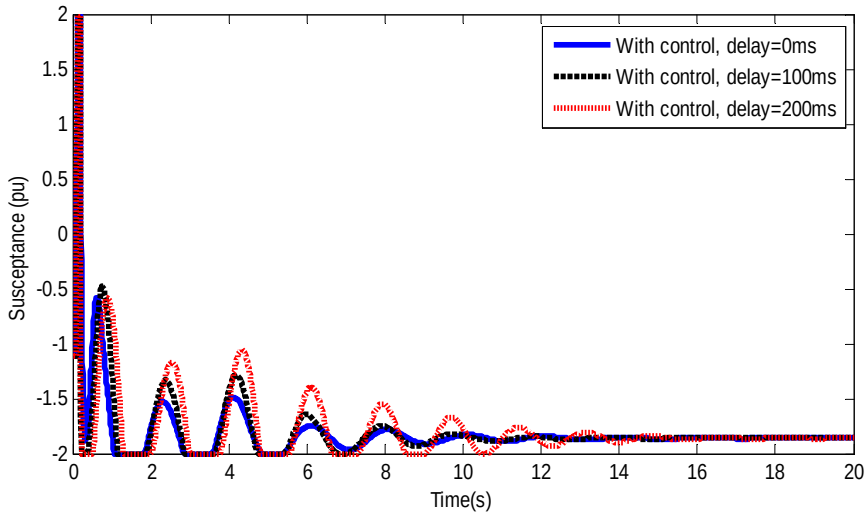

Figure 4.14 Output of the SVC under different time delays

4.6 Conclusion

This chapter presents a new linear design approach on the robust FACTS wide-area damping control to enhance the power stability of large power system. The free-weighting matrices are introduced to converter the optimization object with nonlinear matrix inequality constrains into a set of LMI constrains, which is convenient to the linear design for the FACTS wide-area robust damping controller. Furthermore, a nonlinear optimization algorithm is presented to search out the optimal control gain matrix with the maximum delay independent of the wide-area feedback control signals. Thus, it can effectively improve the negative effects for the time-varying delays on the control performance, which is also in practice to the large power networks with wide-area control system. In practice, after the acceptable system equivalent, the proposed method is simple and easy to be applied into the large power system. The nonlinear simulations on both the four-machine two-area and the sixteen-machine five-area system have shown that the presented robust FACTS wide-area controller not only improves the system oscillation stability, but also has robustness against the variations of time delay aroused by the wide-area transmission and processing information in WAMS.

Chapter References

[4-1] **D. C. Savelli, P. C. Pellanda, N. Martins, N. J. P. Macedo, A. A. Barbosa, and G. S. Luz.** *Robust signals for the TCSC oscillation damping controllers of the Brazilian North-South interconnection considering multiple power flow scenarios and external disturbances.* IEEE Power Engineering Society General Meeting, 2007.

[4-2] **R. Grunbaum, M. de Grijp, and V. Moshi.** *Enabling long distance AC power transmission by means of FACTS.* AFRICON, Sept. 2009.

[4-3] **N. R. Chaudhuri, S. Ray, R. Majumder, and B. Chaudhuri.** *A case study on challenges for robust wide-area phasor POD.* IEEE Power & Energy Society General Meeting, 2009.

[4-4] **P. Korba, M. Larsson, B. Chaudhuri, B. Pal, R. Majumder, R. Sadikovic, and G. Andersson.** *Towards real-time implementation of adaptive damping controllers for FACTS devices.* IEEE Power Engineering Society General Meeting, 2007.

[4-5] **M. Zarghami, M. L. Crow, and S. Jagannathan.** *Nonlinear control of FACTS controllers for damping interarea oscillations in power systems.* IEEE Transactions on Power Delivery. Vol. 25, No. 4, pp. 3113-3121, Oct. 2010.

[4-6] **K. Gu.** Discretized LMI set in the stability problem for linear uncertain time-delay systems. Int. J. Control, 1997, 68 (4): 923-934

[4-7] **K. Gu.** *A generalized discretization scheme of Lyapunov functional in the stability problem of linear uncertain time-delay systems*. Int. J. Robust & Nonlinear Control, 1999, 9 (1): 1-4

[4-8] **K. Gu.** *A further refinement of discretized Lyapunov functional method for the stability of time-delay systems*. Int. J. Control, 2001, 74 (10): 967-976.

[4-9] **E. Fridman, U. Shaked.** *Delay-dependent stability and H_∞ control: constant and time-varying delays.* Int. J. Control, 2003, 76 (1): 48-60.

[4-10] **E. Fridman, U. Shaked.** *On delay-dependent passivity.* IEEE Transactions on Automatic Control, 2002, 47 (4): 664 -669

[4-11] **H. Gao, C. Wang.** *Comments and further results on 'A descriptor system approach to H1 control of linear time- delay systems'*. IEEE Transactions on Automatic Control, 2003, 48 (3): 520~ 525

[4-12] **Q. L. Han.***Stability criteria for a class of linear neutral systems with time-varying discrete and distributed delays.* IMA Journal of Math. Contr. and Info., 2003, 20(4): 371~ 386

[4-13] **F. Liu, M. Wu, Y. He, Y.C. Zhou, and R. Yokoyama.** *Delay-dependent Robust Stability Analysis for Interval Neural Networks with Time-varying Delay.* IEEJ, accepted, 2010.

[4-14] **F. Liu, M. Wu, Y. He, Y.C. Zhou, and R. Yokoyama.** *New Delay-dependent Stability Criteria for T-S Fuzzy Systems with a Time-varying Delay.* Proceedings of the 17th World Congress, the International Federation of Automatic Control. Seoul, Korea, 2008.

[4-15] **F. Liu, M. Wu, Y. He, Y.C. Zhou, and R. Yokoyama.** *New Delay-dependent Stability Analysis and Stabilizing Design for T-S Fuzzy Systems with a Time-varying Delay.* 27th Chinese Control Conference, Kunming, China, 2008.

[4-16] **Q.Y. Jiang, Z.Y. Zou, and Y.J. Cao.** *Wide-area TCSC controller design in consideration of feedback signals' time delays.* IEEE Power Engineering Society General Meeting, 2005.

[4-17] **P. Kundur.** *Power Stability and Control.* New York: McGraw-Hill, 1994.

[4-18] **G. Rogers.** *Power System Oscillations.* Norwell, MA: Kluwer, 1999.

[4-19] **H. Gao, J. Lam, C. Wang, and Y. Wang.** *Delay-dependent output-feedback stabilization of discrete-time systems with time-varying state delay.* IEE Proceedings of Control Theory and Application. Vol. 151, No. 6, pp. 691-698, Nov. 2004.

[4-20] **L. El Ghaoui, F. Oustry, and M. AitRami.** *A cone complementarity linearization algorithm for static output-feedback and related problems.* IEEE Transactions on Automatic Control. Vol. 42, No. 8, pp. 1171-1176, Aug. 1997.

[4-21] **M. Chilali, P. Gahinet, and P. Apkarian.** *Robust pole placement in LMI regions. IEEE Trans Automat Control.* Vol. 44, No. 12, pp. 2257–2270, Dec. 1999.

Chapter 5
Output-Feedback-Type Controller Design with Considering Signal Time-Varying Delay for FACTS Wide Area Damping Control Strategy

5.1 Introduction

In this chapter, a design approach with considering time-varying delay of control-input will be presented for FACTS output-feedback-type wide area damping controller design. The control concept and basic controller structure will be described in advance. Then, a discrete-time linearized plant model is introduced for the discrete-time controller design. Based on the plant model, the controller design procedure is presented in detail, which includes the stabilization analysis, iterative algorithm of control gain, and the process of time-varying delay. Finally, two typical test system, that is the four-machine two-area benchmark system for oscillation damping study and the sixteen-machine five-area test system (New England test system (NETS) and New York power system (NYPS) interconnected system), are studied in detail to validate the control concept and the designed damping controller.

5.2 Description of FACTS Wide Area Output-feedback Damping Control

Figure 5.1 shows the basic structure of the wide area output-feedback damping control associated to the series-type FACTS device (TCSC) expressed with the dynamic control model, which can be used to describe the basic control concept on WAMS-based TCSC wide area output-feedback-type power oscillation damping to enhance the stability of the power system.

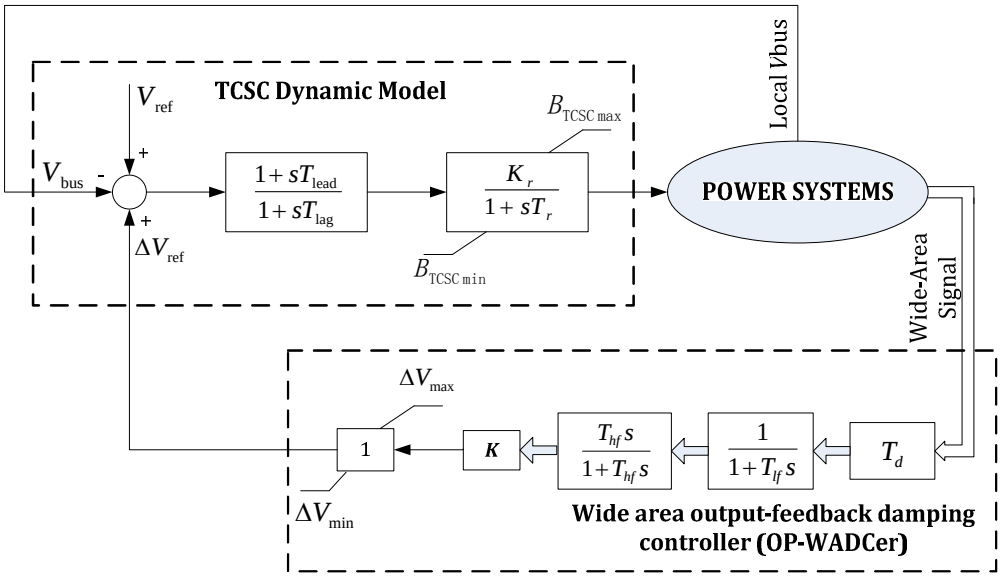

Figure 5.1 Basic structure of FACTS wide area output-feedback damping control

As Figure 5.1 shows, as one kind of supplementary control scheme of the TCSC device, the control-output of the wide area output-feedback damping controller (OP-WADCer) is one part of the control-input of the TCSC device, which can satisfy the additional damping control demand by adjusting the susceptance within a certain range to provide the effective damping on the inter-area oscillations. For the control-input of the OP-WADCer, it selects the suitable wide-area signal that can achieve the optimal damping performance for the concerned inter-area oscillation modes. Generally, the wide-area signals could be the remote generator rotor speed or angle, the bus angle, or the line active power, etc. Basically, such optimal selection on the wide-area signal can be performed by the conventional modal analysis method and based on the maximum observability/controllability index.

As for the structure of the TCSC OP-WADCer as shown in Figure 5.1, the high-pass and the low-pass filters (HPF and LPF) are used to process the control-input signal with the purpose of remaining the concerned oscillation mode information. Different from the state-feedback control discussed in the above chapter, for the OP-WADCer in here, there is no the state observer. The measured wide area control signal directly feed into the control gain K through HPF and LPF. The feedback-control gain K only consider the control-input variables not the system state variables, thus compared to the

state-feedback control, it is simpler and more convenient for the practical application. Furthermore, for the TCSC OP-WADCer design, the important part is the solution of the output-feedback control gain *K*, which fundamentally determines the damping performance of WADCer. Generally, there are mainly two type of the output-feedback control gain, that is the static and the dynamic type. For the static type, it is just a constant value, while for the dynamic type it is represented as the state space form. At present, for the output-feedback control, many research results are about the static type. Different from this, in this chapter, the dynamic output-feedback control gain will be studied to further improve the dynamic performance of power system. In addition, it should be noted that for the wide area signal, it inevitably exist a certain time delay, which may reduce the damping performance to a certain degree. Thus, in this chapter, a newly linear design approach will be presented to optimize the output-feedback control gain *K* with the efficient consideration of the negative effect of time delay on the damping performance.

5.3 Discrete-Time System with Considering Time-vary Delay

Generally, there are two types of linearized model for power system. One is the continuous-time model like discussion in the previous chapters. The other one is the discrete-time model discussed in this section. Such model can be converted by the continuous-time model or be obtained by the real-time analysis data of power system. For the power system with the control-input and control-output, its discrete-time model has the following standard form:

$$\begin{cases} x(k+1) = Ax(k) + Bu(k) \\ y(k) = Cx(k) \end{cases} \tag{5.1}$$

For the stabilization of the time-delay power system, we consider a dynamic output feedback controller described by

$$\begin{bmatrix} x_c(k+1) \\ u(k) \end{bmatrix} = \begin{bmatrix} A_c & B_c \\ C_c & D_c \end{bmatrix} \begin{bmatrix} x_c(k-\tau(k)) \\ y(k-\tau(k)) \end{bmatrix} \tag{5.2}$$

Where $u(k)$ is the controller output, $x_c(k)$ is the controller states.

Then the closed loop system is obtained by combining the linearized power system(5.1) and the controller(5.2), and can be described by the following equation:

$$\xi(k+1) = \widehat{A}\xi(k) + \overline{B}\xi(k-\tau(k)) \tag{5.3}$$

where $\xi(k) = [x^T(k) \quad x_c^T(k)]^T$

$$\widehat{A} = \begin{bmatrix} A & 0 \\ 0 & 0 \end{bmatrix} \quad , \quad \overline{B} = \begin{bmatrix} BD_cC & BC_c \\ B_cC & A_c \end{bmatrix} = \widehat{B}\widehat{K}\widehat{C}$$

$$\widehat{B} = \begin{bmatrix} B & 0 \\ 0 & I \end{bmatrix} \quad , \quad \widehat{C} = \begin{bmatrix} C & 0 \\ 0 & I \end{bmatrix}$$

and $\widehat{K} = \begin{bmatrix} D_c & C_c \\ B_c & A_c \end{bmatrix}$ is to be determined. Then, the problem of designing a dynamic output feedback controller (5.2) can be transformed into the problem of design a static output feedback(SOF) controller[5-1],

$$u(k) = \widehat{K}y(k-\tau(k)) \tag{5.4}$$

for the system

$$\begin{cases} \xi(k+1) = \widehat{A}\xi(k) + \widehat{B}u(k) \\ y(k) = \widehat{C}\xi(k) \end{cases} \tag{5.5}$$

Connecting the SOF controller (5.4) to the system(5.5), the following closed-loop system can be obtained

$$\xi(k+1) = \widehat{A}\xi(k) + \widehat{A}_\tau\xi(k-\tau(k)) \tag{5.6}$$

Where $\widehat{A}_\tau = \widehat{B}\widehat{K}\widehat{C}$, and the time-varying delay satisfied with $h_1 \le \tau(k) \le h_2$.

5.4 Design of FACTS Wide Area Output-feedback Damping Controller

This section will present a stability criterion for the time-delay power system by using free-weighting matrices approach[5-2][5-3]. It can be used to design the output feedback stabilization controllers.

Theorem 1 For given integers h_1 and h_2 with $h_1 \le \tau(k) \le h_2$, system(5.1) can be stabilized by controller(5.5) if there exist $P = P^T > 0,\ L = L^T > 0,\ Q_i = Q_i^T > 0, (i = 1,2),\ R = R^T > 0,$

$Z_i = Z_i^T > 0, (i = 1,2),$ $W_i = W_i^T > 0, (i = 1,2),$ $X = \begin{bmatrix} X_{11} & X_{12} \\ * & X_{22} \end{bmatrix},$

$Y = \begin{bmatrix} Y_{11} & Y_{12} \\ * & Y_{22} \end{bmatrix},\ N = \begin{bmatrix} N_1^T & N_2^T \end{bmatrix}^T,\ M = \begin{bmatrix} M_1^T & M_2^T \end{bmatrix}^T,\ S = \begin{bmatrix} S_1^T & S_2^T \end{bmatrix}^T$ and $\widehat{K}$ such that the following matrices are satisfied with:

$$\begin{bmatrix} \Phi & \Xi_1^T & h_2\Xi_2^T & (h_2 - h_1)\Xi_2^T \\ * & -L & 0 & 0 \\ * & * & -h_2 W_1 & 0 \\ * & * & * & (h_2 - h_1)W_2 \end{bmatrix} < 0 \tag{5.7}$$

$$PL = I,\quad Z_i W_i = I,\ i = 1,2 \tag{5.8}$$

$$\Psi_1 = \begin{bmatrix} X & N \\ * & Z_1 \end{bmatrix} > 0 \tag{5.9}$$

$$\Psi_2 = \begin{bmatrix} X + Y & M \\ * & Z_1 + Z_2 \end{bmatrix} > 0 \tag{5.10}$$

$$\Psi_3 = \begin{bmatrix} Y & S \\ * & Z_2 \end{bmatrix} > 0 \tag{5.11}$$

where

$$\Phi = \begin{bmatrix} -P+Q_1+Q_2+(h_2-h_1+1)R+N_1+N_1^T+h_2X_{11}+(h_2-h_1)Y_{11} & -N_1+N_2^T+M_1-S_1+h_2X_{12}+(h_2-h_1)Y_{12} & S_1 & -M_1 \\ * & -N_2-N_2^T-R+M_2+M_2^T-S_2-S_2^T+(h_2-h_1)Y_{22} & S_2 & -M_2 \\ * & * & -Q_1 & 0 \\ * & * & * & -Q_2 \end{bmatrix}$$

$$\Xi_1 = [\hat{A} \;\; \hat{A}_\tau \;\; 0 \;\; 0]$$
$$\Xi_2 = [\hat{A}-I \;\; \hat{A}_\tau \;\; 0 \;\; 0]$$

Proof: Define

$$\eta(l) = \xi(l+1) - \xi(l) \tag{5.12}$$

It is clear from (5.12) that

$$\xi(k+1) = \xi(k) + \eta(k)$$

and

$$\begin{aligned} \eta(k) &= \xi(k+1) - \xi(k) \\ &= (\hat{A}-I)\xi(k) + \hat{A}_\tau \xi(k-\tau(k)) \end{aligned}$$

Choose a Lyapunov functional candidate to be

$$\begin{aligned} V(k) &= V_1(k)+V_2(k)+V_3(k)+V_4(k) \\ V_1(k) &= \xi^T(k)P\xi(k) \\ V_2(k) &= \sum_{i=k-h_1}^{k-1} \xi^T(i)Q_1\xi(i) + \sum_{i=k-h_2}^{k-1} \xi^T(i)Q_2\xi(i) \\ V_3(k) &= \sum_{l=k-h_2}^{k-h_1} \sum_{i=l}^{k-1} \xi^T(i)R\xi(i) \\ V_4(k) &= \sum_{i=-h_2}^{-1} \sum_{l=k+i}^{k-1} \eta^T(i)Z_1\eta(i) + \sum_{i=-h_2}^{-h_1-1} \sum_{l=k+i}^{k-1} \eta^T(i)Z_2\eta(i) \end{aligned} \tag{5.13}$$

In which, $P = P^T > 0$, $Q_i = Q_i^T > 0, (i=1,2)$, $R = R^T > 0$, $Z_i = Z_i^T > 0, (i=1,2)$, are to be determined.

Defining $\Delta V(k) = V(k+1) - V(k)$ yields

$$\begin{aligned}\Delta V_1(k) &= \xi^T(k+1)P\xi(k+1) - \xi^T(k)P\xi(k) \\ &= \zeta^T(k)\Xi_1^T P\Xi_1\zeta(k) - \xi^T(k)P\xi(k)\end{aligned} \tag{5.14}$$

where $\zeta(t) = [\xi^T(k) \quad \xi^T(t-\tau(k)) \quad \xi^T(t-h_1) \quad \xi^T(t-h_2)]^T$

and

$$\begin{aligned}\Delta V_2(k) &= \sum_{i=k+1-h_1}^{k} \xi^T(i)Q_1\xi(i) + \sum_{i=k+1-h_2}^{k} \xi^T(i)Q_2\xi(i) - \sum_{i=k-h_1}^{k-1} \xi^T(i)Q_1\xi(i) - \sum_{i=k-h_2}^{k-1} \xi^T(i)Q_2\xi(i) \\ &= \xi^T(k)(Q_1+Q_2)\xi(k) - \xi^T(k-h_1)Q_1\xi(k-h_1) - \xi^T(k-h_2)Q_2\xi(k-h_2)\end{aligned} \tag{5.15}$$

$$\begin{aligned}\Delta V_3(k) &= (h_2-h_1+1)\xi^T(k)R\xi(k) - \sum_{l=k-h_2}^{k-h_1} \xi^T(l)R\xi(l) \\ &\le (h_2-h_1+1)\xi^T(k)R\xi(k) - \xi^T(k-\tau(k))R\xi(k-\tau(k))\end{aligned} \tag{5.16}$$

$$\begin{aligned}\Delta V_4(k) &= h_2\eta^T(k)(Z_1+Z_2)\eta(k) - h_1\eta^T(k)Z_2\eta(k) - \sum_{l=k-h_2}^{k-1} \eta(l)Z_1\eta(l) - \sum_{l=k-h_2}^{k-h_1-1} \eta(l)Z_2\eta(l) \\ &= h_2\zeta^T(k)\Xi_2^T(Z_1+Z_2)\Xi_2\zeta(k) - h_1\zeta^T(k)\Xi_2^T Z_2\Xi_2\zeta(k) - \sum_{l=k-\tau(k)}^{k-1} \eta(l)Z_1\eta(l) - \sum_{l=k-\tau(k)}^{k-h_1-1} \eta(l)Z_2\eta(l) - \sum_{l=k-h_2}^{k-\tau(k)-1} \eta(l)(Z_1+Z_2)\eta(l) \\ &= \zeta^T(k)\Xi_2^T[h_2Z_1 + (h_2-h_1)Z_2]\Xi_2\zeta(k) - \sum_{l=k-\tau(k)}^{k-1} \eta(l)Z_1\eta(l) - \sum_{l=k-\tau(k)}^{k-h_1-1} \eta(l)Z_2\eta(l) - \sum_{l=k-h_2}^{k-\tau(k)-1} \eta(l)(Z_1+Z_2)\eta(l)\end{aligned} \tag{5.17}$$

From Newton-Leibniz formula, the following equations for any matrices N, M and S with appropriate dimensions are true:

$$0 = 2\zeta_1^T(k)N[\xi(k) - \xi(k-\tau(k)) - \sum_{l=k-\tau(k)}^{k-1} \eta(l)] \tag{5.18}$$

$$0 = 2\zeta_1^T(k)M[\xi(k-\tau(k)) - \xi(k-h_2) - \sum_{l=k-h_2}^{k-\tau(k)-1} \eta(l)] \tag{5.19}$$

$$0 = 2\zeta_1^T(k)S[\xi(k-h_1) - \xi(k-\tau(k)) - \sum_{l=k-\tau(k)}^{k-h_1-1} \eta(l)] \tag{5.20}$$

where $\zeta_1(k) = [\xi^T(k) \quad \xi^T(t-\tau(k))\ ]^T$

On the other hand, for any appropriated dimensioned matrix $X = X^T \geq 0$ and $Y = Y^T \geq 0$, the following equation is true:

$$\begin{aligned} 0 &= \sum_{l=k-h_2}^{k-1} \zeta_1^T(k) X \zeta_1(k) - \sum_{l=k-h_2}^{k-1} \zeta_1^T(k) X \zeta_1(k) \\ &= h_2 \zeta_1^T(k) X \zeta_1(k) - \sum_{l=k-h_2}^{k-\tau(k)-1} \zeta_1^T(k) X \zeta_1(k) - \sum_{l=k-\tau(k)}^{k-1} \zeta_1^T(k) X \zeta_1(k) \end{aligned} \tag{5.21}$$

$$\begin{aligned} 0 &= \sum_{l=k-h_2}^{k-h_1-1} \zeta_1^T(k) Y \zeta_1(k) - \sum_{l=k-h_2}^{k-h_1-1} \zeta_1^T(k) Y \zeta_1(k) \\ &= (h_2 - h_1) \zeta_1^T(k) Y \zeta_1(k) - \sum_{l=k-h_2}^{k-\tau(k)-1} \zeta_1^T(k) Y \zeta_1(k) - \sum_{l=k-\tau(k)}^{k-h_1-1} \zeta_1^T(k) Y \zeta_1(k) \end{aligned} \tag{5.22}$$

Then adding the right sides of (5.17)-(5.21) to the $\Delta V(k)$ yields

$$\begin{aligned} \Delta V(k) \leq\ & \zeta^T(k) \Xi_1^T P \Xi_1 \zeta(k) - \xi^T(k) P \xi(k) + \xi^T(k)(Q_1 + Q_2)\xi(k) - \xi^T(k-h_1) Q_1 \xi(k-h_1) - \xi^T(k-h_2) Q_2 \xi(k-h_2) \\ & + (h_2 - h_1 + 1)\xi^T(k) R \xi(k) - \xi^T(k-\tau(k)) R \xi(k-\tau(k)) \\ & + \zeta^T(k) \Xi_2^T [h_2 Z_1 + (h_2 - h_1) Z_2] \Xi_2 \zeta(k) - \sum_{l=k-\tau(k)}^{k-1} \eta(l) Z_1 \eta(l) - \sum_{l=k-\tau(k)}^{k-h_1-1} \eta(l) Z_2 \eta(l) - \sum_{l=k-h_2}^{k-\tau(k)-1} \eta(l)(Z_1 + Z_2)\eta(l) \\ & + 2\zeta_1^T(k) N [\xi(k) - \xi(k-\tau(k)) - \sum_{l=k-\tau(k)}^{k-1} \eta(l)] \\ & + 2\zeta_1^T(k) M [\xi(k-\tau(k)) - \xi(k-h_2) - \sum_{l=k-h_2}^{k-\tau(k)-1} \eta(l)] \\ & + 2\zeta_1^T(k) S [\xi(k-h_1) - \xi(k-\tau(k)) - \sum_{l=k-\tau(k)}^{k-h_1-1} \eta(l)] \\ & + h_2 \zeta_1^T(k) X \zeta_1(k) - \sum_{l=k-h_2}^{k-\tau(k)-1} \zeta_1^T(k) X \zeta_1(k) - \sum_{l=k-\tau(k)}^{k-1} \zeta_1^T(k) X \zeta_1(k) \\ & + (h_2 - h_1) \zeta_1^T(k) Y \zeta_1(k) - \sum_{l=k-h_2}^{k-\tau(k)-1} \zeta_1^T(k) Y \zeta_1(k) - \sum_{l=k-\tau(k)}^{k-h_1-1} \zeta_1^T(k) Y \zeta_1(k) \end{aligned}$$

$$\begin{aligned} &= \zeta^T(k) \{ \Phi + \Xi_1^T P \Xi_1 + \Xi_2^T [h_2 Z_1 + (h_2 - h_1) Z_2] \Xi_2 \} \zeta(k) - \sum_{l=k-\tau(k)}^{k-1} \zeta_2^T(k,l) \Psi_1 \zeta_2(k,l) \\ &- \sum_{l=k-h_2}^{k-\tau(k)-1} \zeta_2^T(k,l) \Psi_2 \zeta_2(k,l) - \sum_{l=k-\tau(k)}^{k-h_1-1} \zeta_2^T(k,l) \Psi_3 \zeta_2(k,l) \end{aligned} \tag{5.23}$$

where $\zeta_2(k) = [\zeta_1^T(k),\ \ \eta^T(l)]^T$

Therefore, if $\Psi_i \geq 0 (i=1,2,3)$ and $\Phi + \Xi_1^T P \Xi_1 + \Xi_2^T [h_2 Z_1 + (h_2 - h_1) Z_2] \Xi_2 > 0$, then $\Delta V(k) < 0$. By using Schur complements[5-4], it can be obtained $\Phi + \Xi_1^T P \Xi_1 + \Xi_2^T [h_2 Z_1 + (h_2 - h_1) Z_2] \Xi_2 > 0$ is equal to

$$\begin{bmatrix} \Phi & \Xi_1^T P & h_2 \Xi_2^T Z_1 & (h_2 - h_1) \Xi_2^T Z_2 \\ * & -P & 0 & 0 \\ * & * & -h_2 Z_1 & 0 \\ * & * & * & (h_2 - h_1) Z_2 \end{bmatrix} < 0 \tag{5.24}$$

For the inequality (5.24), pre- and post-multiplying its left and right sides by $diag\{ I, P^{-1}, Z_1^{-1}, Z_2^{-1} \}$ yields

$$\begin{bmatrix} \Phi & \Xi_1^T & h_2 \Xi_2^T & (h_2 - h_1) \Xi_2^T \\ * & -P^{-1} & 0 & 0 \\ * & * & -h_2 Z_1^{-1} & 0 \\ * & * & * & (h_2 - h_1) Z_2^{-1} \end{bmatrix} < 0 \tag{5.25}$$

Defining $L = P^{-1}$, $W_i = Z_i^{-1} (i = 1, 2)$ in (5.25), we can find that (5.7) and (5.8) hold. So, based on the above analysis, it can be concluded if the conditions (5.7)-(5.11) are satisfied, the system (5.1) can be stabilized by a dynamic output feedback controller with controller $\hat{K}$.

Since the condition (5.8) is not LMI form, we cannot use a convex optimization algorithm to solve the controller gain $\hat{K}$. However, we can also use the cone complementarity linearization algorithm to convert this problem into nonlinear minimization problem like in Chapter 4. So we omit it here.

5.5 Cases Study

In this chapter, the design method of FACTS wide area output-feedback control are also applied into two test systems with series-type FACTS device (TCSC), that is the benchmark test system [5-5] (four-machine two-area test system) for oscillation damping control and the NETS-NYPS interconnected system [5-6] (sixteen-machine five-area test system) to verify the correctness and effectiveness of the presented control concept and controller design approach.

5.5.1 Four-Machine Two-Area System

To enhance the interconnected ability, a series-type FACTS device (TCSC) is installed between Area 1 (G1 and G2) and Area 2, as Figure 5.2 shows. Many research results have shown that the benchmark test system exists at the potential inter-area oscillation between G1-G2 located in Area 1 and G3-G4 located in Area 2. Such oscillation could be excited if there are some disturbances (e.g. load shedding) or faults (e.g. line-to-ground fault). To damp the inter-area oscillation, the wide area control strategy is embedded in the TCSC controller, and the power flow in the tie-line 9-10 is selected as the wide area control-input. After linearizing the test system in the environment of power system toolbox (PST), the TCSC output-feedback-type wide area damping controller (OP-WADCer), which considers the varying-delay of wide area control-input, can be designed according to the presented design approach mentioned in the above section.

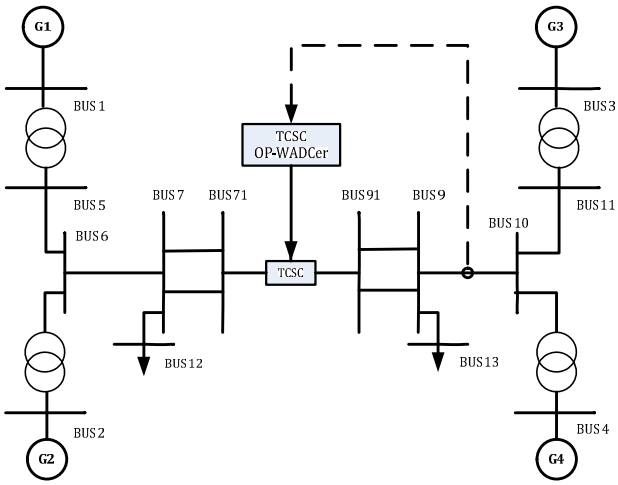

Figure 5.2 Four-machine two-area test system with series-type FACTS device

For the linearized model of the test system including series-type FACTS device, its model order is 57, which is inconvenient to implement the controller design method mentioned in this chapter, hence, the balanced truncation method is used to reduce the order of the test system from 57 to 4. Figure 5.3 gives the frequency response of the full and the reduced order system. The reduced order system is closed to the full order system within 2-10 rad/sec, which indicates that the

reduced order system can reflect the dynamic characteristics of the full order system, and also validates the effectiveness of the model reduction algorithm.

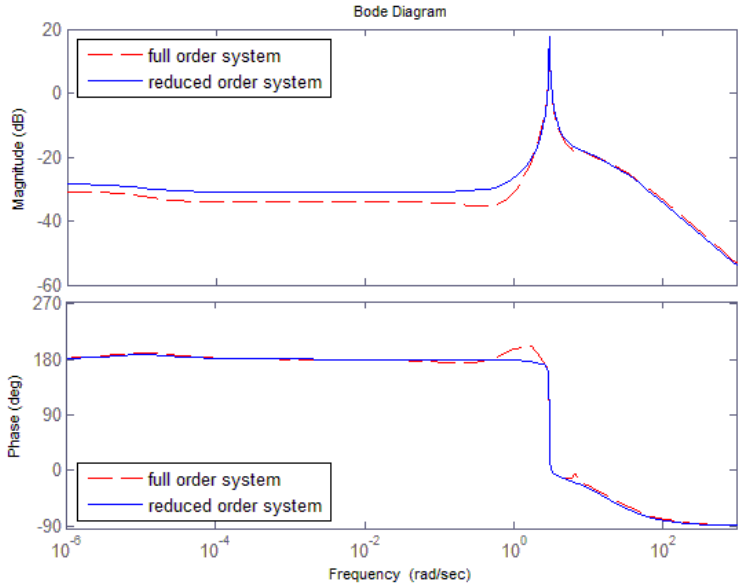

Figure 5.3 Frequency response of the full and the reduced order system

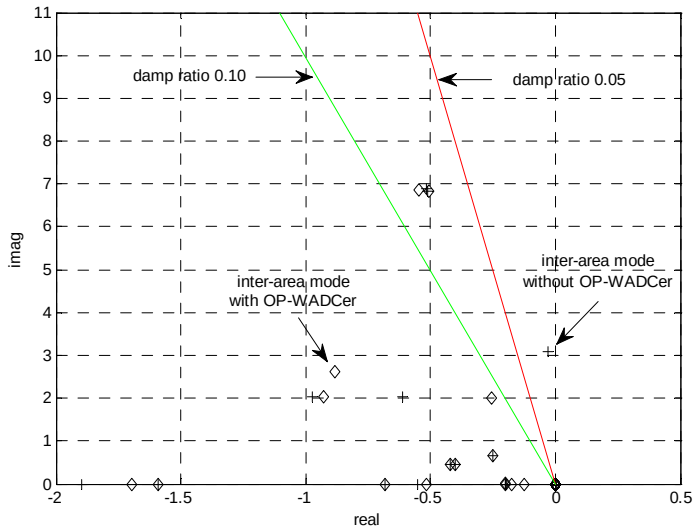

Figure 5.4 Dominant eigenvalues of the test system with or without OP-WADCer

The eigenvalue method is used to analyze the damping performance of the designed OP-WADCer. Figure 5.4 shows the dominant eigenvalues of the test system. In this figure, it can be seen that if

there is no OP-WADCer, the test system contains a typical inter-area oscillation mode with the very weak damping ratio. Its oscillation frequency f and damping ratio ρ is 0.4918 Hz and 0.0092, respectively. Such oscillation is unstable and cannot reach the acceptable minimum damping ratio ρ_{min}=0.050. But for the system with OP-WADCer, the inter-area mode greatly shifts to the left half of the S-plane, and its damping ratio ρ reaches to 0.256, which means that such unstable mode is stabilized greatly.

As said in this chapter, the proposed method can represent the robustness even the wide area control signal exists a certain delay time. To validate this advantage, the eigenvalue method is also performed to further analyze the dominant mode on the condition of various time delay of the wide area control signal. Table 5.1 shows the corresponding results. From this, it can be seen that when the delay time is controlled in the region of 0-400 ms, the designed OP-WADCer maintains good damping performance with the sufficient damping ratio 0.10 (ρ>0.10). Even the delay time reaches to 450 ms, the OP-WADCer can still keep on the effective damping performance (ρ>0.05). In general, for the application of PMUs, the wide area time delay can be controller within 300 ms, thus, from the above analysis, it can be seen that the designed OP-WADCer has the good damping ability on the dominant inter-area oscillation mode, even there are a certain delay time for the wide area control signal.

Table 5.1 Dominant inter-area mode when the control input of OP-WADCer suffers different delay time

Delay time (ms)	Dominant eigenvalue	Frequency f (Hz)	Damping ratio ρ
0	-6.29e-001 ± 2.38e+000i	0.3787888	0.256
100	-9.16e-001 ± 2.44e+000i	0.3883381	0.351
200	-1.48e+000 ± 2.57e+000i	0.4090282	0.497
300	-1.44e+000 ± 4.18e+000i	0.6652677	0.326
400	-5.57e-001 ± 4.28e+000i	0.6811832	0.129
450	-2.96e-001 ± 4.22e+000i	0.6716339	0.0701
500	-1.04e-001 ± 4.13e+000i	0.6573099	0.0252

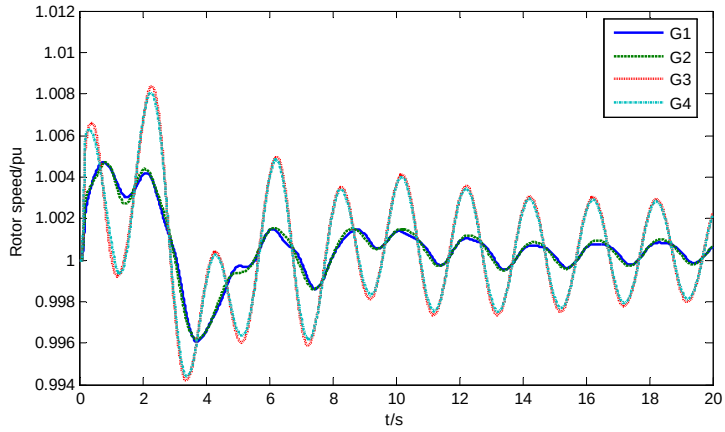

(a)

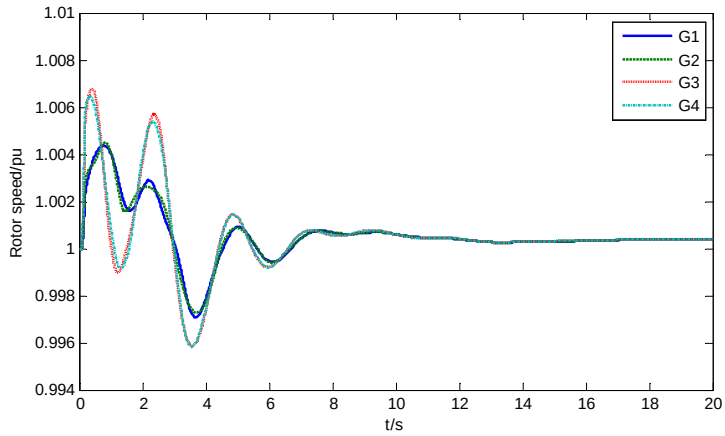

(b)

Figure 5.5 Dynamic response of generator rotor speed of the four-machine two-area system, (a) without TCSC OP-WADCer; (b) with TCSC OP-WADCer

The large disturbance, that is the line-to-ground fault nearby bus 13 of line 13-15, is simulated to validate the damping performance of the designed TCSC OP-WADCer. Such disturbance occurred at 0.1 s, and is cleared at 0.2 s. Figure 5.5 shows the comparison about the dynamic responses of the rotor speed of G1-G4 located in the test system with or without TCSC OP-WADCer. From Figure 5.5(a), it can be seen that when there is no TCSC OP-WADCer, it exists serious power oscillations among generators located in the test system. However, when the system is installed the TCSC OP-

WADCer, such oscillations are damped very well (see Figure 5.5(b)). Furthermore, Figure 5.6 shows the phenomenon of power-angle oscillation between different generators (G1 and G3) located in different Areas (Area 1 and Area 2). From this, it can be further seen that the big disturbance also leads to unstability of the relative angle between different generators located in different areas. But when implementing the TCSC OP-WADC strategy, such unstable phenomenon is eliminated completely within around 10 s (see Figure 5.6).

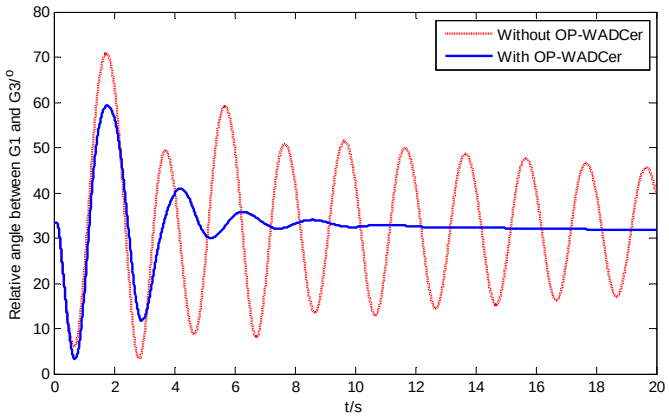

Figure 5.6 Dynamic response of relative angle between G1 and G3 of the four-machine two-area system with or without TCSC OP-WADCer

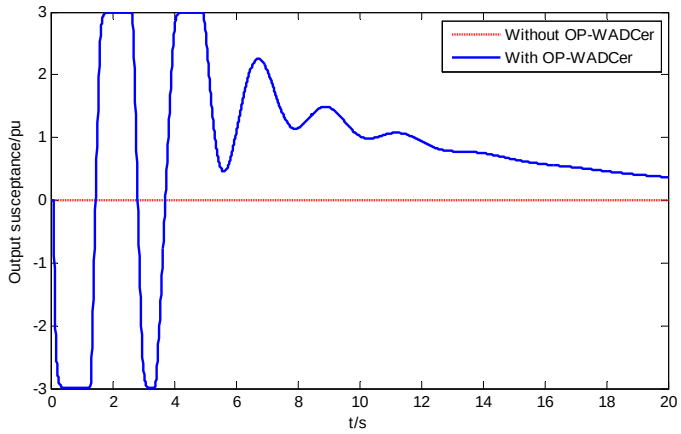

Figure 5.7 Control output response of the four-machine two-area system with or without TCSC OP-WADCer

Figure 5.7 shows the control output response of the TCSC controller. From this, it can be clearly seen that the TCSC device provides the effective susceptance to damp the inter-area oscillation, which validates the effectiveness of the designed TCSC OP-WADCer. Moreover, Figure 5.8 shows the dynamic response of the power flow in the tie-line 3-20. From this, it can be also seen that there is power oscillation that endangers the transmission stability and security of power system. But the designed TCSC OP-WADCer can damp such oscillation and guarantee the stability and security very well, which also validates the technical superiority of FACTS wide area damping strategy.

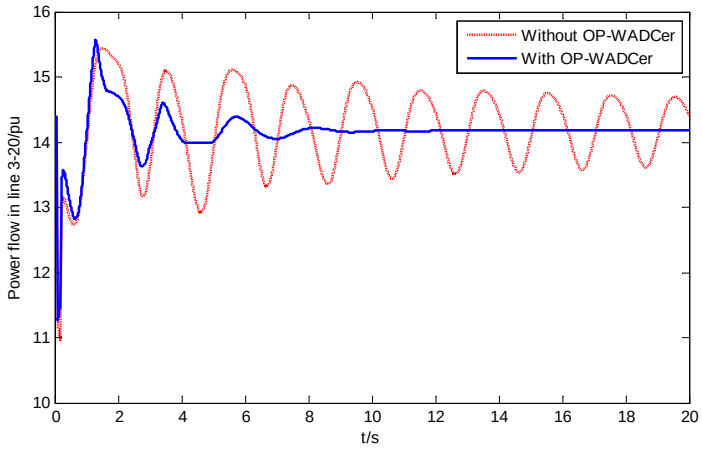

Figure 5.8 Dynamic response of the power flow in tie-line 3-20 of the four-machine two-area test system with or without TCSC OP-WADCer

For the wide area control strategy, the delay effects of wide area signal on control performance should be considered carefully. In this chapter, the varying delay of wide area signal is included when design the TCSC wide area damping controller. To evaluate the robustness and the performance of the TCSC OP-WADCer, the different delay time of wide area signal is simulated, and Figure 5.9 represents the damping performance when the designed TCSC OP-WADCer suffers various time delay of wide area control-input. From this, it can be clearly seen that even the time delay reaches to 500ms, the designed TCSC OP-WADCer still keep on effective damping performance, which validates the control theory and the controller design approach presented in this chapter.

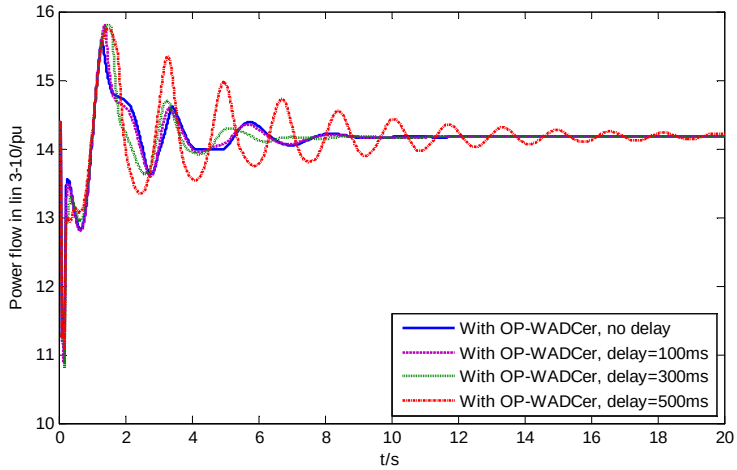

Figure 5.9 Effects of different time delay of wide area control signal on damping performance for the four-machine two-area test system with or without TCSC OP-WADCer

5.5.2 Sixteen-Machine Five-Area Test System

The control concept and design approach for FACTS OP-WADCer is further validated through the more complex power system that is the NETS-NYPS (New England Test System and New York Power System) interconnected system. As discussed in the above chapters, this test system includes the sixteen machines and is divided into five areas. The detailed system parameters can be seen in [5-6]. In this chapter, the series-type FACTS device is installed to interconnect bus-51 with bus-50. The purpose for the FACTS application is to enhance the interconnected ability of such multi-machine multi-area system. Here, the FACTS device is also used to construct wide area damping control strategy to prevent the inter-area oscillation. From the conventional modal analysis method, it can be found that if the line power flow is available for the selection of wide area control-input, the power flow in line 52-68 represents highest observability/controllability. Thus, it is selected as the control-input for TCSC OP-WADCer.

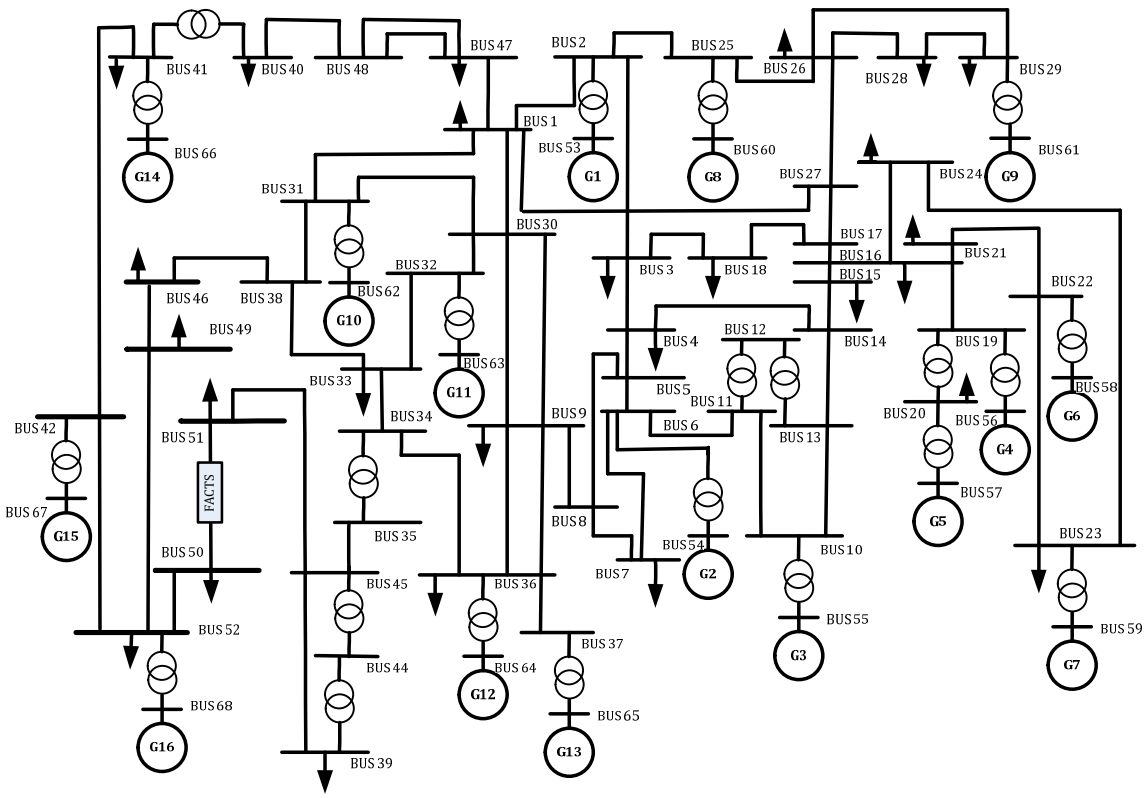

Figure 5.10 Sixteen-machine five-area test system (NETS-NYPS interconnected system) with series-type FACTS device

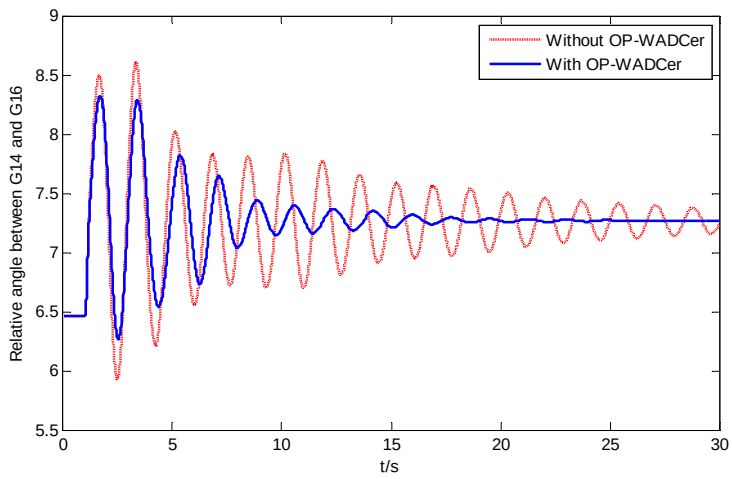

(a)

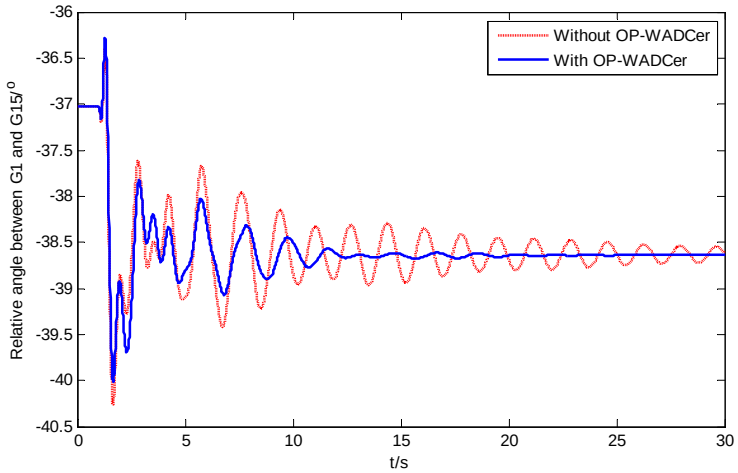

(b)

Figure 5.11 Dynamic responses of relative angle between different generators located in different areas of the sixteen-machine five-area test system, (a) between G14 and G16; (b) between G1 and G15.

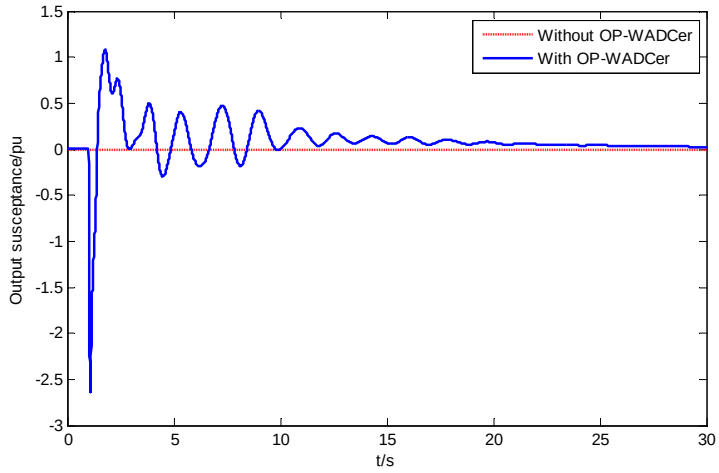

Figure 5.12 Control output response of the sixteen-machine five-area test system with or without TCSC OP-WADCer

A large disturbance (line-to-ground fault near by bus-49 of line 46-49) is set at the 1.0 s with the duration of 0.1 s is simulated in this chapter to validate the designed TCSC OP-WADCer. Figure 5.11 shows the dynamic responses of relative angle between different generators located in different

areas. From this, it can be clearly seen that the designed TCSC OP-WADCer can effectively damp the inter-area oscillations between different generators. In addition, Figure 5.12 represents the output susceptance of TCSC device. From this, it can be further seen that the TCSC plays the effective action for oscillation damping control, which further verifies the effectiveness of the TCSC OP-WADCer designed by means of the presented approach.

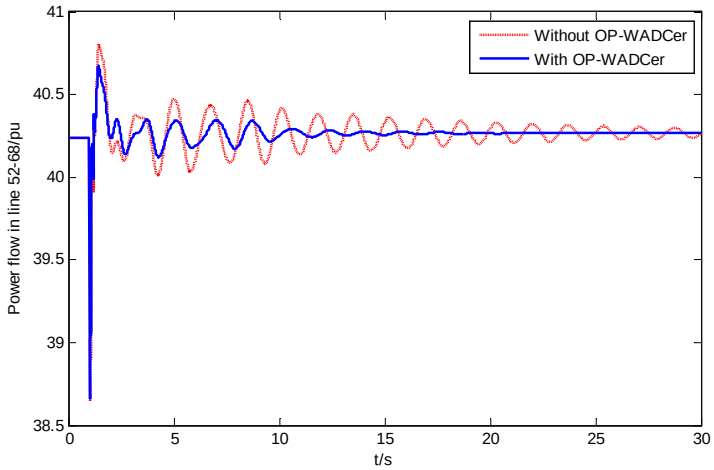

(a)

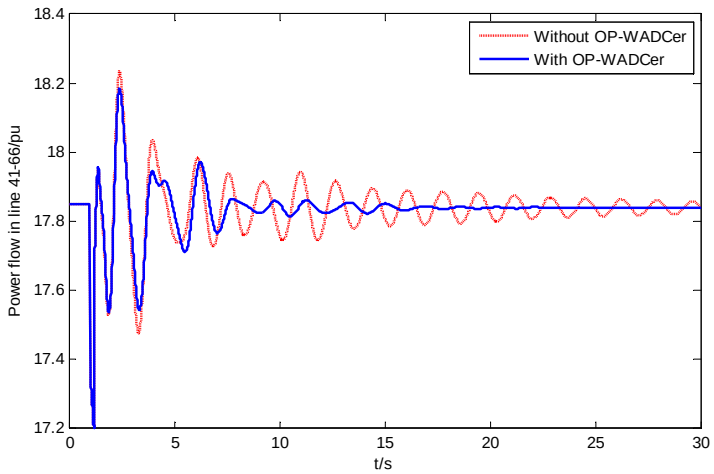

(b)

Figure 5.13 Dynamic responses of the tie-line power flow in the sixteen-machine five-area test system, (a) in the tie-line 52-68; (b) in the tie-line 41-66.

Furthermore, Figure 5.13 represents the dynamic responses of the power flow in the tie-lines. From this, it can be also seen that for the test system without TCSC OP-WADCer, the line-to-ground fault excites the serious power oscillations in the tie-lines. However, when the system is installed with TCSC OP-WADCer, such oscillations can be damped within 15 s. Moreover, in order to evaluate the effects of the time delay on the wide area damping performance, various time delays are considered for wide area signal. Figure 5.14 represents the damping performance under different time delays. From this, it can be clearly seen that although the wide area signal exists a certain delay, the designed TCSC OP-WADCer still maintains good damping performance, which further validates the control concept and design approach mentioned in this chapter.

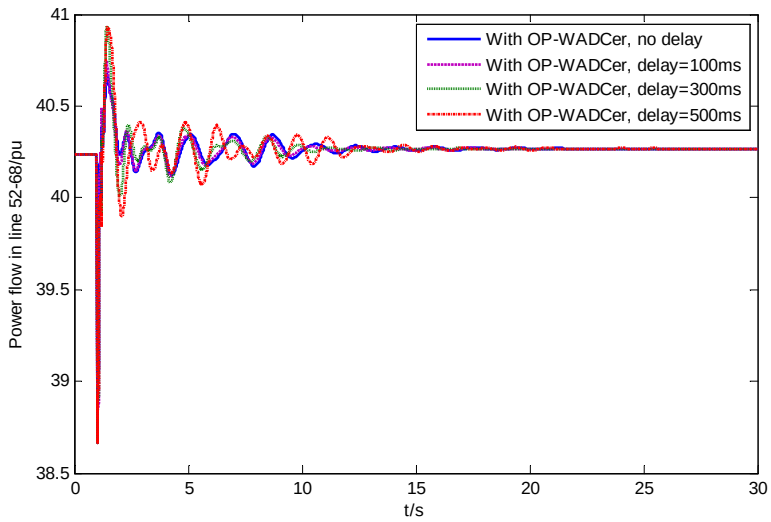

Figure 5.14 Effects of different time delay of wide area control signal on damping performance for the sixteen-machine five-area test system with or without TCSC OP-WADCer

5.6 Conclusion

In this chapter, a dynamic output-feedback-type controller structure is proposed for FACTS wide area damping control strategy. Such controller can implement direct feedback control with considering signal delay of wide area control input, and at the same time can represent a certain robustness against changing of operating conditions. The control concept and the control structure are briefly described, and the discrete-time system model is established with considering time-vary

delay of wide area feedback signal. Then, the stability criterion is discussed in the framework of LMIs, and the controller parameters are determined by the presented theorem. The detailed case studies validated the control concept and the design method of FACTS output-feedback-type control strategy, and further showed the good damping performance and the robustness on the various operating conditions of large-scale interconnected systems.

Chapter References

[5-1] **Y. L. Abdel-Magid, M. Bettayeb.** *Power system output feedback stabilizer design via genetic algorithms*. Genetic algorithms in engineering systems: innovations and applications, 1997. Galesia 97. pp.56-62, 1997.

[5-2] **F. Liu, R. Yokoyama, Y. C. Zhou, M. Wu.** *SVC Robust Additional Damping Controller Design for Power System with Considering Time-delay of Wide-area Signals.* Ninth International Conference on Environment and Electrical Engineering (EEEIC2010), May 16-18, 2010, Prague, Czech

[5-3] **F. Liu, R. Yokoyama, Y. C. Zhou, M. Wu.** *TCSC Wide-Area Damping Controller to Enhance the Damping of Inter-area Oscillation for Power Systems with Considering the Time Delay of Wide-Area Signals*. 2010 International Conference on Power System Technology (POWERCON2010), October, 24-28, 2010, Hangzhou, China

[5-4] **H. Gao, J. Lam, C. Wang, and Y. Wang.** *Delay-dependent output-feedback stabilization of discrete-time systems with time-varying state delay.* IEE Proceedings of Control Theory and Application. Vol. 151, No. 6, pp. 691-698, Nov. 2004.

[5-5] **P. Kundur.** *Power Stability and Control.* New York: McGraw-Hill, 1994.

[5-6] **G. Rogers.** *Power System Oscillations.* Norwell, MA: Kluwer, 1999.

Chapter 6
Wide Area Coordinated Robust Damping Control Strategy of Multiple FACTS Devices for Stability Enhancement of Large-Scale Power Systems

6.1 Introduction

In the practical large-scale interconnected systems, there is not only one but several wide area damping controllers together to stabilize power oscillations and improve stability of power systems. In such a case, the coordination of multiple controllers should be considered carefully [6-1] [6-2] [6-3]. Otherwise, if each controller is designed independently, although each controller can get the effect control performance for the concerned oscillation mode, the interaction among multiple controllers may damage the overall control performance, and the overall stability enhancement maybe not gained. For this consideration, a wide area coordinated damping control strategy is proposed in this chapter. It utilizes multiple FACTS control devices to construct wide area control network. A robust design approach is correspondingly proposed to simultaneously tune all the considered FACTS wide area damping controllers. The controller interaction is considered sufficiently to reduce or even to eliminate the effect of one controller on another one. Besides these, the time-varying delay of each wide area control signal is also considered to maintain control performance.

6.2 Basic Concept of Multiple FACTS Wide Area Coordinated Damping (WACD) Control Strategy

The basic concept of wide-area robust damping control for multiple FACTS devices can be described as shown in Figure 6.1. For the large-scale power systems including kinds of FACTS devices (e.g. shunt-type and series-type FACTS devices), the supplementary control function associated to each FACTS devices can be available for the implementation of wide-area damping control to enhance the overall stability of large-scale power systems.

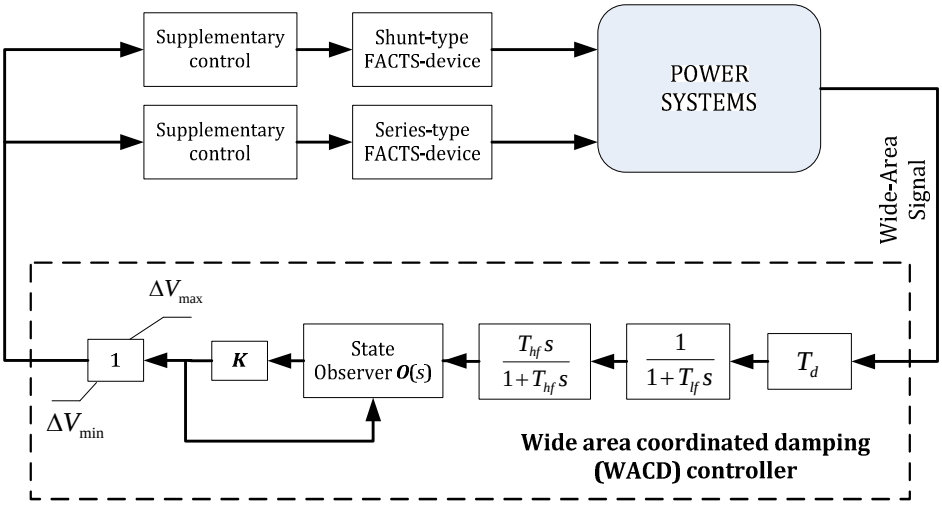

Figure 6.1 Basic framework of robust wide-area coordinated damping (WACD) control of multiple FACTS devices

From the basic framework as shown in Figure 6.1, it can be seen that the wide-area control signals should be determined in advance before constructing wide-area damping control. Generally, kinds of operating variables such as line power flow, line current, rotor speed of remote generator, and so on, can be selected as the wide-area control input. The classic residue method can be used to choose the suitable control input [6-4] [6-5]. In addition, for the wide-area control, the effect of the time delay of the wide area signals on the wide-area control performance should be considered carefully. In this chapter, the Pade approximation [6-6] [6-7] is used to represent the time delay characteristic of the wide area control signals, and the linear robust control theory and design method based on linear matrix inequality is used handle with the robust control problem of the time delay power system.

Furthermore, according to the structure of the wide area robust damping controller as shown in Figure 6.1, it can be seen that the high-pass and the low-pass filters (HPF and LPF) are used to process the wide-area control signals. Besides this, it is worth to say that in this chapter, the designed controller is the typical state-feedback controller, however, in practice, it could be impossible to realize the observation of all the operating states of the large-scale power systems, therefore, the state observer is introduced to converse such state-feedback control as one kind of output-feedback control. In this chapter, the state observer is designed with the classic but practical pole-placement method.

6.3 Robust Design for Multiple FACTS WACD Controller

6.3.1 Problem Formulation

When consider the uncertainty and disturbance of power system, from chapter 2, the linearized power system with series-type FACTS device (TCSC) and shunt-type FACTS device (SVC) can be described as

$$\begin{cases} \dot{x}(t) = Ax(t) + B_1u(t) + B_2\omega(t) \\ z(t) = \begin{bmatrix} Cx(t) + D_2\omega(t) \\ D_1u(t) \end{bmatrix} \end{cases} \tag{6.1}$$

For a given scalar $\gamma > 0$, the performance of the system is defined to be

$$J(\omega) = \int_0^\infty z^T(t)z(t) - \gamma^2\omega^T(t)\omega(t)dt \tag{6.2}$$

The H_∞ robust control problem addressed in this chapter can be stated as described as: for a memory state-feedback controller, find a value for the gain $K \in \Re^{m\times n}$, in the control law

$$u(t) = Kx(t - \tau(t)) \tag{6.3}$$

Such that for any time-varying delay , satisfying

$$\begin{cases} 0 \le \tau(t) \le h \\ \dot{\tau}(t) \le \mu \end{cases} \tag{6.4}$$

The closed-loop system (6.1) should be asymptotically stable under the condition $\omega(t) = 0$;

$J(\omega) < 0$ for all non-zero $\omega(t)$ under the zero initial condition and a given $\gamma > 0$.

So the system(6.1) can be described as

$$\begin{cases} \dot{x}(t) = Ax(t) + B_1Kx(t - \tau(t)) + B_2w(t) \\ z(t) = \begin{bmatrix} Cx(t) + D_2w(t) \\ D_1Kx(t - \tau(t)) \end{bmatrix} \end{cases} \tag{6.5}$$

6.2 Bounded Real Lemma (BRL)

Before the delay-dependent H∞ robust design for the supplementary wide-area stabilizing control of FACTS devices, a new delay-dependent bounded real lemma (BRL) of the closed-loop system (6.5) is derived by using FWM approach. Before discussion, the following lemmas will be employed in the proofs of our results. And the notion $*$ stands for the symmetric matrix.

Lemma 1[6-8]: For given matrice $Q = Q^T$, H, and E with appropriate dimensions,

$$Q + HF(t)E + E^T F^T(t) H^T < 0$$

hold for all $F(t)$ satisfying all $F(t)F^T(t)H^T < I$ if and only if there exists $\varepsilon > 0$ such that

$$Q + \varepsilon HH^T + \varepsilon EE^T < 0$$

Lemma 2[6-9]:There exists a symmetric matrix X such that

$$\begin{bmatrix} P_1 + X & Q_1 \\ * & R_1 \end{bmatrix} > 0, \quad \begin{bmatrix} P_2 - X & Q_2 \\ * & R_2 \end{bmatrix} > 0,$$

if and only if

$$\begin{bmatrix} P_1 + P_2 & Q_1 & Q_2 \\ * & R_1 & 0 \\ * & * & R_2 \end{bmatrix} > 0$$

Theorem 1 Consider system (6.1) with $u(t) = 0$. Given scalar $h \geq 0$, μ, and $\gamma > 0$, the system is asymptotically stable and satisfies $J(\omega) < 0$ for all non-zero $\omega(t)$ under the zero initial condition if there exist matrices $P > 0$, $Q_i > 0, i = 1,2$, $Z > 0$ and $X > 0$ and any appropriately dimensioned matrices N, M such that the following LMIs hold:

$$\Omega = \begin{bmatrix} \Phi & h\Xi^T Z & \Pi_1^T & \Pi_2^T \\ * & -hR & 0 & 0 \\ * & * & -I & 0 \\ * & * & * & -I \end{bmatrix} < 0 \tag{6.6}$$

$$\Omega_1 = \begin{bmatrix} X_{11} & X_{12} & X_{13} & N_1 \\ * & X_{22} & X_{23} & N_2 \\ * & * & X_{33} & N_3 \\ * & * & * & Z \end{bmatrix} > 0 \tag{6.7}$$

$$\Omega_2 = \begin{bmatrix} X_{11} & X_{12} & X_{13} & M_1 \\ * & X_{22} & X_{23} & M_2 \\ * & * & X_{33} & M_3 \\ * & * & * & Z \end{bmatrix} > 0 \tag{6.8}$$

where

$$\Phi = \begin{bmatrix} PA + A^T P + N_1 + N_1^T + Q_1 + Q_2 + hX_{11} & PB_1K - N_1 + N_2^T + M_1 + hX_{12} & N_3^T - M_1 + hX_{13} & PB_2 \\ * & -(1-\mu)Q_1 - N_2 - N_2^T + M_2 + M_2^T + hX_{22} & -N_3^T + M_3^T - M_2 + hX_{23} & 0 \\ * & * & -Q_2 - M_3 - M_3^T + hX_{33} & 0 \\ * & * & * & -\gamma^2 I \end{bmatrix}$$

$$\Xi = \begin{bmatrix} A & BK & 0 & B_2 \end{bmatrix}$$

$$\Pi_1 = \begin{bmatrix} C & 0 & 0 & D_2 \end{bmatrix}$$

$$\Pi_2 = \begin{bmatrix} 0 & D_1K & 0 & 0 \end{bmatrix}$$

Proof: Construct the following Lyapunov candidate function:

$$V(x_t) = x^T(t)Px(t) + \int_{t-\tau(t)}^{t} x^T(s)Q_1x(s) + \int_{t-h}^{t} x^T(s)Q_2x(s) + \int_{-h}^{0}\int_{t+\theta}^{t} \dot{x}^T(s)Z\dot{x}(s)dsd\theta \tag{6.9}$$

where $P = P^T > 0$, $Q_i = Q_i^T > 0, i = 1,2$, $Z = Z^T > 0$.

Calculating the derivative of $V(x_t)$ along the solutions of system (6.1) and using the FWMs approach, it obtained:

$$
\begin{aligned}
\dot{V}(x_t) &= \dot{x}^T(t)Px(t) + x^T(t)P\dot{x}(t) + x^T(t)Q_1x(t) - (1-\dot{\tau}(t))x^T(t-\tau(t))Q_1x(t-\tau(t)) \\
&+ x^T(t)Q_2x(t) - x^T(t-h)Q_2x(t-h) + h\dot{x}^T(t)Z\dot{x}(t) - \int_{t-h}^{t}\dot{x}^T(s)Z\dot{x}(s)ds \\
&\le x^T(t)(PA + A^TP)x(t) + 2x^T(t)PB_1Kx(t-\tau(t)) + 2x^T(t)PB_2w(t) \\
&\quad + x^T(t)(Q_1+Q_2)x(t) - (1-\mu)x^T(t-\tau(t))Q_1x(t-\tau(t)) - x^T(t-h)Q_2x(t-h) \\
&\quad + h\dot{x}^T(t)Z\dot{x}(t) - \int_{t-h}^{t}\dot{x}^T(s)Z\dot{x}(s)ds \\
&\quad + 2[x^T(t)N_1 + x^T(t-\tau(t))N_2 + x^T(t-h)N_3][x(t) - x(t-\tau(t)) - \int_{t-\tau(t)}^{t}\dot{x}(s)ds] \\
&\quad + 2[x^T(t)M_1 + x^T(t-\tau(t))M_2 + x^T(t-h)M_3][x(t-\tau(t)) - x(t-h) - \int_{t-h}^{t-\tau(t)}\dot{x}(s)ds] \\
&\quad + h\xi^T(t)X\xi(t) - \int_{t-h(t)}^{t}\xi^T(t)X\xi(t)ds \\
&= \xi_1^T(t)[\Phi + h\Xi^TR\Xi]\xi_1(t) - \int_{t-\tau(t)}^{t}\xi_2^T(t,s)\Psi_1\xi_2(t,s)ds - \int_{t-h}^{t-\tau(t)}\xi_2^T(t,s)\Psi_2\xi_2(t,s)ds + \gamma^2\omega^T(t)\omega(t)
\end{aligned}
\tag{6.10}
$$

Where

$$
\Phi = \begin{bmatrix}
PA + A^TP + N_1 + N_1^T + Q_1 + Q_2 + hX_{11} & PB_1K - N_1 + N_2^T + M_1 + hX_{12} & N_3^T - M_1 + hX_{13} & PB_2 \\
* & -(1-\mu)Q_1 - N_2 - N_2^T + M_2 + M_2^T + hX_{22} & -N_3^T + M_3^T - M_2 + hX_{23} & 0 \\
* & * & -Q_2 - M_3 - M_3^T + hX_{33} & 0 \\
* & * & * & -\gamma^2 I
\end{bmatrix}
$$

$$
\Xi = \begin{bmatrix} A & B_1K & 0 & B_2 \end{bmatrix}
$$

$$
\xi(t) = \begin{bmatrix} x^T(t) & x^T(t-\tau(t)) & x^T(t-h) \end{bmatrix}^T
$$

$$
\xi_1(t) = \begin{bmatrix} x^T(t) & x^T(t-\tau(t)) & x^T(t-h) & \omega^T(t) \end{bmatrix}^T
$$

$$
\xi_2(t,s) = \begin{bmatrix} x^T(t) & x^T(t-\tau(t)) & x^T(t-h) & \dot{x}^T(s) \end{bmatrix}
$$

$$
\Psi_1 = \begin{bmatrix}
X_{11} & X_{12} & X_{13} & N_1 \\
* & X_{22} & X_{23} & N_2 \\
* & * & X_{33} & N_3 \\
* & * & * & Z
\end{bmatrix}
$$

$$\Psi_2 = \begin{bmatrix} X_{11} & X_{12} & X_{13} & M_1 \\ * & X_{22} & X_{23} & M_2 \\ * & * & X_{33} & M_3 \\ * & * & * & Z \end{bmatrix}$$

From the inequality of Eq. (6.10), it can be obtained

$$\begin{aligned} &\dot{V}(x_t) + z^T(t)z(t) - \gamma^2\omega^T(t)\omega(t) \\ &\quad \le \xi_1^T(t)[\Phi + h\Xi^T R\Xi]\xi_1(t) - \int_{t-\tau(t)}^{t} \xi_2^T(t,s)\Psi_1\xi_2(t,s)ds - \int_{t-h}^{t-\tau(t)} \xi_2^T(t,s)\Psi_2\xi_2(t,s)ds + z^T(t)z(t) \\ &\quad = \xi_1^T(t)[\Phi + h\Xi^T Z\Xi + \Pi_1^T\Pi_1 + \Pi_2^T\Pi_2]\xi_1(t) - \int_{t-\tau(t)}^{t} \xi_2^T(t,s)\Psi_1\xi_2(t,s)ds - \int_{t-h}^{t-\tau(t)} \xi_2^T(t,s)\Psi_2\xi_2(t,s)ds \end{aligned} \tag{6.11}$$

where $\Pi_1 = \begin{bmatrix} C & 0 & 0 & D_2 \end{bmatrix}$, $\Pi_2 = \begin{bmatrix} 0 & DK & 0 & 0 \end{bmatrix}$

If $\Psi_i \ge 0, (i = 1,2)$ and the LMI (6.6) is true , using **Lemma 1** and **2**, it is easy to obtain $\Phi + h\Xi^T Z\Xi < 0$, which means system(6.1) is asymptotically stable with $\omega(t) = 0$.

On the other hand, if $\Psi_i \ge 0, (i = 1,2)$ and the LMI (6.6) is true, it is also easy to obtain $\Phi + h\Xi^T Z\Xi + \Pi_1^T\Pi_1 + \Pi_2^T\Pi_2 < 0$, then $\dot{V}(x_t) + z^T(t)z(t) - \gamma^2 w^T(t)w(t) < 0$.

That is

$$z^T(t)z(t) - \gamma^2 w^T(t)w(t) < -\dot{V}(x_t) \tag{6.12}$$

On both sides of Eq. (6.12), integral from 0 to ∞ with respect to *t* yields

$$\int_0^\infty [z^T(t)z(t) - \gamma^2 w^T(t)w(t)]dt < V(0) - V(\infty)\,. \tag{6.13}$$

It is straightforward to see

$$\int_0^\infty [z^T(t)z(t) - \gamma^2 w^T(t)w(t)]dt < 0 \tag{6.14}$$

6.2 H_∞ Controller Design

This section extends Theorem 1 to the design of an $H\infty$ controller for system (8.1) under control law (6.3).

Theorem 2 Consider closed-loop system (6.5). For given scalar $h \geq 0$, μ, and $\gamma > 0$, if there exist matrices $L > 0$, $\widehat{Q}_i > 0, i = 1,2$, $W > 0$ and $Y > 0$ and any appropriately dimensioned matrices $\widehat{N}, \widehat{M}$ and V such that the following matrix inequalities hold:

$$\begin{bmatrix} \widehat{\Phi}_{11} & \widehat{\Phi}_{12} & \widehat{\Phi}_{13} & B_2 & hLA^T & LC^T & 0 \\ * & \widehat{\Phi}_{11} & \widehat{\Phi}_{23} & 0 & hV^T B^T & 0 & V^T D_1 \\ * & * & \widehat{\Phi}_{33} & 0 & 0 & 0 & 0 \\ * & * & * & -\gamma^2 I & hB_2^T & D_2^T & 0 \\ * & * & * & * & -hI & 0 & 0 \\ * & * & * & * & * & -I & 0 \\ * & * & * & * & * & * & -I \end{bmatrix} < 0 \tag{6.15}$$

$$\begin{bmatrix} Y_{11} & Y_{12} & Y_{13} & \widehat{N}_1 \\ * & X_{22} & X_{23} & \widehat{N}_2 \\ * & * & X_{33} & \widehat{N}_3 \\ * & * & * & LW^{-1}L \end{bmatrix} > 0 \tag{6.16}$$

$$\begin{bmatrix} Y_{11} & Y_{12} & Y_{13} & \widehat{M}_1 \\ * & Y_{22} & Y_{23} & \widehat{M}_2 \\ * & * & Y_{33} & \widehat{M}_3 \\ * & * & * & LW^{-1}L \end{bmatrix} > 0 \tag{6.17}$$

where

$$\widehat{\Phi}_{11} = AL + LA^T + \widehat{N}_1 + \widehat{N}_1^T + \widehat{Q}_1 + \widehat{Q}_2 + hY_{11}$$
$$\widehat{\Phi}_{12} = B_1 V - \widehat{N}_1 + \widehat{N}_2^T + \widehat{M}_1 + hY_{12}$$
$$\widehat{\Phi}_{13} = \widehat{N}_3^T - \widehat{M}_1 + hY_{13}$$
$$\widehat{\Phi}_{22} = -(1-\mu)\widehat{Q}_1 - \widehat{N}_2 - \widehat{N}_2^T + \widehat{M}_2 + \widehat{M}_2^T + hY_{22}$$
$$\widehat{\Phi}_{23} = -\widehat{N}_3^T + \widehat{M}_3^T - \widehat{M}_2 + hY_{23}$$
$$\widehat{\Phi}_{33} = -\widehat{Q}_2 - \widehat{M}_3 - \widehat{M}_3^T + hY_{33}$$

Then the system is asymptotically stable and satisfies $J(\omega) < 0$ for all non-zero $\omega(t)$ under the zero initial condition and a stabilizing H_∞ Controller $u(t) = VL^{-1}x(t)$.

Define

$$\Pi = diag\{P^{-1} \quad P^{-1} \quad P^{-1} \quad I \quad Z^{-1} \quad I \quad I\}$$
$$\Theta = diag\{P^{-1} \quad P^{-1} \quad P^{-1} \quad P^{-1}\}$$

Pre- and post-multiply Ω in (6.6) by Π; pre- and post-multiple $\Omega_i, i = 1,2$ in (6.7) and (6.8) by Θ and make the following changes in the variables:

$$L = P^{-1}$$
$$\widehat{N}_i = P^{-1}N_iP^{-1}, i = 1,2,3$$
$$\widehat{M}_i = P^{-1}M_iP^{-1}, i = 1,2,3$$
$$\widehat{Q}_i = P^{-1}Q_iP^{-1}, i = 1,2$$
$$Y = P^{-1}XP^{-1}$$
$$W = Z^{-1}$$

Then, (6.15)-(6.17) are derived using the Schur complement[6-10]. This completes the proof.

Note that the conditions in Theorem 2 are no longer LMI conditions due to the terms $LW^{-1}L$ in (6.16) and (6.17). As mentioned in Chapter 4, we can solve this nonconvex problem by using the idea for solving a cone complementarity problem. So we omit it here.

6.4 Cases Study

6.4.1 Four-Machine Two-Area Test System with Multiple FACTS Devices

To validate the designed multiple FACTS wide-area damping controller, the four-machine two-area test system [6-11], which is also the benchmark system for the oscillation damping study, is simulated in this chapter. Here, such test system is modified by placing one series-type FACTS device (TCSC) to enhance the interconnected ability and meanwhile one shunt-type FACTS device (SVC) to satisfy the voltage profile of Bus-7, as shown in Figure 6.2. Such test system is divided into two areas, in which, G1 and G2 belong to Area-1, and G3 and G4 belong to Area-2.

The modal analysis indicates that there is a typical inter-area oscillation mode between Area-1 and -2. Such mode is further represented as the oscillation between G1 (in Area-1) and G3 (in Area-2). Furthermore, the results of the residue analysis indicate that if the current in line 9-10 is selected as the wide-area control input for the multiple FACTS wide-area damping controller, the high controllability can be achieved. Therefore, the current in line 9-10 is chosen, and the formed FACTS-WACD controller has been simply represented in Figure 6.1. The controller parameter can be obtained according to the robust design method presented in the above section.

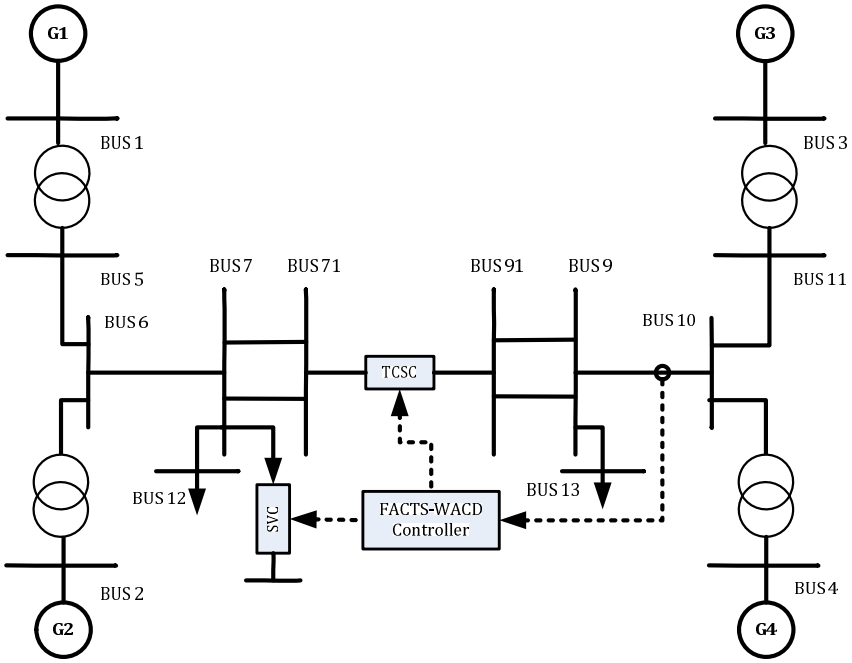

Figure 6.2 Modified four-machine two-area test system installed with multiple FACTS devices

To reveal the damping performance of the designed multiple FACTS WACD controller, a large disturbance (three-phase-to-ground fault nearby bus 13 of line 13-9) is carried out at 0.1 s with the duration of 0.1 s. Figure 6.3 shows the dynamic responses of the rotor speed of each generator located in the different areas of the test system. From Figure 6.3(a), it can be clearly seen for the test system without the multiple FACTS WACD controller, the disturbance exists the typical inter-area oscillation between Area 1 (G1 and G2) and Area 2 (G3 and G4). Different from this, for the test system installed with the designed WACD controller, from Figure 6.3(b), it can be clearly seen that such oscillation is damped quickly, which validates the effectiveness of the design approach for the multiple FACTS WACD control strategy.

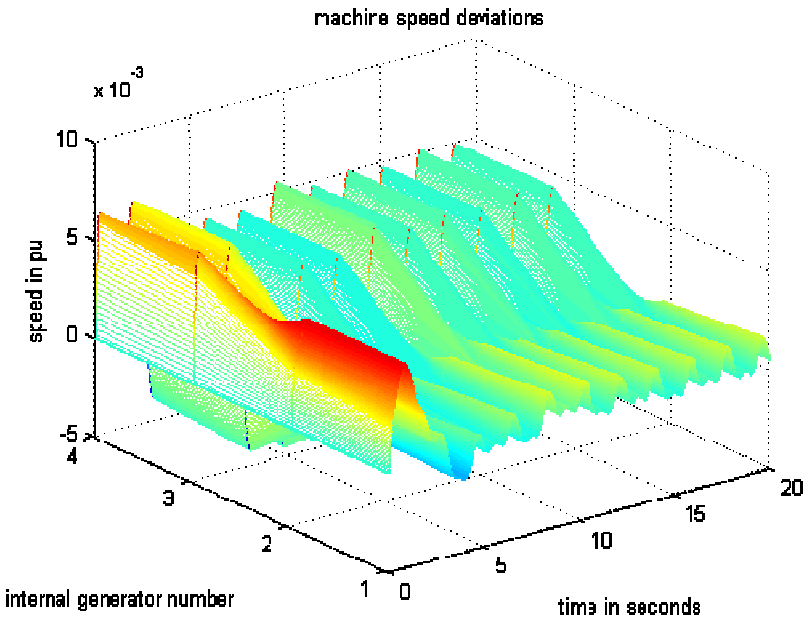

(a)

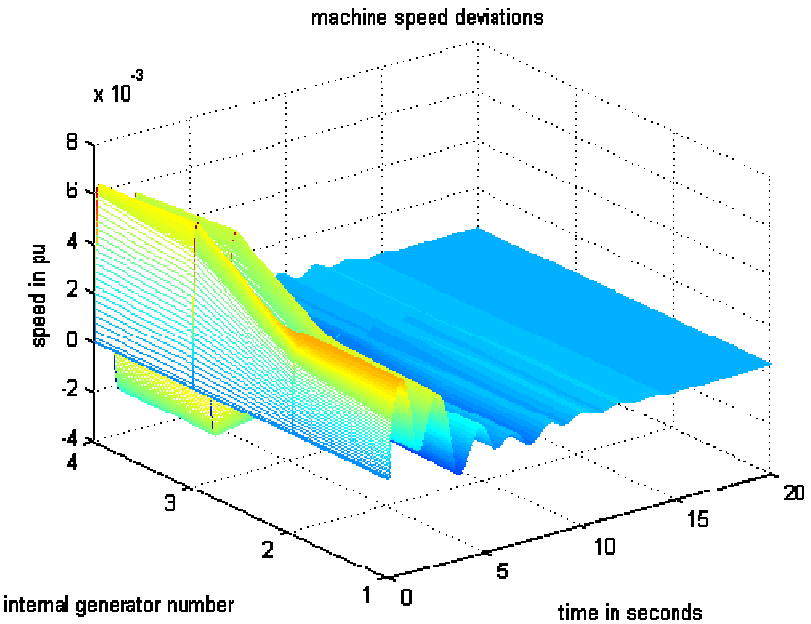

(b)

Figure 6.3 Dynamic response of generator rotor speed of the four-machine two-area test system, (a) without multiple FACTS WACD controller; (b) with multiple FACTS WACD controller

Furthermore, Figure 6.4 represents the dynamic response of the relative angle between G1 (located in Area 1) and G3 (located in Area 2). From this, it further indicates the obvious feature of the inter-area oscillation in the interconnected system. But when the test system is installed with multiple FACTS WACD controller, such serious inter-area oscillation mode is damped effectively. In addition, Figure 6.5 further represents the dynamic response of the power flow in the tie transmission line. From this, it can be also seen that the serious power oscillation in the tie-line is damped very well with the application of multiple FACTS wide area damping control strategy.

To evaluate the effects of signal time delay on the wide area damping performance, different time delays are acted on both the SVC and the TCSC wide area signal. Here, the delays of both the control-input and the control-output signals are wholly equivalent to such defined time delays. Figure 6.6 shows the dynamic responses of the test system with different time delays of the wide area signals. From this, it is clearly seen that even there exists various delays for multiple FACTS wide area control signals, the designed WACD controller can maintain the good damping performance on the inter-area oscillation.

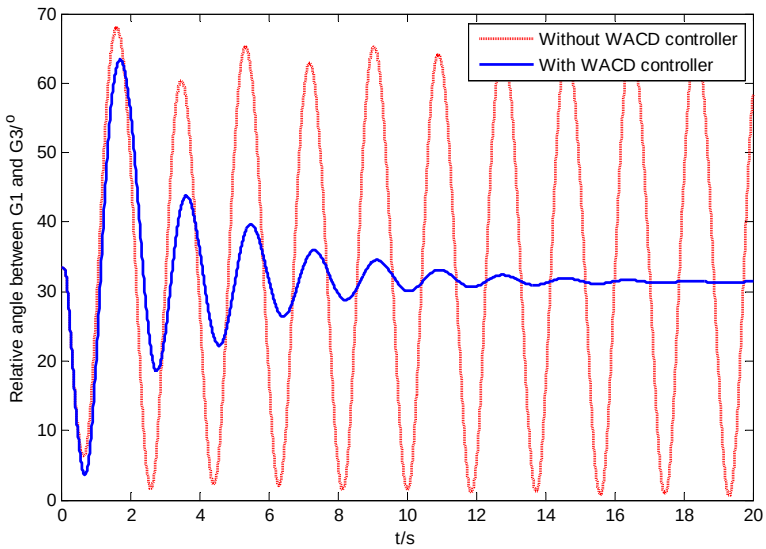

Figure 6.4 Dynamic response of relative angle between G1 and G3 located in the four-machine two-area test system with or without multiple FACTS WACD controller

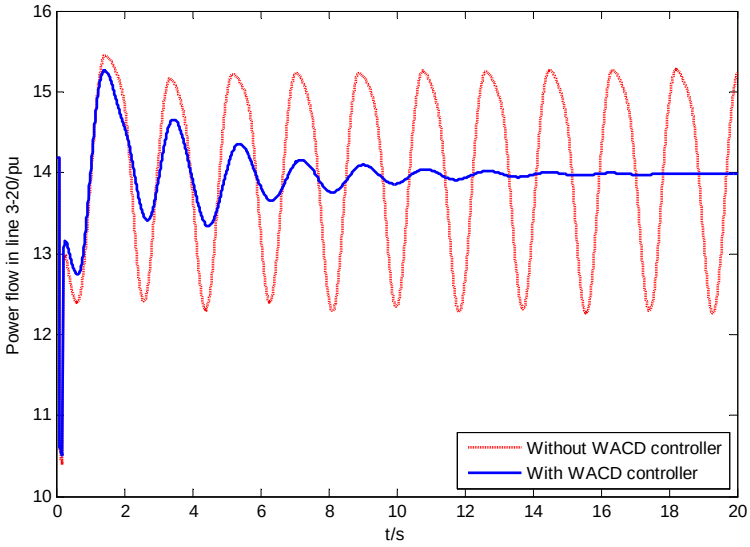

Figure 6.5 Dynamic response of power flow in the tie-line 3-20 of the four-machine two-area test system with or without multiple FACTS WACD controller

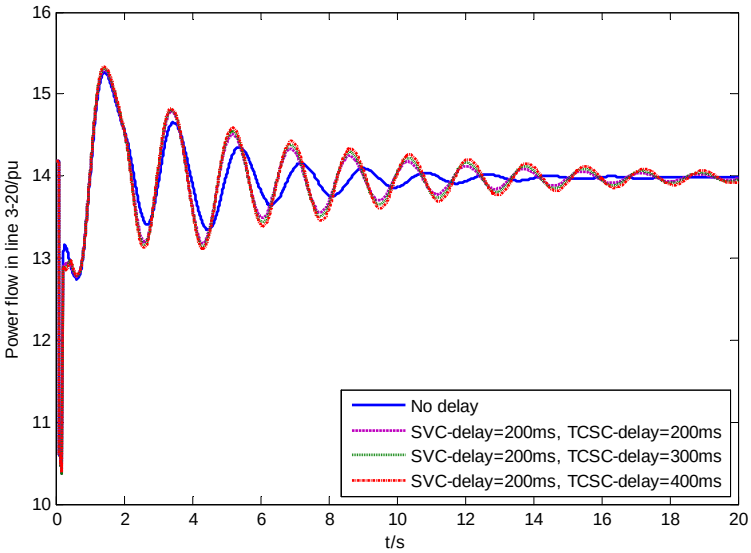

Figure 6.6 Effects of different time delay of wide area signals on damping performance for the four-machine two-area test system with or without multiple FACTS WACD controller

6.4.2 Sixteen-Machine Five-Area Test System with Multiple FACTS Devices

In this section, the sixteen-machine five-area test system (NETS-NYPS interconnected system) [6-12] is used to further validate the presented control concept and the designed multiple FACTS WACD controller in the large-scale power systems. Figure 6.7 shows the single-line diagram of the NETS-NYPS interconnected system. To enhance the interconnected ability and improve bus voltage stability, one series-type FACTS device (TCSC) is placed between bus 1 and bus 2, and one shunt-type FACTS device (SVC) is placed at bus 51. The power flow in the tie-line 68-52 is selected as the wide area control-input signal for both the SVC and TCSC, and the WACD controller is in charge of distributing wide area control-output signal to each SVC and TCSC device located in the different areas of the large-scale power system.

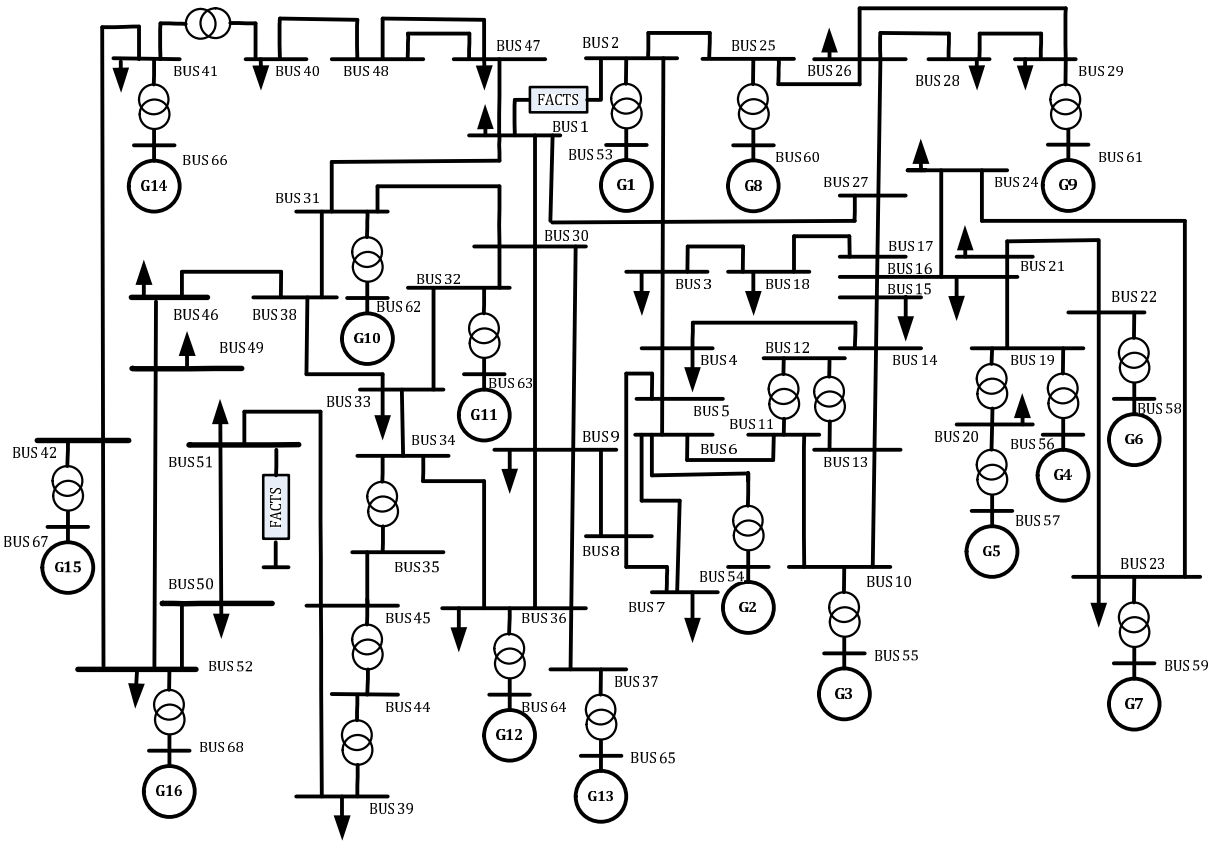

Figure 6.7 Modified NETS-NYPS interconnected system installed with multiple FACTS devices

A serious line-to-ground fault is carried out nearby the bus 47 of the interconnected line 1-47, and it starts at 1.0 s and continues 0.1 s before fault clearing. Figure 6.8 shows the dynamic responses of the relative angle between different generators located in different areas of the NETS-NYPS interconnected system with or without multiple FACTS WACD controller. From this, it can be clearly seen that the designed controller can effectively damp the inter-area oscillation between different generators located in different areas. Figure 6.9 further represents the dynamic responses of the output susceptance of the multiple FACTS devices. From this, it can be clearly seen that the both the series-type and the shunt-type FACTS device with WACD controller can play the effective action to prevent the inter-area oscillation, which verifies the correctness of the presented control concept and the designed WACD controller.

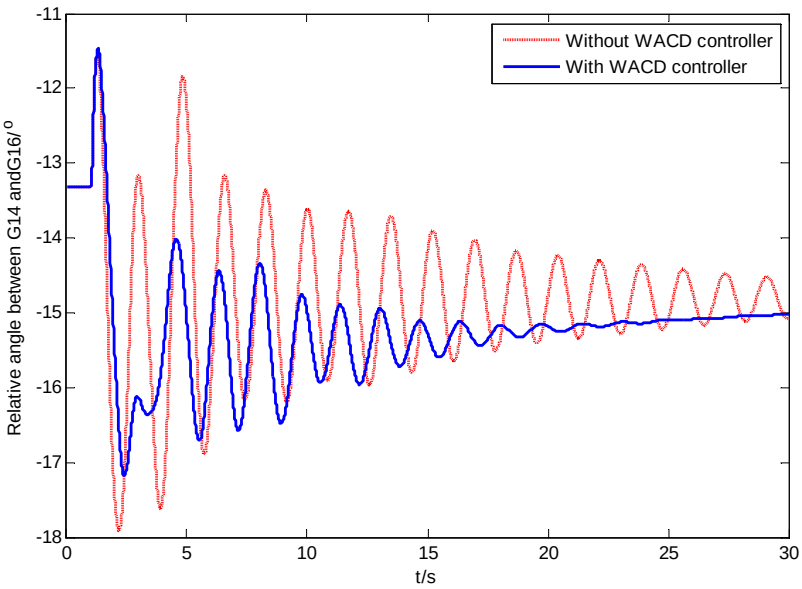

(a)

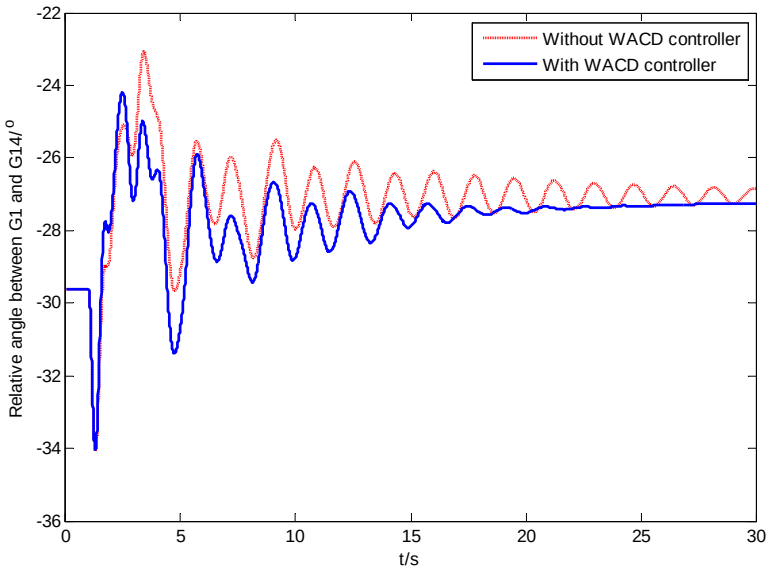

(b)

Figure 6.8 Dynamic responses of the relative angle between different generators located in different areas of the NETS-NYPS interconnected system with or without multiple FACTS WACD controller, (a) between G14 and G16; (b) between G1 and G16.

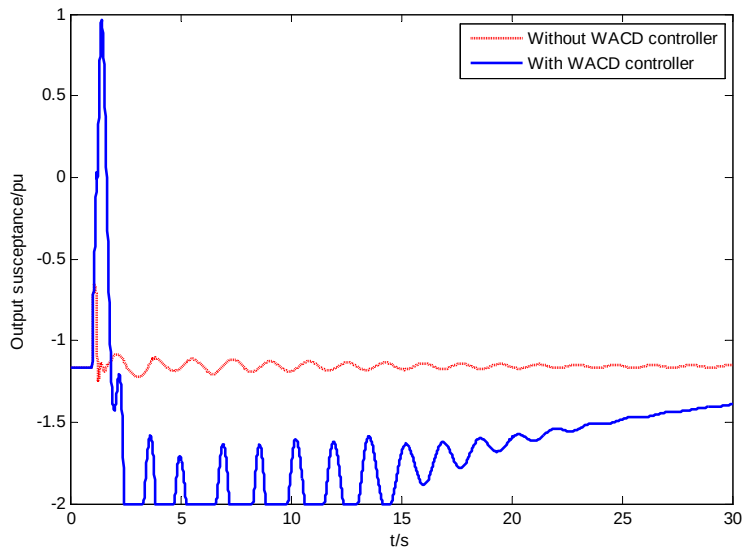

(a)

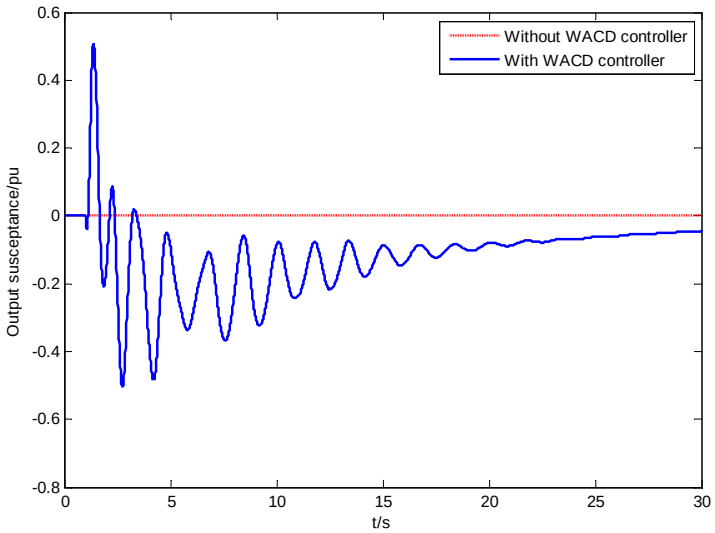

(b)

Figure 6.9 Control output responses of the NETS-NYPS interconnected system with or without multiple FACTD WACD controller, (a) control-output of SVC; (b) control-output of TCSC.

Furthermore, Figure 6.10 represents the dynamic responses of the power flow in the tie-lines of the large-scale power system, which also indicates that the designed multiple FACTS WACD controller can effectively damp the power oscillation in the tie transmission lines, which is advantage to the stability and security operation of large-scale interconnected network. In addition, Figure 6.11 shows the dynamic response of the tie-line power flow of the test system that includes different time delay of wide area signals. From this, it can be also seen that the designed multiple FACTS WACD controller can keep on good damping performance even the wide area signals have a certain time delay caused by the transmission and the processing of wide area signals.

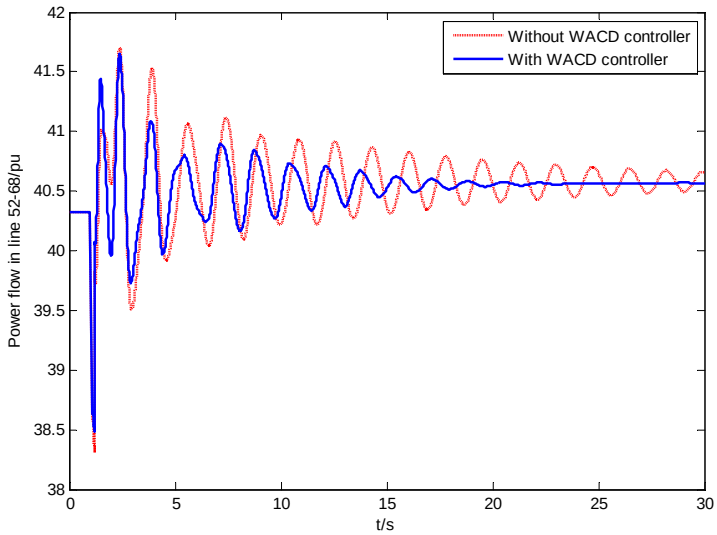

(a)

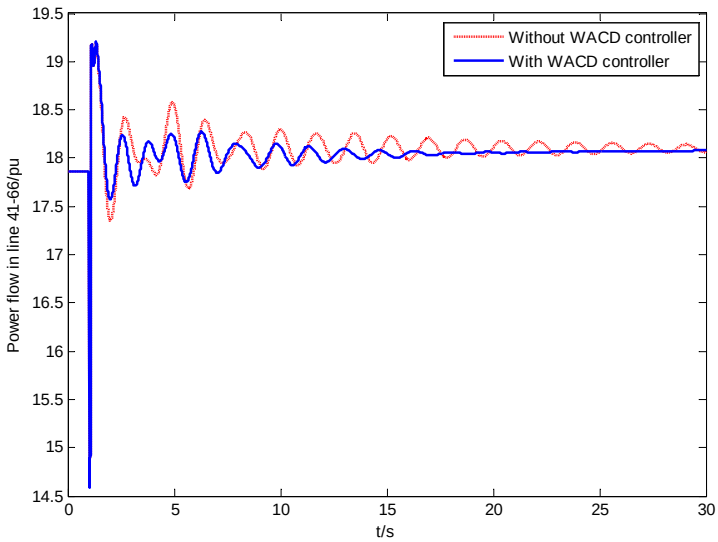

(b)

Figure 6.10 Dynamic responses of the tie-line power flow in the NETS-NYPS interconnected system with or without multiple FACTS WACD controller, (a) in the tie-line 52-68; (b) in the tie-line 41-66.

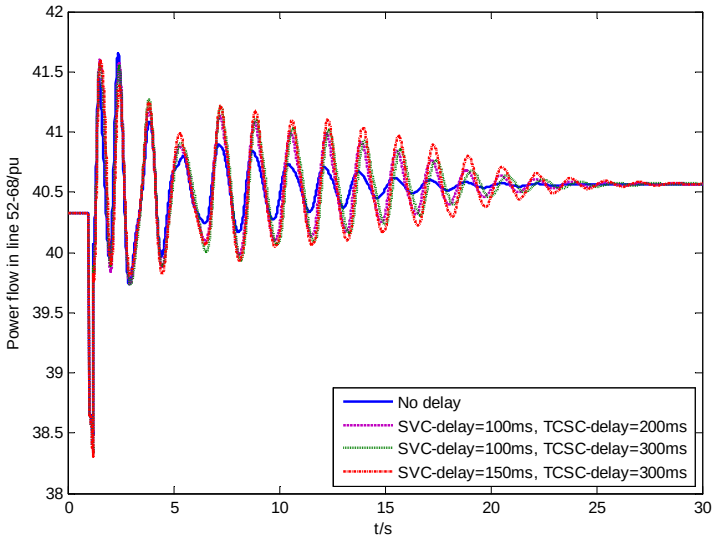

Figure 6.11 Effects of different time delay of wide area signals on damping performance of NETS-NYPS interconnected system with or without multiple FACTS WACD controller

6.5 Conclusion

In this chapter, a wide area coordinated robust damping control strategy is proposed to improve the overall stability of large-scale power systems. For the large-scale power systems, it may include multiple FACTS devices. Here, these FACTS devices are further developed to implement wide area damping control strategy together. The basic concept and the controller structure are discussed briefly, and then a robust design approach is presented to handle with multiple controllers design and the multiple time delays of wide area control signals. Two case studies validate the presented control concept and controller design approach, and further indicates the good damping performance under various operating conditions and when suffering various time-varying delays of different wide area signals.

Chapter References

[6-1] **I. Kamwa, R. Grondin, and Y. Hebert.** *Wide-area measurement based stabilizing control of large power systems-a decentralized/hierarchical approach.* IEEE Transaction on Power Systems. Vol. 16, No. 1, pp. 136–153, Feb. 2001.

[6-2] **E. Johansson, K. Uhlen, A. B. Leirbukt, P. Korba, J. O. Gjerde, and L. K. Vormedal.** *Coordinating power oscillation damping control using wide area measurements.* IEEE/PES Power Systems Conference and Exposition, 2009.

[6-3] **J. M. Davalos Ramirez, V. R. J. Valenzuela.** *Coordination of FACTS-based stabilizers for damping oscillations.* IEEE Power Engineering Review. Vol. 20, No. 12, pp. 46-49, Dec. 2000.

[6-4] **A. Heniche and I. Kamwa.** *Assessment of two methods to select wide-area signals for power system damping control.* IEEE Transactions on Power Systems. Vol. 23, No. 2, pp. 572-581, May 2008.

[6-5] **H. F. Wang, F. J. Swift, and M. Li.** *Indices for selecting the best location of PSSs or FACTS-based stabilisers in multimachine power systems: a comparative study.* IEE Proceedings of Generation, Transmission and Distribution. Vol. 144, No. 2, pp. 155-159, Mar. 1997.

[6-6] **N. R. Chaudhuri, B. Chaudhuri, S. Ray, and R. Majumder.** *Wide-area phasor power oscillation damping controller: a new approach to handling time-varying signal latency.* IET Generation, Transmission & Distribution. Vol. 4, No. 5, pp. 620-630, May 2010.

[6-7] **Y. Yuan, Y. Z. Sun, and L. Cheng.** *Design of delayed-input wide-area FACTS controller using genetic algorithm.* IEEE Power Engineering Society General Meeting, 2007.

[6-8] **V. Rasvan**. *Popov theories and qualitative behavior of dynamic and control systems*. European Journal of Control, 8(3): 190-199, 2002.

[6-9] **S. X. Zhao**. *On absolute stability of control systems with several executive elements*. Scientia Sinica (Ser. A), 31(4): 395-405, 1988.

[6-10] **H. Gao, J. Lam, C. Wang, and Y. Wang.** *Delay-dependent output-feedback stabilization of discrete-time systems with time-varying state delay.* IEE Proceedings of Control Theory and Application. Vol. 151, No. 6, pp. 691-698, Nov. 2004.

[6-11] **P. Kundur.** *Power Stability and Control.* New York: McGraw-Hill, 1994.

[6-12] **G. Rogers.** *Power System Oscillations.* Norwell, MA: Kluwer, 1999.

Chapter 7
Conclusions and Further Works

7.1 Conclusions

This dissertation investigates the wide area damping control strategies to stabilize inter-area oscillations and enhance the stability of large-scale interconnected systems. The quick and flexible control features that FACTS devices can achieve are developed to construct wide area damping controllers, and the advanced robust design approaches are proposed in the LMI framework to guide controller design. Typically, the time delay of wide area signal is considered sufficiently to reduce or even eliminate the effects of the wide area damping controller on the damping performance. The main research achievements of this dissertation are summarized as follows:

(1) *Small signal stability analysis (SSSA) on large-scale interconnected systems.* The practical modal analysis method is used to discuss the stability problem of large-scale interconnected systems. The dominant LFOs especial the inter-area oscillation modes are revealed through modal analysis, which includes the oscillation frequencies and the damping ratios. Besides this, the classic local PSSs with different structures are studied, and their potential limitation on damping inter-area oscillations is also discussed.

(2) *Establishment of wide area damping control network and principle study of wide area damping control strategy.* The basic framework of wide area damping control network is presented, which mainly includes the local PMUs, the WAMS center, the WADC center, and the wide area control devices. In addition, the operating principle of FACTS wide area damping control is theoretically studied according to the SMIB system installed with FACTS device. Furthermore, the general configuration of FACTS wide area damping control is also presented, and the local and the wide area control loops are clarified in this configuration.

(3) *The robust control design method-FWMs approach is employed to design FACTS wide area damping controller.* By way of FWMs approach, the controller design problem is converted into the standard linear design problem in the LMI framework. The iteration algorithm is corresponding proposed to find

the suitable controller parameters. The time delay of wide area control signal is considered sufficiently during the process of controller design. It is worth to note that the utilization of wide area signal makes power system as the typical time-delay system. As discussed in this dissertation, FWMs approach is good to handle with time-delay problem, hence, it is advantage to use such approach to design FACTS wide area damping controller.

(4) *A practical output-feedback-type controller structure is proposed for FACTS wide area damping controller.* The controller design is also converted into the optimization problem with a set of LMI constrains. Unlike the classic output-feedback controller, the proposed one has the dynamic item and can adapts the time-varying delay of wide area signal and the changing of operating conditions. At the same time, unlike the classic state-feedback controller, its controller structure is simple but practical, and it needn't use state observer, thus, it is more advantage to the practical application.

(5) *A robust coordinated control concept and method is proposed for multiple FACTS wide area damping controllers.* In fact, the FWMs approach can be extended to simultaneously design more than one controller. In addition, generally, in a practical power system there are more than one wide area damping controller to act together to improve the overall stability. In this dissertation, a wide area coordinated robust damping control strategy is presented. The multiple series- and shunt-type FACTS devices are utilized to construct wide area control network. A robust design method and algorithm is proposed to design such coordinated controllers. Unlike the classic coordinated controllers, by using the proposed robust coordination method, the time delays of different wide area controllers are considered together, thus, it is advantage to handle with the multi-time-delay problems of multiple wide area controllers.

7.2 Further Works

According to the research results achieved in this dissertation, and combing to the new development of modern power systems and advanced control theory, the following research works can be performed in the future:

(1) *Real application of robust FACTS wide area damping controllers presented in this dissertation.* Although several control concept and controller structures have been proposed, their validations are performed

by using nonlinear simulation on the 4-machine 2-area benchmark system (Kunder system) and the 16-machine 5-area interconnected systems (NETS-NYPS). In the future, the real interconnected systems (e.g., Chinese interconnected systems) can be used to further validate the control concept and controller design approaches presented in this dissertation.

(2) *Analysis of time-delay stability region of large-scale power systems including PMUs/WAMS.* Up to now, there is no mature method to evaluate stability region of power system with time-delay characteristic. In fact, the wide application of PMUs/WAMS makes the power system as the typical time-delay system. As discussed in this dissertation, the time-delay may endanger the control performance of wide area damping controller. Besides this, it may also influence the processing result of wide area information transmitted by WAMS. Therefore, it is necessary to find some effective solutions to analyze the stability region of time-delay power system.

(3) *New application of FWMs approach for parameter design of different type controllers.* In fact, the proposed FWMs method has the general meaning to handle with the delay problem of controller design. It can be applied not only the wide area damping controller but also other control fields of power systems. In the future, it is worth to perform the related research and extend the application fields of FWMs approach.

List of Publications

Refereed Publications (査読論文)

1. **Fang Liu, Ryuichi Yokoyama, Yicheng Zhou, Min Wu.** *Free-Weighting Matrices-Based Robust Wide-Area FACTS Control Design with Considering Signal Time Delay for Stability Enhancement of Power Systems*. IEEJ Transactions on Electrical and Electronic Engineering, 2011. (Accepted)

2. **Fang Liu, Min Wu, Yong He, Yicheng Zhou, Ryuichi Yokoyama.** *Delay-dependent Robust Stability Analysis for Interval Neural Networks with Time-varying Delay*. IEEJ Transactions on Electrical and Electronic Engineering, 6(4), 345-352, 2011.

3. **Fang Liu, Min Wu, Yong He, Ryuichi Yokoyama.** *Improved Delay-dependent Stability Analysis for Uncertain Stochastic Neural Networks with Time-varying Delay*. Neural Computing and Applications, 20, 441-449, 2011.

4. **Fang Liu, Ryuichi Yokoyama, Yicheng Zhou, Min Wu.** *Oscillation Damping Effects of Power System Stabilizer with Eigenvalue Analysis Method*. International Journal of Power and Energy Systems, 30(4), 241-247, 2010.

5. **Fang Liu, Min Wu, Yong He, Ryuichi Yokoyama**. *New Delay-dependent Stability Criteria for T-S Fuzzy Systems with Time-varying Delay*. Fuzzy Sets and Systems, 161(15), 2033-2042, 2010.

6. **Fang Liu, T. Niimura, Ryuichi Yokoyama, Yicheng Zhou, Min Wu**. *H_∞ Controller Design for SVC to Enhance System Damping and Voltage Stability with Time-delay of Wide-area Signals*. International Journal of Electronics, Electrical and Communication Engineering, 1(1), 51-60, 2009.

7. **Min Wu, Fang Liu, Peng Shi, Yong He, Ryuichi Yokoyama.** *Improved Free-Weighting Matrix Approach for Stability Analysis for Discrete-time Recurrent Neural Networks with Time-varying Delay*. IEEE Trans on Circuits and Systems, II, 55(7), 690-694, 2008.

8. **Min Wu, Fang Liu, Peng Shi, Yong He, Ryuichi Yokoyama.** *Exponential Stability Analysis for Neural Networks with Time-Varying Delay*. IEEE Trans on Systems, Man and Cybernetics, Part B, 38(4), 1152-1156, 2008.

9. **Fang Liu, Min Wu, Yong He.** *Further Improvement of Free-weighting Matrix Approach for The Stability Analysis of Neural Networks with Time-varying Delay*. Computing Technology and Automation, 1 (27), 1-6, 2008.(Chinese)

International Conference (国際学会)

10. **Fang Liu, Ryuichi Yokoyama, Yicheng Zhou, Min Wu.** *Design of Damping Controllers of Multi-FACTS Devices with considering Time-delay of Wide-area Signals*, 46th International Universities' Power Engineering Conference (UPEC2011), September 5-8, Soest, Germany, 2011. (Accepted)

11. **Fang Liu, Ryuichi Yokoyama, Yicheng Zhou, Min Wu.** *TCSC Output-Feedback Damping Controller Design to Damp Power Systems Oscillation with Consider-ing Signal's Delay*, IEEE Trondheim Powertech 2011, June, 19-23, Trondheim, Norway, 2011.

12. **Fang Liu, Ryuichi Yokoyama, Yicheng Zhou, Min Wu.** *TCSC Wide-Area Damping Controller to Enhance the Damping of Inter-area Oscillation for Power Systems with Considering the Time Delay of Wide-Area Signals*. 2010 International Conference on Power System Technology (POWERCON2010), October, 24-28, 2010, Hangzhou, China.

13. **Fang Liu, Ryuichi Yokoyama, Yicheng Zhou, Min Wu.** *SVC Robust Additional Damping Controller Design for Power System with Considering Time-delay of Wide-area Signals*. Ninth International Conference on Environment and Electrical Engineering (EEEIC2010), May 16-18, 2010, Prague, Czech.

14. **Fang Liu, Ryuichi Yokoyama, Yicheng Zhou, Min Wu.** *Study on Oscillation Damping Effects of Multi-Band Power System Stabilizer Arrangement with Eigenvalue Analysis Method*. IASTED International Conference Modelling, Simulation, and Identification (MSI 2009), October 12-14, 2009, Beijing, China.

15. **Fang Liu, Ryuichi Yokoyama, Yicheng Zhou, Min Wu.** *Reactive Power Compensation Characteristics of a New SVC for Industry Custom Power System.* International Conference on Power Systems Transients

(IPST2009), June 2-6, 2009, Kyoto, Japan.

16. **Fang Liu, Ryuichi Yokoyama, Yicheng Zhou, Min Wu.** *Overview of Wide-Area Damping Control and Method to Against Power System Oscillation with Consideration of time-delay*. Power Engineering and Power Systems Engineering, IEE Japan, September 15-17, 2009, Tokyo, Japan.

17. **Fang Liu, Min Wu, Yong He, Yicheng Zhou, Ryuichi Yokoyama.** *New Delay-dependent Stability Criteria for T-S Fuzzy Systems with a Time-varying Delay*. Proceedings of the 17th World Congress, the International Federation of Automatic Control. 254-258, July 6-11, 2008, Seoul, Korea.

18. **Fang Liu, Min Wu, Yong He, Yicheng Zhou, Ryuichi Yokoyama.** *New Delay-dependent Stability Analysis and Stabilizing Design for T-S Fuzzy Systems with a Time-varying Delay*. The 27th Chinese Control Conference (CCC08), 4, 340-344, July, 2008, Kunming, China.

Book (著書)

19. **Fang Liu, Ryuichi Yokoyama, Yicheng Zhou, Min Wu**. CHAPTER 4, *<<Modeling, Simulation and Identification>>*, 63-80, ISBN 978-953-307-136-7, Sciyo Publication, 2010.